Technical Report Documentation Page

1. Report No.	2. Government Accession No.	3. Recipient's Catalog No.
UMTRI-85-44		

4. Title and Subtitle	5. Report Date
THREE-DIMENSIONAL OCCUPANT DYNAMICS SOFTWARE: STEERING ASSEMBLY MODEL	October 1985
	6. Performing Organization Code
7. Author(s)	8. Performing Organization Report No.
D.H. Robbins	UMTRI-85-44
9. Performing Organization Name and Address University of Michigan Transportation Research Institute Institute of Science and Technology Ann Arbor, Michigan 48109	10. Work Unit No. (TRAIS)
	11. Contract or Grant No. P.O. CP004552
12. Sponsoring Agency Name and Address Current Product Engineering General Motors Technical Center Warren, Michigan 48090	13. Type of Report and Period Covered FINAL REPORT Jan. 1984 - Aug. 1985
	14. Sponsoring Agency Code

15. Supplementary Notes

16. Abstract

Rather than the development of software, existing options available in the three-dimensional crash victim simulation software were used to generate a steering assembly linkage data set module. This procedure was adopted for a variety of reasons including:

-- Availability of the software so no code development was required
-- Precedence based on work at British Leyland
-- Flexibility to model a variety of steering assembly linkages and energy absorption concepts

Development of a steering assembly model was found to be flexible and was demonstrated. A comparison between predictions and data from an impact sled test indicated similar results.

17. Key Words	18. Distribution Statement
Crash Victim Simulation Occupant Dynamics Occupant Protection Steering Assembly Modeling	Unlimited

19. Security Classif. (of this report)	20. Security Classif. (of this page)	21. No. of Pages	22. Price
None	None	97	

UMTRI-85-44

THREE-DIMENSIONAL OCCUPANT DYNAMICS SOFTWARE: STEERING ASSEMBLY MODEL

D. H. Robbins

Transportation Research Institute
Institute of Science and Technology
The University of Michigan
Ann Arbor, Michigan 48109

Final Report
October 1985

Prepared for

Current Product Engineering
General Motors Technical Center
Warren, Michigan 48090

TABLE OF CONTENTS

LIST OF FIGURES

LIST OF TABLES

1.0 INTRODUCTION AND OBJECTIVES

The three-dimensional occupant dynamics software package (3D-CVS), originally developed at Calspan Corporation (1), is a powerful tool for studying linkage dynamics and forcible interactions between a linkage and its physical environment. Subprograms, which have been developed for applying the software to problems in occupant protection, can be used to simulate restraint harnesses, air cushions, and occupant equilibrium positioning.

The 3D-CVS package suffers from a lack of input/output software to make the task of the user easier. In addition, few validations have been conducted to show that the software produces results similar to those observed in laboratory dynamic tests. Because of these factors, most applications of the 3D-CVS have been experimental in nature. In order to move toward the time when the 3D-CVS can be used with some confidence in realistic research, development, and design applications, work has been initiated in areas both of user aids and software expansion/improvement.

One of the projects, the subject of this report, has been to improve the capabilities of the 3D-CVS in order to model various steering assembly concepts. Rather than the development of software to accomplish this goal, existing options available in the software were used to generate a steering assembly linkage data set module. For a traditional assembly this linkage should allow column and wheel rotation, column collapse, shear capsule effects, interactions between the wheel rim and the occupant, as well as the possibility for intrusion of the assembly into the occupant compartment. There is precedence for this approach in work reported by British Leyland (2).

Non-traditional assemblies may use different concepts for the placement of energy-absorbing components. This could result from development of steering linkage concepts which route the column away from proximity to a plane passing through the center-line of the driver. The concept of a data set development solution to the steering assembly model problem rather than a software modification solution was adopted for a variety for reasons including:

- Availability of the software as no code development is required.
- Precedence based on the work of British Leyland.
- Flexibility to model a variety of steering assembly linkages and energy absorption concepts.

In conclusion, the objective was to use existing capabilities of the 3D-CVS in developing models of existing and new steering assembly concepts.

Part 2 of the report discusses the details of the selection of modeling concepts. The development of the data set, based on an impact sled experiment, is discussed in Part 3. Graphic results of the simulation and comparisons with the test are given in Part 4. The remainder of the report presents Conclusions and Recommendations as well as references.

2.0 SELECTION OF CONCEPT

2.1 Initial Concepts

The initial concept, shown in Figure 1, includes four masses. A wheel rim mass is connected through two joints to the upper column mass. The upper column strokes with respect to the lower column. The lower column sleeve is attached to the vehicle. The connecting link between rim and column, which can be thought to represent spokes, also is assigned a mass value. The remaining mass is the mobile point at the lower end of the column. This mass could become active in the case of intrusion from the engine compartment.

The wheel rim was modeled as a contact ellipsoid which would generate forces upon contact with vehicle occupant segments such as the head, chest, and abdomen. Collapse and rotation of the rim was simulated by rotation of the link connecting rim with column. Forces generated by the deformation process were the result of torques generated at the two joints.

A guide bracket was included to represent one of the known modes of column resistance to rotation. This concept was modeled as a sphere attached to the upper column mass which was contained in a sleeve with three sides. The three sides were modeled as planar contact surfaces capable of applying frictional and normal forces to the column. The fourth side was left open so that the column could drop out of the bracket.

The other two spheres on the upper column mass were intended to absorb energy much like the ball bearings do in many current designs. The two spheres had diameters slightly larger than the distance between the four sides of a hollow sleeve. Because of this, normal forces were

always generated by the contacts. Tangential forces, produced by friction of the spheres plowing through the hollow sleeve, were intended to model the collapse of the column. Column rotation was possible in that the two spheres were restrained in the hollow sleeve only by the force-deformation relationship of the contacts.

Although this concept had features which were eventually used in the final model, it was rejected became of a lack of degrees of freedom of the wheel with respect to the column. The reason for this was the observation during tests that the wheel rim could move and deform in a plane perpendicular to the long axis of the column.

2.2 First Implementation

Figure 2 describes schematically the first concept, much of which was implemented as a data set. The same technique was used for column collapse as was used in the first concept. However, instead of a rigid link connecting the wheel to the column, a sphere was attached to the wheel mass which was restrained from motion by being located within a six-sided box comprised of contact surfaces attached to the upper column. The collapse, shear, and rotation of an energy-absorbing hub is illustrated in a series of drawings at the bottom of Figure 2. Rim rotation is resisted by frictional torques generated when the sphere rotates inside the box. Rim motion perpendicular to the column (shear) is resisted by normal forces. Likewise, collapse of the rim in the direction of the axis of the column is resisted by normal forces generated by the sphere on the surfaces comprising the box.

When construction was initiated for that portion of the data set which dealt with the wheel mass and its attachment to the column, it was found extremely difficult to relate available test data to the

parameters and modeling techniques illustrated in the bottom and right schematics shown in Figure 2. To complete the data set, the arrangement of contact surfaces and ellipsoids that is illustrated in Figure 3, is used. The top schematic shows a side view of the column mass. Attached to this mass are two spheres which guide the direction of any column collapse and resist motion. Six contact surfaces are also attached to this mass. They are arranged in the configuration of a box to resist three-dimensional motion of the steering wheel when it interacts with ellipsoids attached to the torso. The bottom schematic shows side and front views of the wheel/rim model. The large ellipsoid, having the general dimension of the outline of the rim, is used to sense forcible contact with the chest and abdomen ellipses. The three small spheres sense interactions with the six contact surfaces attached to the column mass, that are arranged in the configuration of a box. These spheres, which may be thought to represent the behavior of spokes attached to the rim, model the resistance of motion by the wheel rim as it interacts with the column.

The complete implementation of the column in this configuration is shown in Figure 4 which is the computer-generated plot produced at the initiation of the computer exercise. Figure 5 shows the position of the occupant and vehicle interior at a time of 20 milliseconds into the computer run. Although the occupant has barely begun to move relative to the vehicle at this early point in the simulation, the column mass has rotated so that the spheres are no longer restrained by the sleeve. In addition, symmetry is lost as shown by the rotation of the surfaces attached to the column mass. It appears that the problem started immediately after initiation of the run.

Two problems with the analysis used in developing the computer code were identified which precipitated this problem. These are:

1. the lack of a model of static friction (motion must exist for friction to be applied).
2. the reduction of force to zero when an ellipsoid has passed completely through a contact surface (a particularly severe problem when the dimensions of the ellipsoid are small).

The first of these problems is particularly severe and was the primary cause of the failure. At the beginning of the run, tangential friction forces between the spheres on the column and the sleeve were predicted to be zero even though penetration was non-zero. The normal forces produced as the result of these contacts, were also non-zero. When the vehicle deceleration caused the beginnings of motion, a relative velocity between the column and the vehicle was initiated which precipitated a rapid buildup of friction forces. For computational reasons which are not totally understood, the integration procedure was not able to handle the buildup of several frictional forces simultaneously, and instability resulted. The properties of the second problem with the code worsened the overall effect. The use of very small integration steps did help somewhat but did not remove the overall instability. By the end of the review of results, it appeared that the problem was present from the beginning, perhaps pointing at limitations in the integration procedure as well as the physics. As a result, the first data set implementation was dropped.

A byproduct of a code lacking the capability for modeling static friction is the related problem of modeling initial equilibrium states. This prevents the use of realistic models for the initial positioning of vehicle occupants. It should be noted that this problem also exists in the MVMA-2D Code (3).

2.2 Final Concept

The final concept used an alternative to friction for energy-absorption in the column. Figure 6 shows modified views of the column and wheel/rim models. A spring-damper element is attached to the column center of mass. This element acts along the center line of the column. The other end of the spring-damper is attached to the vehicle. The force-deflection characteristics were obtained from test data supplied by General Motors. The spheres attached to the column mass serve to stabilize the motion of the energy-absorbing element as it moves within the sleeve. The diameter of the spheres was reduced so that they now fit within the sleeve. As the column rotates, normal forces are generated which tend to resist the motion. Plowing is not included in this data set. It could be added by providing a second sleeve, larger than the first, which could begin to generate tangential friction forces when the column is already in motion.

Likewise, the friction concept for resisting motion was not used in simulating the interaction between the wheel/rim mass and the column mass. Spring-dampers were attached from the center of each sphere to a point on a plane parallel to the initial plane of the wheel. The purpose of the spring-dampers is to resist deformation of the wheel rim with respect to the column. Rotation of the wheel is allowed for contacts at any point on the rim. The force-deflection data were obtained in static tests of the rim by pressing a platen onto the rim top or bottom in separate tests. Using different data for the rim top and rim bottom allows for differentiation of impacts to different parts of the rim by the chest, head, and abdomen. As shown in Figure 6, the spheres are still retained to stabilize the wheel from lateral motions.

The large ellipsoid for the wheel still is useful for chest, abdomen, and head contact. The hub contact surface attached to the column is sensitive to chest contact.

Figure 7, 8, and 9 show side, front, and top views of the occupant seated in the vehicle at the initiation of the computer run. The names of the various contact surfaces (identical to those used in the data set) have been added to clarify the definitions.

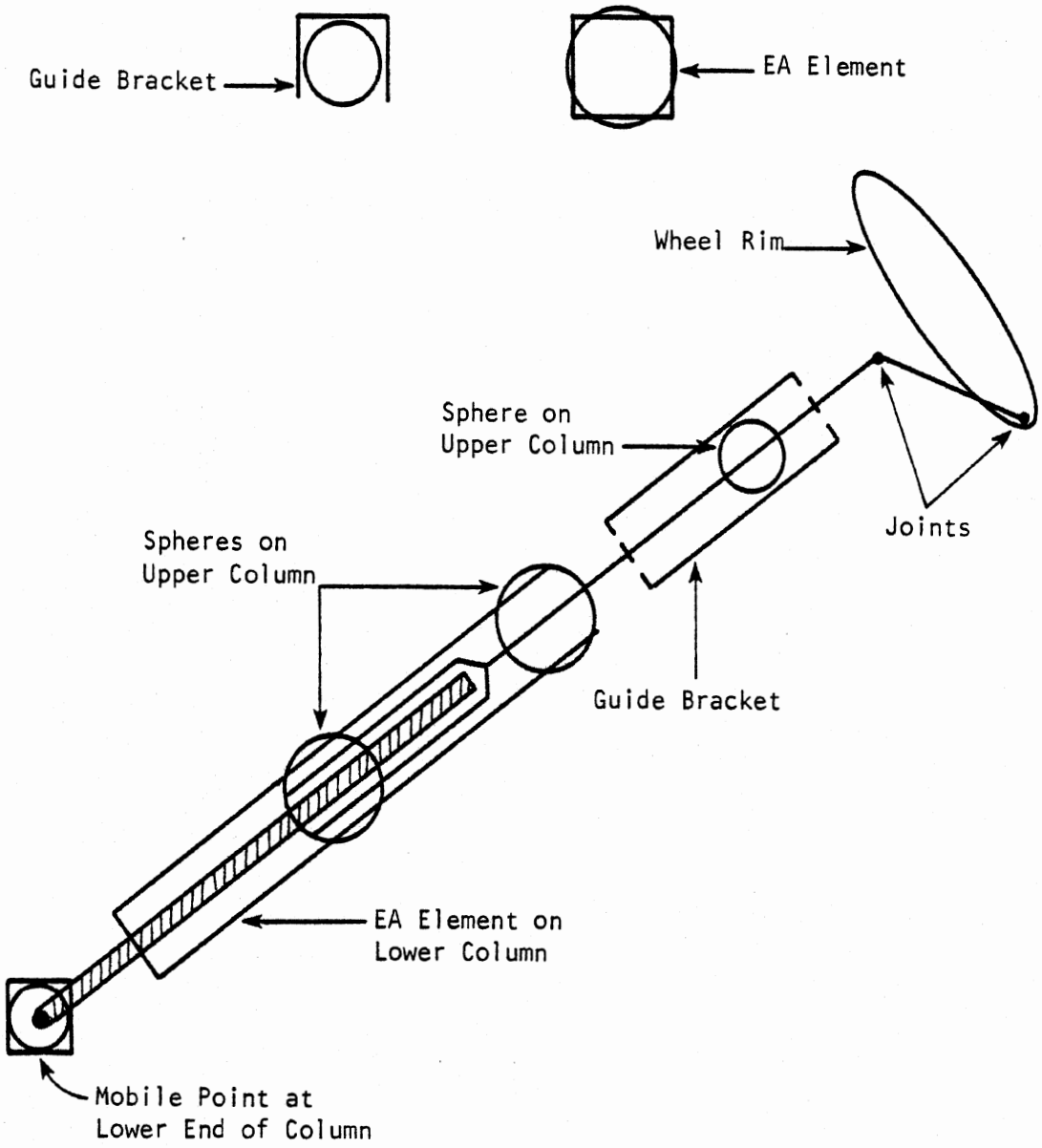

Figure 1. Initial 4-mass wheel/column concept. Pivoted wheel.

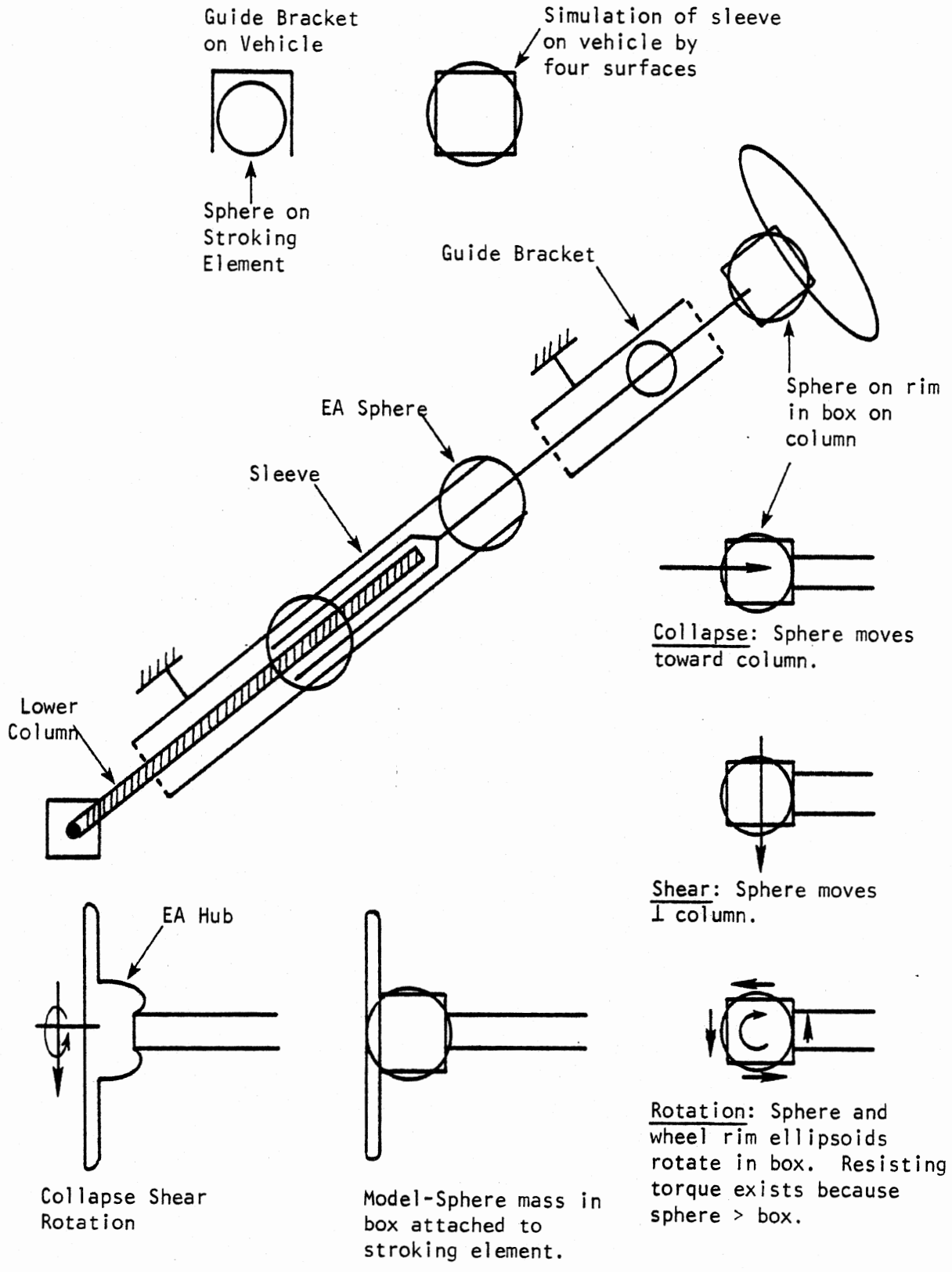

Figure 2. Initial 2-mass wheel/column concept. Energy absorption by friction.

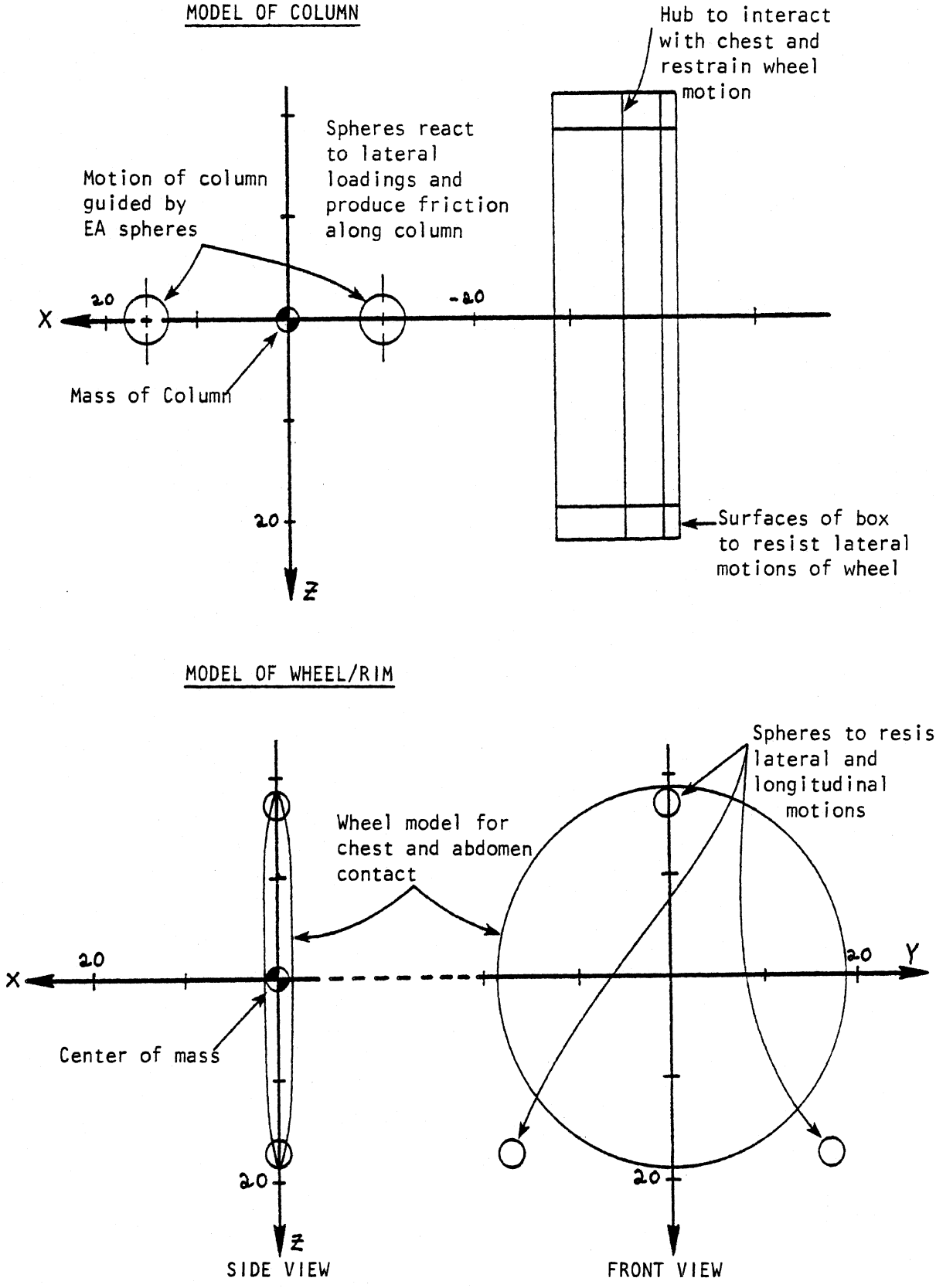

Figure 3. Schematic of the two column masses for the initial 2-mass wheel/column concept.

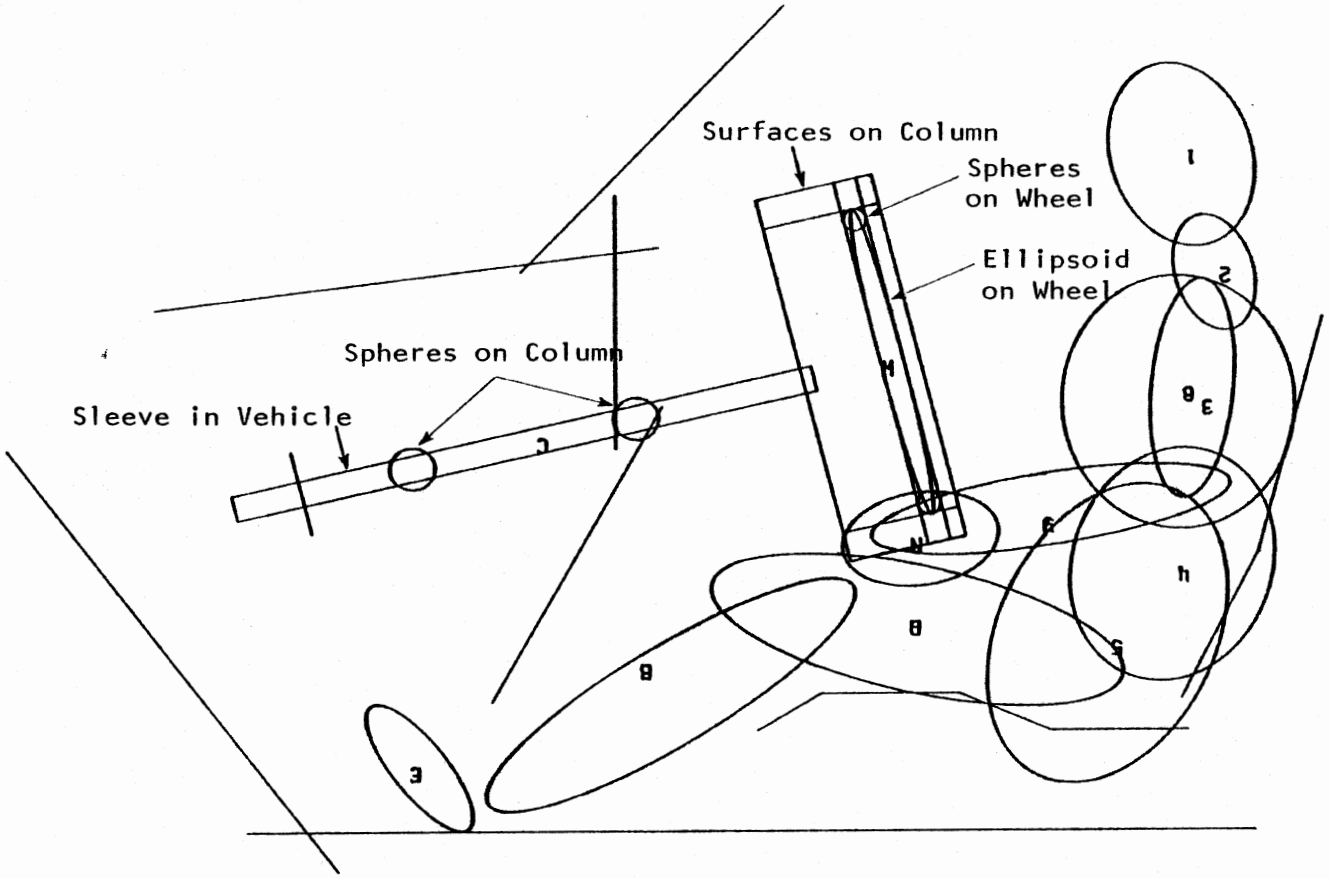

Figure 4. Side view of occupant for initial 2-mass wheel/column concept. t=0ms.

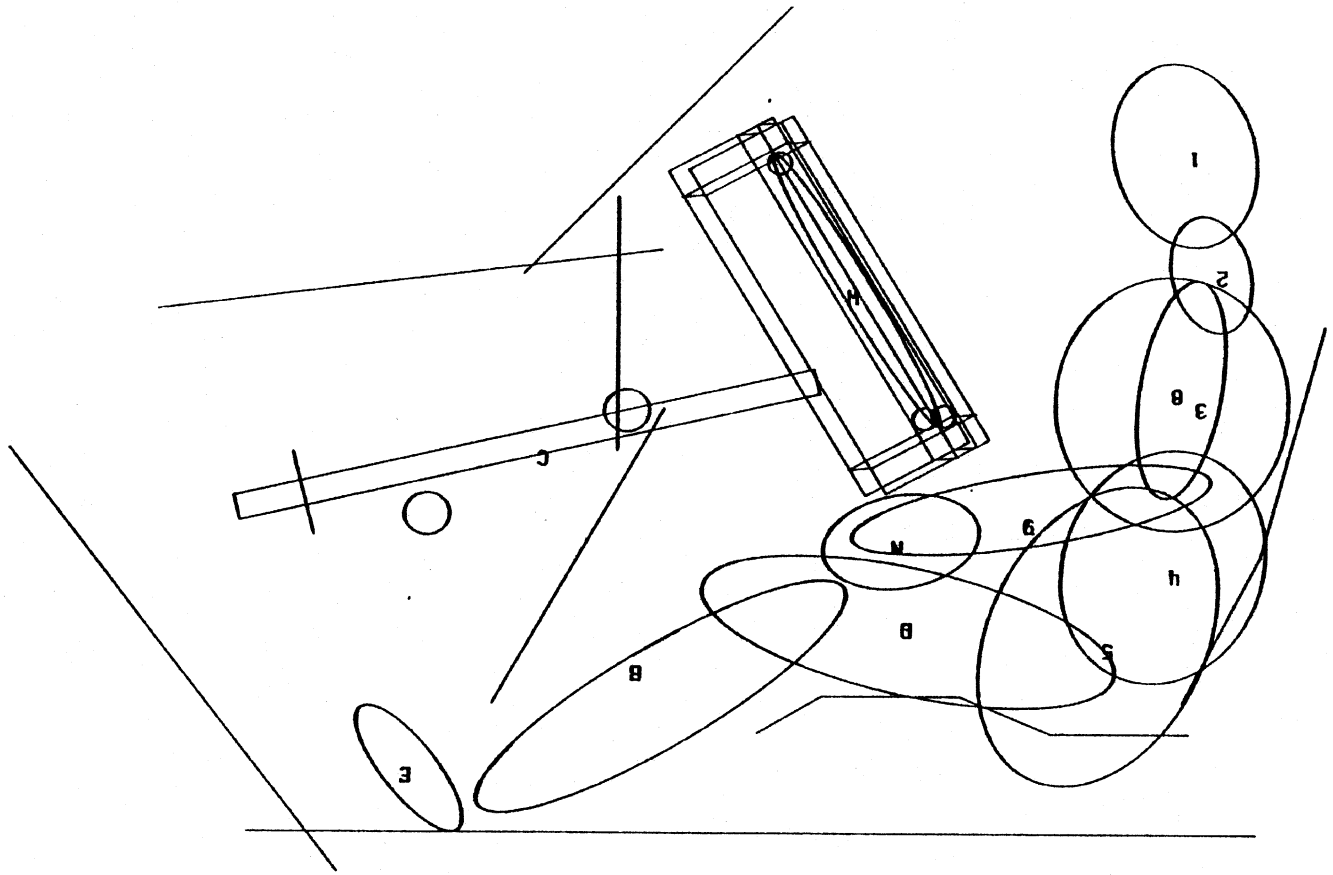

Figure 5. Side view of occupant for initial 2-mass wheel/column concept. t=20ms.

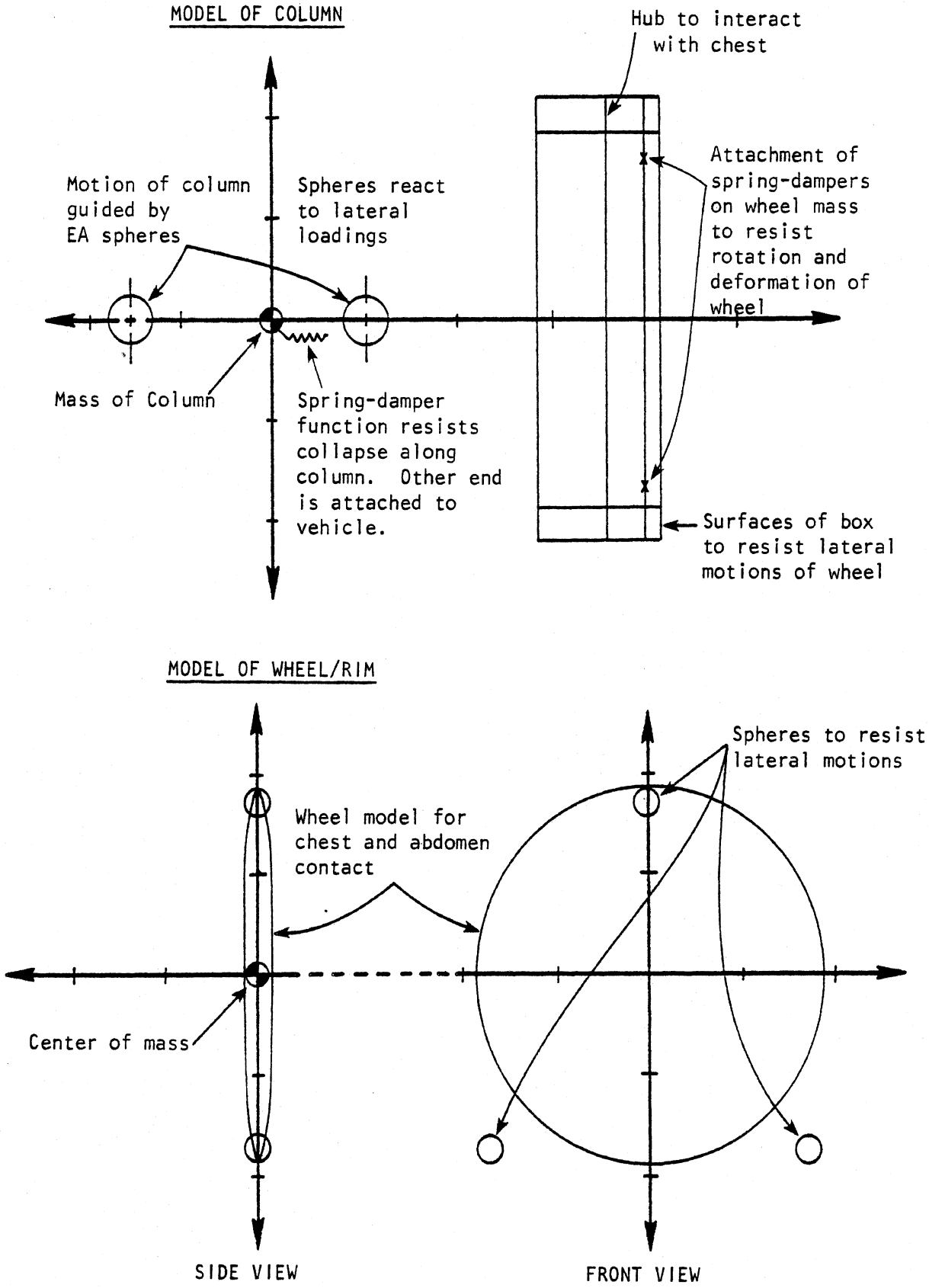

Figure 6. Schematic of the two column masses for the final wheel/column concept using spring-damper elements.

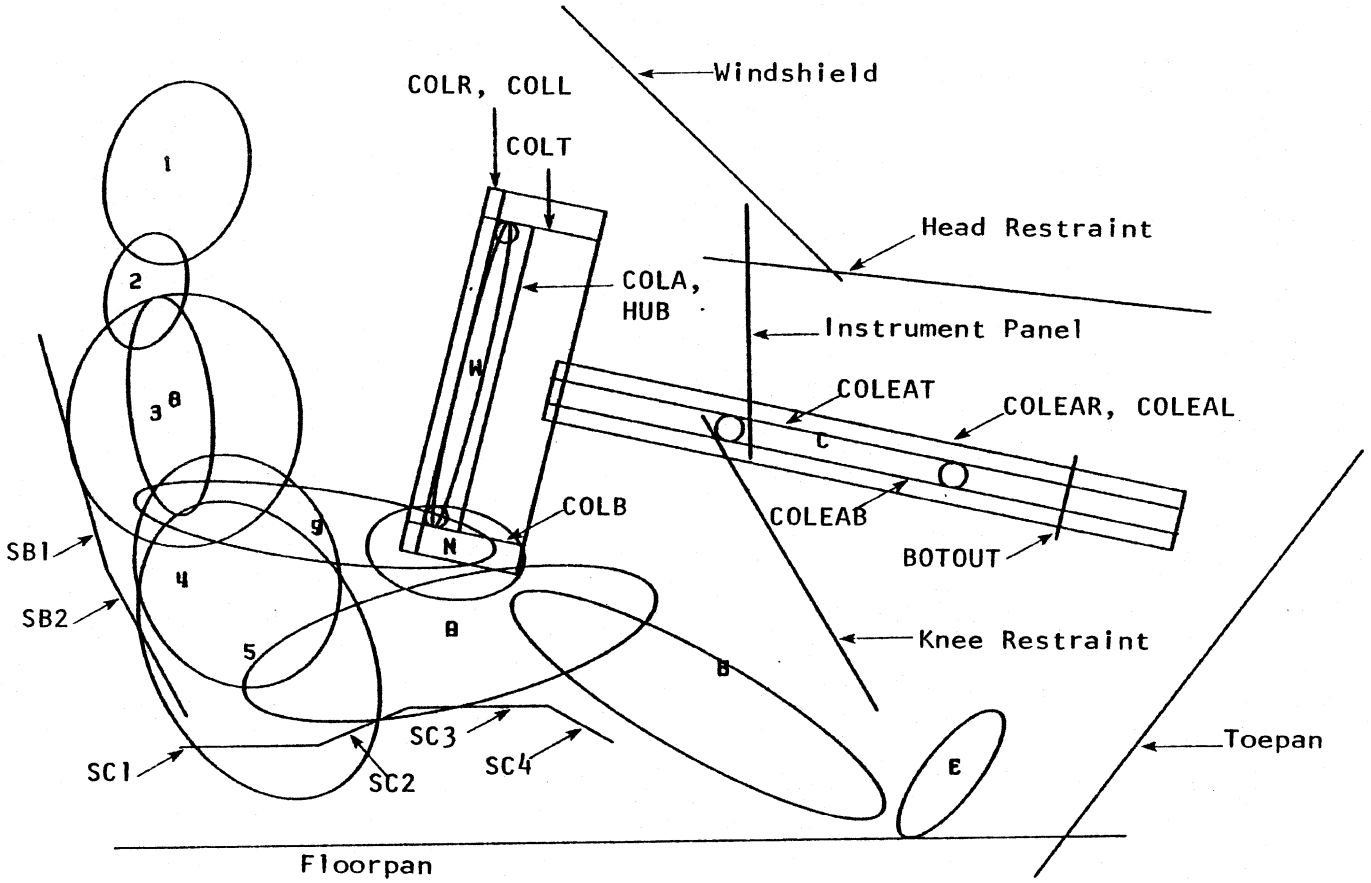

Figure 7. Side view of occupant for final wheel/column concept. t=0ms.

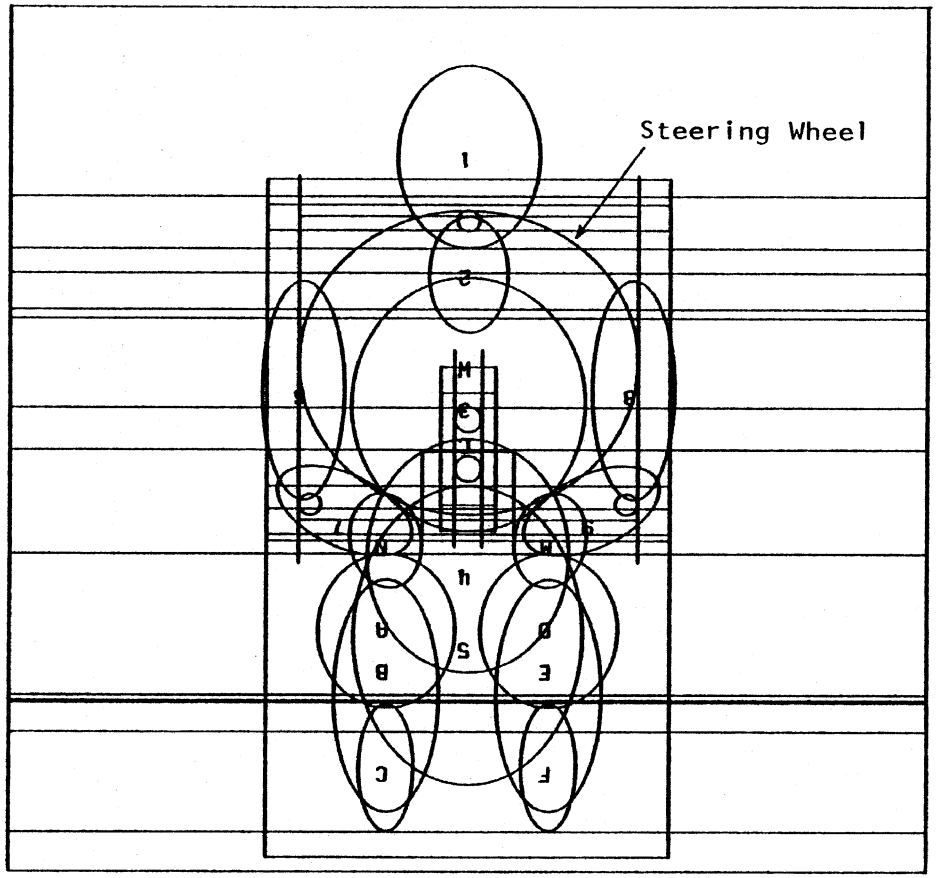

Figure 8. Front view of occupant for final wheel/column concept. t=0ms.

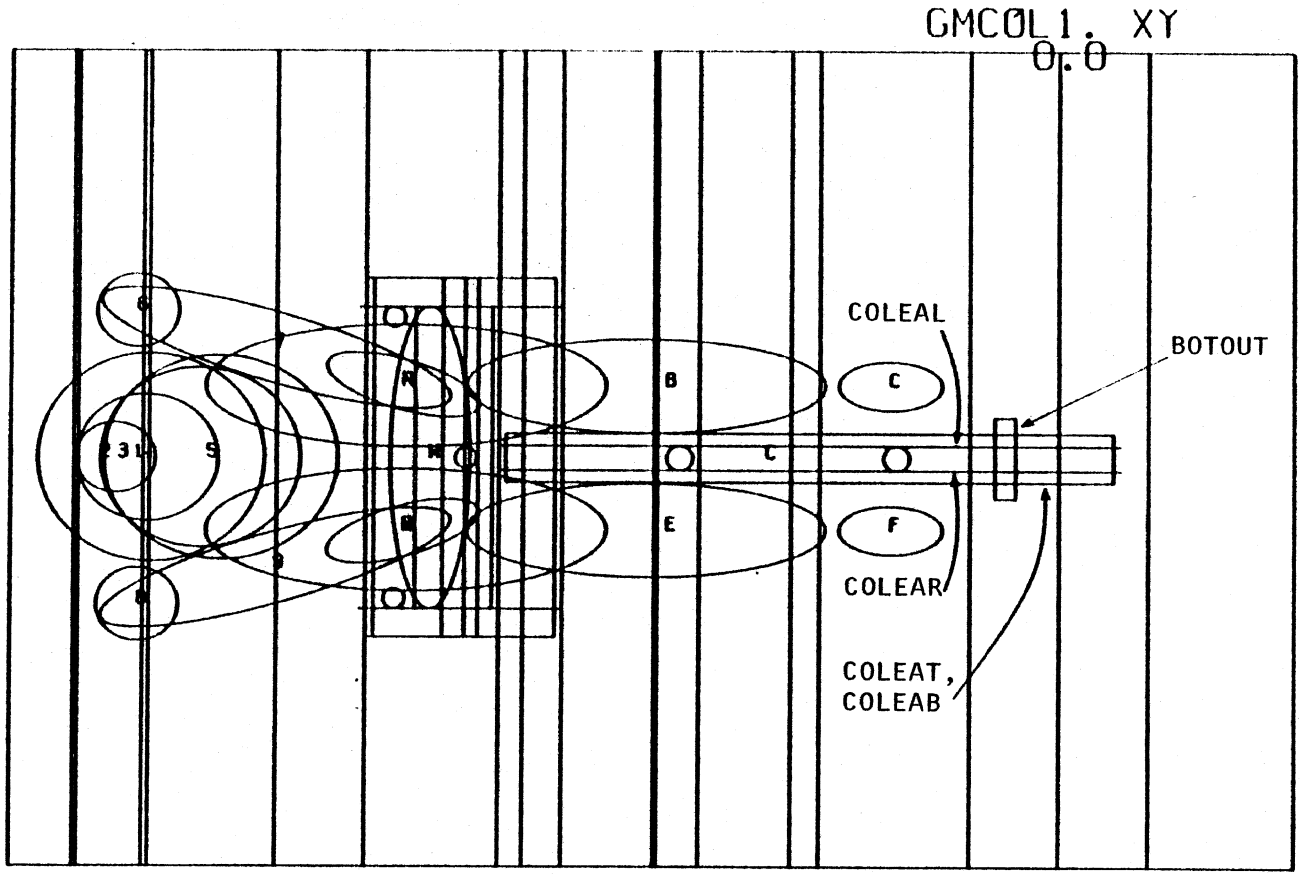

Figure 9. Top view of occupant for final wheel/column concept. t=0ms.

3.0 DEVELOPMENT OF DATA SET

3.1 The Test

In order to prove that the model would actually simulate a real column system, data from an impact sled test was provided by General Motors. This test provide geometric data and the vehicle deceleration. The spatial location of various vehicle components as well as four important targets on the test dummy are shown in Figure 10. Some additional information on collapse of the column was provided separately. Tests were conducted to determine the force-deflection properties of the rim with respect to the column.

Data describing the dummy and the remainder of the force-deflection characteristics of vehicle components were obtained from a data set provided by General Motors during a related modeling project. These data probably do not reflect the most recent dummy data which are available for use with the 3D-CVS Code. Also, it is not known how well the force-deflection data for the vehicle interior components (in particular, the seat, instrument panel, and knee restraint) describe the properties of the similar components in the impact sled test buck.

3.2 The Initial Baseline Data Set

At the beginning of the project, a baseline data set was provided by General Motors for use with the three-dimensional CVS Code. This data set simulates an unrestrained passenger in a frontal barrier impact. The occupant model appears to be based on the original fifteen mass linkage proposed by Calspan Corporation. Left and right hands have been added. The data set is included as Table 1.

Many changes were made to this data set in order to develop the final steering column simulation. The location of changes have been

indicated in the listing. Line 5 indicates changes to the A4-card. It was found necessary to decrease the integration time step in order to simulate the complex and stiff behavior of the column. The change to line 9, a B2-card, moves the abdomen contact ellipsoid forward in the segment in order to pick up the contact with the lower portion of the steering wheel rim. The changes to lines 15 and 18, also B2-cards, decreases the dimensions of the foot contact ellipsoids in order to aid in establishing initial equilibrium. Two B2-cards were added after line 24 in order to define the steering column and wheel mass properties.

A variety of changes were also made to the B-cards describing the joint properties. After line 56, four cards were added for null joints connecting the column and wheel masses with the remainder of the segments. An apparent inconsistency between the left and right hip joint parameters was found on line 62 and was changed (B4-cards). Several changes were made to the properties of the shoulder, elbow, and hip joints (B4-cards) on lines 71-80. This was done to stabilize the motion which occurred during interactions of the hands and with the instrument panel. Non-zero linear flexural spring characteristics were added for the elbows and wrists (lines 73,77,79,80). The very stiff quadratic spring coefficient was reduced for the wrists (lines 79,80) while the cubic spring coefficients were reduced to zero for the elbows (lines 73,77). The energy dissipation was reduced to 0.5 for all six segments for both the flexural and torsional degrees of freedom. Non-zero linear torsional spring coefficients were also added to all six. In addition, the quadratic spring coefficient for tension was reduced for the wrists (lines 79,80). After line 80 two cards were added for

the null joints connecting the column and wheel masses with the remainder of the segments.

Non-zero viscous coefficients were added to all occupant joints on the B5-cards in an additional effort to stabilize the motions. In the case of Euler joints, non-zero values were added mostly for the precession and nutation axes (lines 81-112). The values for the viscous coefficients are those report by Fleck et al. (1). An error was corrected on line 105 (Coulomb friction) for right shoulder precession. Coulomb friction was increased for both wrists (lines 111,112). In addition, the maximum torque allowed for a joint to remain locked was increased for the elbows and wrists (lines 102-103,108-109,111-112). As for the other B-cards, two additional cards for null joint properties were added to occupant for the presence of the unconnected column and wheel masses.

At the end of the B6-cards (after line 129) convergence test parameters were inserted for the wheel and column masses. Because these separate masses have linear as well as rotational degrees of freedom, six test values were included.

The C-cards (lines 131-136) were modified to use the velocity and deceleration data obtained during the impact sled test. The D1-card was modified to reflect the change in the number of contact surfaces, the number of added ellipsoids, and the three spring-dampers. The D2-cards (lines 138-265) defining the vehicle contact surfaces have been completely replaced by the new vehicle and wheel/column model. Four cards (D5) were added after line 265 to define the additional column and wheel contact ellipsoids. After line 266 one additional blank D7-card was added because the number of segments had increased beyond 18. After

this D7-card a total of four cards was added to define the four spring-dampers (D8).

Of the 26 functions included in the baseline data set (lines 267-390), 21 were retained, renumbered, and in some cases, renamed. This information is summarized in Table 2. The additional sixteen functions which were developed for the new data set defined the column and wheel force-interaction functions as well as the interactions of the occupant with the wheel and column. It should be noted that all the functions listed above have been obtained from the baseline data set as no known data were available to describe these functions for the case of the impact sled test.

The F-cards included in the baseline data set (lines 392-451) were not used. This reflects the complete rearrangement of contact surfaces, force interaction functions, and number of segments. Some modifications were necessary for the G-cards. These include addition of two G2-cards after line 454 to define the initial linear position of the wheel and column masses. Two G3-cards have been added after line 471 to define the angular orientation of these two masses. Changes were also made to the angular orientation of upper legs, lower legs, and feet (lines 460-465) in order to establish initial equilibrium. The remaining G- and H-cards (lines 472-1020) were not used as the output structure of the UMTRI version of the 3D-CVS is somewhat different from that used at General Motors as described by Robbins, et al. (4).

3.3 The Complete Final Data Set

Table 3 is a listing of the final data set including the energy-absorbing steering column and deformable wheel rim. The major

differences between this data set and the baseline presented in Table 1 are:

- addition of wheel and column masses, interactions, and constraints
- use of impact sled test data for defining vehicle deceleration
- use of geometric description of impact sled test buck to define the vehicle.
- use of UMTRI version of 3D-CVS output structure

The locations of the changes have been described in detail in Part 3.2.

Two additional tables are included to supplement Table 3. Table 4 is a list of the allowed contacts defined on the F-cards. The surface or ellipse and the contacts it makes with other ellipses are listed as well the identification numbers. Table 5 is a supplement to Table 2. It lists the new force-deflection functions which were defined.

UNIVERSAL DRIVER SLED FIXTURE

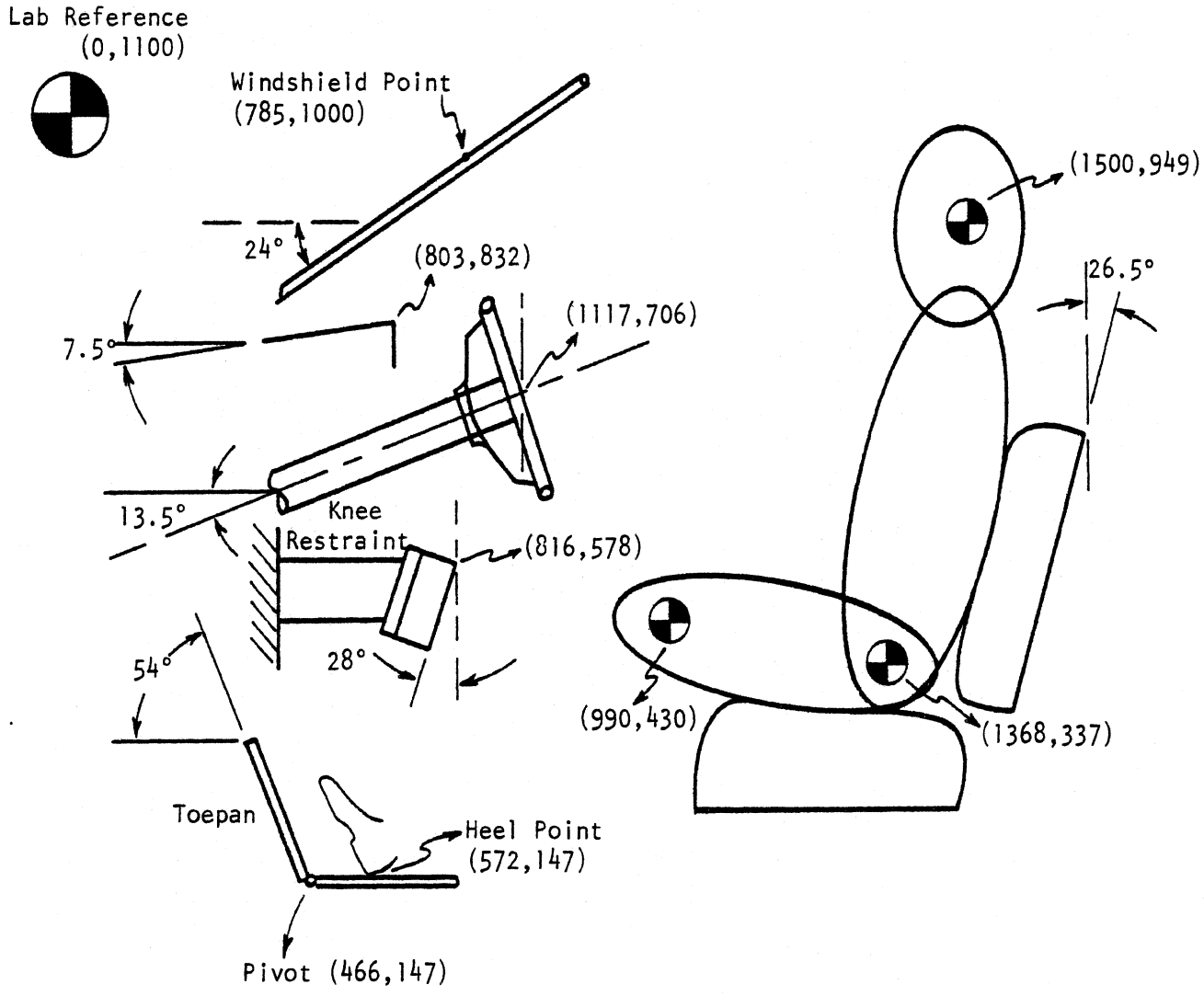

Figure 10. Universal driver sled test fixture.

```
Listing of GMCVS1.D at 16:20:49 on OCT  3, 1985 for CCId=SUVH                    Page    1

    1      07 JUN 1983
    2       SAMPLE PROBLEM# # 1
    3      UNRSTR PASSR,FRONTAL BARRIER IMPACT, NO PITCH
    4      CM. KG.SEC.      0.0          0.0       980.66
    5        6 020 0.00100 0.00025  0.001 0.000025
    6     01 00500 0 0 0 000 0 0 0 00000 0  0100
    7          17    16
    8       LT 517.331 2.479 2.479 1.468 12.00 12.50 18.50  1.70 0.000 -.350
    9       CT 4 5.760 .3650 .3650 .2790 11.00 11.00 14.00 1.660 0.000 0.000
   10       UT 317.227 2.504 2.504 2.170 12.75 12.75 15.00 3.610 0.000 0.000
   11        N 2 1.545 0.060 0.060 0.006  4.30  4.30  7.00 1.670 .0000 0.000
   12        H 1 4.545 .2190 .2060 .2060  7.75  7.75 11.00 1.500 .0000 0.000
   13      LUL A 6.091 .6860 .6860 .1310  7.50  7.50 23.10 -0.94 .0000 .0000
   14      LLL B 3.300 .7650 .7650 .0970  5.75  5.75 23.70 -4.22 .0000 .0000
   15       LF C 1.227 .0550 .0550 .0150  4.00  4.00 10.00 .0000 .0000 .0000
   16      RUL D 6.091 .6860 .6860 .1310  7.50  7.50 23.10 -.940 .0000 .0000
   17      RLL E 3.300 .7650 .7650 .0970  5.75  5.75 23.70 -4.22 .0000 .0000
   18       RF F 1.227 .0550 .0550 .0150  4.00  4.00 10.00 .0000 .0000 .0000
   19      LUA 6 2.000 .1160 .1160 .0250  4.50  4.50 13.00  0000  .000 .0000
   20      LLA 7 2.273 .3600 .3600 .0320  4.25  4.25 20.80 1.15 .0000 .0000
   21      RUA 8 2.000 .1160 .1160 .0250  4.50  4.50 13.00 .0000 0.00 .0000
   22      RLA 9 2.273 .3600 .3600 .0320  4.25  4.25 20.80 1.15 .0000 .0000
   23       LH N 0.800 .0115 .0115 .0012  5.50  3.05  9.00 .000 .000  .0000
   24       RH M 0.80  .0115 .0115 .0012  5.50  3.05  9.00 .000 .0000 .0000
   25        P O   1  -2 -4.25          -4.32          .0000  6.53
   26                      0.0    0.0     0.0    0.0    0.0    0.0
   27        W P   2  -2 -1.60          -6.48          .0000 13.93
   28                      0.0    0.0     0.0    0.0    0.0    0.0
   29       NP Q   3  -2 -2.54         -15.59          .0000 .0000
   30
   31       HP R   4  -2 0.000          -9.59          .0000 4.780
   32
   33       LH W   1  -4 -2.45 -8.85  2.57    0.0 .0000-23.99
   34                     -90.   90.                  4.76       27.0   -70.0
   35       LK X   6   1  0.00 .0000 16.18    0.0 .0000-16.36
   36                                               43.0
   37       LA G   7  -4-0.250 .0000 22.04  5.36 .0000 -4.09
   38                     90.                90.                        79.0
   39       RH V   1  -4 -2.45  8.85  2.57    0.00.0000-23.99
   40                     90.    90.                  4.76       -27.    70.
   41       RK Z   9   1   0.0 .0000 16.18    0.0 .0000-16.36
   42                                               43.0
   43       RA H  10  -4-0.250 .0000 22.04  5.36 .0000 -4.09
   44                     90.                90.                        79.0
   45       LS S   3  -4  0.45-18.00-14.59    0.0 .0000-13.06
   46                           90.                                -55.    -65.
   47       LE T  12  -4   0.0 .0000 13.07    0.0 .0000-15.11
   48                     90.0               90.                  8.0     70.
   49       RS U   3  -4  0.45 18.00-14.59    0.0 .0000-13.06
   50                          -90.                               55.0    65.
   51       RE V  14  -4   0.0 .0000 13.07    0.0 .0000-15.11
   52                     90.                90.                 -8.     70.
   53       LW J  13   1   0.0 .0000 10.20    0.0 .0000 -5.11
   54                     0.0 .0000                  -10.  00.0
   55       RW K  15   1   0.0 .0000 10.20    0.0 .0000 -5.11
   56                     0.0 .0000                  -10.  00.0
   57     115.8 0.000 .2000 0.500 90.000      115.8 .0000 .2000 0.500 70.000
   58     115.8 0.000 0.200 0.500 90.000      115.8  .000 0.200 0.5   70.0
```

Add two segment cards for column and wheel masses (B2).

Add four cards for null joints connecting column and wheel masses with remainder of segments (B3).

Table 1. Listing of Baseline Unrestrained Occupant Data Set (Page 1 of 9).

```
 59   30.0   .108   .0000 0.500 60.000     150.   .108   .0000 0.500 60.000
 60   30.0   .108   .0000 0.500 60.000     150.   .108   .0000 0.500 60.000
 61   6.000  .2500  .0000 0.500 10.000    2.972  .1088 0.000 0.500 100.00
*62   16.0   160.    160.  0.5   60.0       0.    -90.0  0.0
 63    0.00- 10.00  10.0  0.950 45.000    0.000  .000  0.000 0.950
 64   1.00   10.00  10.00 0.950 50.000    1.0    10.0   10.   0.950  42.
 65   0.     0.
 66   6.000  .2500  .0000 0.500 10.000    2.972  .1088 0.000 .500   100.
 67   16.0   160.   160.0  .5   60.0       0.0   0.     0.
 68          10.00  10.00 0.950 45.000                              0.950  0.000
 69   1.00   10.00  10.00 0.950 50.000    1.0    10.0   10.   0.950  42.
 70   0.     0.
*71   14.    00.0   00.0  0.950 125.00     ____                    0.950  60.0
 72   0.     0.
*73   ____   20.0   20.0  0.950 45.000     ____                    0.950  70.000
 74   0.     0.
*75   14.    00.0   00.0  0.950 125.00     ____                    0.950  60.0
 76   0.     0.     00.0
*77   ____   20.0   20.0  0.950 45.000     ____                    0.950  70.00
 78   0.     0.
*79          600.          0.950 60.000            600.           0.950  60.000
*80          600.          0.950 60.000            600.           0.950  60.000
 81   0.0    1000.  200.0  174.5  .0                        0.0    0.0
 82   0.0    1000.  200.0  105.0  .0                        0.0    0.0
 83   0.0    20.0   200.0  174.5  .0                        0.0    0.0
 84   0.0    20.0   200.0  180.9  .0                        0.0    0.0
*85   0.0    500.0  200.0  180.9  .0                        0.0    0.0
 86   0.0    500.0  200.0  180.9  .0                        0.0    0.0
 87   0.0    500.0  200.0  180.9  .0
 88   0.0    125.0  10.0   15.4   .0                        0.0    0.0
 89   0.0    20.0   10.0   30.    .0                        0.0    0.0
 90   0.0    20.0   10.0   30.    .0
 91   0.0    0.0    10.0
 92   0.0    500.0  200.0  180.9  0.0                       0.0    0.0
 93   0.0    500.0  200.0  180.9  0.0                       0.0    0.0
*94   0.0    500.0  200.0  180.9  0.0
 95   0.0    125.0  10.0   15.4   .0                        0.0    0.0
 96   0.0    20.0   10.0   30.    .0
 97   0.0    20.0   10.0   30.    .0
 98   0.0    0.0    10.0   0.0
*99   0.0    125.0  400.0  65.0   0.0                       0.0    0.0
*100  0.0    50.0   400.0  65.0
 101  0.0    0.0    400.0  0.0
*102  0.0    175.0  100.0  16.3   0.0                       0.0    0.0
*103  0.0    175.0  100.0  16.3
 104  0.0    0.0    100.0
*105  0.0    120.0  400.0  65.0   0.0                       0.0    0.0
*106  0.0    50.0   400.0  65.0
 107  0.0    0.0    400.0  0.0
*108  0.0    175.0  100.0  16.3   0.0                       0.0    0.0
*109  0.0    175.0  100.0  16.3
 110  0.0    0.0    100.0
*111  0.0    12.0   100.0  13.3   0.00
*112  0.0    12.0   100.0  13.3   0.00
 113                                    00.0 00.10 00.10 00.01 00.01 00.01
 114                                    00.0 00.10 00.1
 115                                    00.0 00.10 00.10
 116                                    00.0 00:10 00.10
```

Add two cards for null joints connecting column and wheel masses with remainder of segments (B4).

Add two cards for null joint properties (B5).

Table 1. Listing of Baseline Unrestrained Occupant Data Set (Page 2 of 9).

```
117                                          00.0 00.10 00.10
118                                          00.0 00.10 00.10
119                                          00.0 00.10 00.10
120                                          00.0 00.10 00.10
121                                          00.0 00.10 00.10
122                                          00.0 00.10 00.10
123                                          00.0 00.10 00.10
124                                          00.0 00.10 00.10
125                                          00.0 00.1  00.1
126                                          00.0 00.1  00.1
127                                          00.0 00.1  00.1
128                                          00.0 00.1  00.1
*129                                         00.0 00.1  00.1
130     FRONT BARRIER PULSE,  PRIMARY VEHICLE MOTION
131      0.0   0.0   0.0  1369. 0.000  0.0   0.0   0.0     59  0.0 0.002     00
*132    0.0   0.0   1.0  7.0   17.0  19.0  18.0  12.5  8.5   5.0  2.0   22.5
*133    27.5  15.0  18.0 20.5  37.0  33.0  22.5  14.5  15.5  20.0 22.0  25.0
*134    23.0  25.5  26.0 25.5  22.5  21.5  21.0  25.0  24.0  23.0 22.0  20.0
*135    17.0  15.0  12.5 10.5  10.0  10.0   7.5   5.0   1.0   0.0 -3.0  -3.0
*136    -2.5  -2.0  -2.0 -1.5  -1.0  -0.5   0.0   0.0   0.0   0.0  0.0   0.0
*137     32     0     0    0
138      1        WINDSHIELD
139    -224.8          50.0        -91.2
140    -277.5          50.0        -121.2
141    -224.8         -50.0        -91.2
142      2          DASHBOARD 1
143    -200.1          50.0        -36.4
144    -209.2         50.0         -71.5
145    -200.1         -50.0        -36.4
146      3        BOTTOM I.P.
147    -230.0           50.        -57.2
148    -242.4           50.        -59.5
149    -230.0          -50.        -57.2
150      4        LOWER I.P.
151    -242.4           50.        -59.5
152    -246.2           50.        -75.5
153    -242.4          -50.        -59.5
154      5        MID I.P.
155    -246.2           50.        -75.5
156    -242.9           50.        -93.1
*157   -246.2          -50.        -75.5
158      6        FR SEAT BACK1
159    -323.8          20.0        -58.82
160    -315.3          20.0        -41.42
161    -323.8         -20.0        -58.82
162      7        FR SEAT BACK2
163    -330.9          20.0        -86.72
164    -323.8          20.0        -58.82
165    -330.9         -20.0        -86.72
166      8      FR SEAT CUSHION1
167    -316.0          30.0        -37.72
168    -301.0          30.0        -37.72
169    -316.0         -30.0        -37.72
170      9         FLOORBOARD
171    -280.           50.0        -19.2
172    -180.0          50.0        -20.1
173    -280.          -50.0        -19.2
174      10          TOEBOARD
```

→ Add two cards for column and wheel masses (B6).

Table 1. Listing of Baseline Unrestrained Occupant Data Set (Page 3 of 9).

```
175      -225.8          50.0       -19.5
176      -200.1          50.0       -36.4
177      -225.8         -50.0       -19.50
178      11        UPPER I.P.
179       -242.9       50.0        -93.1
180       -224.8       50.0        -91.4
181       -242.9      -50.         -93.1
182      12         FRONT SEAT BACK3
183      -332.2         20.0       -108.12
184      -330.9        20.0        -86.72
185      -332.2        -20.0       -108.12
186      13       LOWER I.P.
187      -242.4          50.        -59.5
188      -246.2          50.        -75.5
189      -242.4         -50.        -59.5
190      14        MID I.P.
191      -246.2          50.        -75.5
192      -242.9          50.        -93.1
193      -246.2         -50.        -75.5
194      15      FR SEAT CUSHION2
195      -301.0          30.0       -37.72
196      -291.0          30.0       -42.12
197      -301.0         -30.0       -37.72
198      16      FR SEAT CUSHION3
199      -291.0          30.0       -42.12
200      -276.0          30.0       -42.12
201      -291.0         -30.0       -42.12
202      17      FR SEAT CUSHION4
203      -276.0          30.0       -42.12
204      -268.9          30.0       -37.72
205      -276.0         -30.0       -42.12
206      18           SILL
207      -332.8          50.0      -19.0
208      -200.1          50.0      -19.0
209      -332.8         -50.0      -19.00
210      19      ROOF PANEL 1
211      -282.6          50.0       -119.8
212      -277.9          50.0       -121.3
213      -282.6         -50.0       -119.8
214      20      ROOF PANEL 2
215      -282.6          50.        -119.8
216      -301.0          50.        -126.5
217      -282.6         -50.        -119.8
218      21         BOTTOM I.P.
219      -230.0          50.        -57.2
220      -242.4          50.        -59.5
221      -230.0         -50.        -57.2
222      22       LOWER I.P.
223      -242.4          50.        -59.5
224      -246.2          50.        -75.5
225      -242.4         -50.        -59.5
226      23       MID I.P.
227      -246.2          50.        -75.5
228      -242.9          50.        -93.1
229      -246.2         -50.        -75.5
230      24         HOOD
231      -94.80          50.        -75.2
232      -224.8          50.        -91.2
```

Table 1. Listing of Baseline Unrestrained Occupant Data Set (Page 4 of 9).

```
233      -94.80        -50.        -75.2
234      25        GRILLE
235      -86.80         50.        -60.0
236      -94.80         50.        -75.2
237      -86.80        -50.        -60.0
238      26        BUMPER
239      -84.80         50.        -50.0
240      -84.80         50.        -60.1
241      -84.80        -50.        -50.0
242      27        ROOF PLANE 3
243      -301.0         50.        -126.5
244      -326.0         50.        -127.5
245      -301.0        -50.        -126.5
246      28        SEAT FRAME1
247      -289.0         50.        -30.92
248      -284.4         50.        -35.32
249      -289.0        -50.        -30.92
250      29        SEAT FRAME 2
251      -284.4         50.        -35.32
252      -277.4         50.        -35.42
253      -284.4        -50.        -35.32
254      30         COWL
255      -225.5         50.        -91.1
256      -232.8         50.        -88.65
257      -225.5        -50.        -91.1
258      31         DASH2
259      -209.2         50.        -71.5
260      -228.0         50.        -75.7
261      -209.2        -50.        -71.5
262      32          SILL
263      -332.8         50.0       -19.0
264      -200.1         50.0       -19.0
265      -332.8        -50.0       -19.00
266
267        1    HEADREST FORCE(KG)
268          0.0          -15.          0.0                    0.0
269          4
270          0.0          0.0           5.0          100.      10.0          200.
271          15.0         300.
272        2      SEAT CUSHION FORCE(KG)
273          0.0          -14.          0.0          1.0
274          8
275          0.0          0.0           2.0          20.       4.0           45.
276          6.0          80.           8.0          130.      10.0          200.
277          12.0         300.          14.0         450.
278        3          SEATBACK FORCE(KG)
279          0.0          -16.          0.0          1.0
280          8
281          0.0          0.0           1.0          7.5       2.            20.
282          3.           50.           4.           90.       6.            200.
283          10.          500.          16.          1000.
284        4          TOEBRD FORCE(KG)
285          0.0          -10.                       1.0
286          18
287          0.0          0.0           0.1          14.0      0.2           22.
288          0.3          40.           0.4          56.       0.5           74.
289          0.6          95.           0.7          115.      0.8           145.
290          1.0          150.          2.0          240.      3.0           300.
```

Add one card for additional column ellipsoid and three cards for additional wheel ellipsoids (D5).

Add one card for NSEG>18 (D7) and four cards for spring/dampers (D8).

Table 1. Listing of Baseline Unrestrained Occupant Data Set (Page 5 of 9).

```
291          4.0         350.          5.0         500.          6.0         900.
292          7.0        1300.          9.0        1650.         10.0        1800.
293        5          WNDSHLD R FUNCTION
294          0.0         -20.          0.0
295          4
296          0.0          1.0          2.0          0.5          9.0          0.25
297         20.           0.0
298        6          WNDSHLD G FUNCTION
299          0.0         -20.          0.0
300          4
301          0.0          0.0          2.0          .75          9.0          0.95
302         20.           0.95
303        8       MID I.P. LOADING(KG)
304          0.0         -20.          0.                        0.0
305          9
306          0.0          0.0          1.0         1200.         1.5         1620.
307          2.        1800.           2.5         1860.         3.0         1910.
308          4.        2010.           6.0         2055.        20.          2160.
309        9          CONSTANT F=0.40
310          0.0          0.0          0.40
311       10          CONSTANT F=0.1
312          0.0          0.0          0.1
313       11       UPP I.P. LOAD(KG)
314          0.0         -24.          0.0                       1.0
315          7
316          0.0          0.0          3.0          80.          6.          120.
317          9.         240.           12.         560.         18.         1150.
318         24.        1800.
319       12          CONSTANT F=0.9
320          0.0          0.0          0.9
321       13          TOEBRD F
322          0.0          0.           0.95
323       14          CONSTANT  F=0.67
324          0.0          0.0          0.67
325       15      UNLOADING G FUNCTION
326          0.0       -1000.          0.0
327          4
328          0.0          0.0          0.5          0.0          0.6          0.95
329       1000.           0.95
330       16      UNLOADING R FUNCTION
331          0.0       -1000.          0.0
332          4
333          0.0          1.0          0.5          1.0          0.6          0.05
334       1000.           0.05
335       17         WNDSHLD FORCE(KG)
336          0.0         -20.          0.0                       1.0
337         16
338          0.0          0.0          1.           70.          2.          110.
339          3.         145.           4.          170.          5.          182.
340          6.         188.           7.          190.          8.          189.
341          9.         176.          10.          166.         11.          153.
342         12.         130.          13.           90.         15.            0.
343         20.           0.
344       18         WSHLD  SPIKE(KG)
345          0.0         -2.5          0.0          1.5          1.0
346         13
347          0.0          0.0          0.4          60.          0.5          120.
348          0.7        160.           0.9         190.          1.0          200.
```

Table 1. Listing of Baseline Unrestrained Occupant Data Set (Page 6 of 9).

```
349          1.2        190.          1.4          160.          1.5          130.
350          1.7         80.          2.0           40.          2.2           20.
351          2.5          0.
352       19        LWR IP LOAD(KG)
353          0.0         -40.           0.0                       0.0
354       17
355          0.0          0.0           1.          200.           2.          320.
356          3.         390.           4.          420.           5.          450.
357          6.         465.           7.          485.           8.          495.
358         11.         525.          13.          550.          15.          600.
359         17.         700.          19.          900.          20.         1070.
360         21.        1300.          40.5       160000.
361       20        HEADER LOAD(KG)
362          0.0         -40.           0.0                       0.0
363          6
364          0.0          0.0          5.08          445.          7.62          980.
365         12.7        980.          20.3         2225.         40.5         16000.
366       21        TOEBRD G
367          0.0         -10.           0.0                       0.0
368          8
369          0.0          0.0           0.2          0.05           0.4          0.13
370         0.65         0.22           1.50         0.55          2.20          0.80
371          2.8         0.92          10.0          0.99
372       22        TOEBRD R
373          0.0         -10.           0.0                       0.0
374          8
375          0.0          0.0           0.2          0.47           0.4          0.37
376         0.65         0.31           1.50         0.26          2.20          0.24
377          2.8         0.22          10.0          0.01
378       23        WNDSHLD F
379          0.0         10.0
380         0.76         0.156           0.0
381       24        ROOFPAN F
382          0.0          0.0           0.80
383       25        SEAT F
384          0.0         10.0
385         0.30          0.1            0.0
386       26        BODY FORCES(KG)
387          0.0         -2.5           0.0                       1.0
388          6
389          0.0          0.0           0.4           4.          1.0           8.
390          1.5          16.           2.0          18.          2.5          30.
391       999
392        1   1   2   5   5   2   2   1   2   2   2   1   4   2   3   3   1
393        1   1   2   2   2
394        1  18   5   5  17  18   5   6  23
395        2  18   5   5  11      16  15  24
396        3  18   7   7  19   0  16  15  12
397        3  18  10  10  19   0  16  15  12
398        4  18   6   6  19   0  16  15  12
399        4  18   7   7  19   0  16  15   9
400        4  18   9   9  19   0  16  15   9
401        4  18  10  10  19      16  15   9
402        4  18   1   1   8      16  15  12
403        5  18   1   1   8   0  16  15  12
404        5  18   2   2   8   0  16  15  12
405        5  18   3   3   8   0  16  15  12
406        5  18  13  13  19      16  15  12
```

Table 1. Listing of Baseline Unrestrained Occupant Data Set (Page 7 of 9).

	407	5	18	15	15	19		16	15	12
	408	6	18	1	1	3	0	16	15	10
	409	6	18	2	2	3	0	16	15	10
	410	7	18	2	2	3	0	16	15	10
	411	7	18	3	3	3	0	16	15	14
	412	8	18	1	1	2		16	15	25
	413	9	18	8	8	4		22	21	13
	414	9	18	11	11	4	0	22	21	13
	415	10	18	8	8	4		22	21	13
*	416	10	18	11	11	4		22	21	13
*	417	11	18	5	5	11		16	15	10
	418	11	18	3	3	11		16	15	10
	419	12	18	5	5	1		16	15	10
	420	13	18	12	12	19		16	15	12
	421	13	18	14	14	19		16	15	12
	422	13	18	13	13	19		16	15	12
	423	13	18	15	15	19		16	15	12
	424	14	18	12	12	19		16	15	12
	425	14	18	14	14	19		16	15	12
	426	15	18	1	1	2		16	15	25
	427	15	18	6	6	2		16	15	25
	428	15	18	9	9	2		16	15	25
	429	16	18	1	1	2		16	15	25
	430	16	18	6	6	2		16	15	10
	431	16	18	9	9	2		16	15	10
	432	17	18	1	1	2		16	15	10
	433	19	18	5	5	10		16	15	24
	434	20	18	5	5	20		16	15	24
	435	21	18	6	6	19		16	15	24
	436	21	18	9	9	19		16	15	24
	437	22	18	17	17	19		16	15	10
	438	22	18	16	16	19		16	15	10
	439	23	18	16	16	26		16	15	10
	440	23	18	17	17	26		16	15	10
	441	2	2	4	0	0	1	0	0	1
	442	1	1	13	13	4		16	15	10
	443	1	1	15	15	4		16	15	10
	444	2	2	16	16	26		16	15	10
	445	2	2	17	17	26		16	15	10
*	446	3	3	13	13	4		16	15	10
	447	3	3	15	15	4		16	15	10
	448	3	3	16	16	26		16	15	10
	449	3	3	17	17	26		16	15	10
	450	6	6	16	16	26		16	15	12
	451	9	9	17	17	26		16	15	12
	452									
	453	10.0		30.0		1.0		15		
*	454	-308.71		0.0		-48.19				
	455	0.0		22.50		0.0				
	456	0.0		15.00		0.0				
	457	0.0		-2.00		0.0				
	458	0.0		-15.00		0.0				
	459	0.0		-15.0		0.0				
*	460	0.0		115.00		0.0				
*	461	0.0		35.000		0.0				
*	462	0.0		90.0		0.0				
*	463	0.0		115.00		0.0				
*	464	0.0		35.000		0.0				

→ Add two cards for position of column and wheel masses (G2).

Table 1. Listing of Baseline Unrestrained Occupant Data Set (Page 8 of 9).

Listing of GMCVS1.D at 16:20:49 on OCT 3, 1985 for CCId=SUVH Page 9

```
*465        0.0      90.0      0.0
 466         0.0       5.0      0.
 467        17.5      81.0      0.       0.0    0.0       0.0    3  2  1
 468         0.0       5.0      00.
 469       -17.5      81.0      0.                                 3  2  1
 470        17.5      81.0      0.                                 3  2  1
 471       -17.5      81.0      0.                                 3  2  1
*472        5   0
 473        1   3   1  40.0  15.0      8   1
 474        1   1   1   4.0  15.0      6   1
 475        2   2   3   4.0  10.0      7   3   4   1   2   4   5
 476        2   2   9  10.0  20.0     16   9   1   6
 477        2   2  10   4.0  30.0      9  11   1   7
1001
1001.1
1001.2      1  10  40  57  55   2  23  49  34  33  30
1002          6   1          0.0        0.0        0.0
1003              2
1004              3          0.0        0.0        0.0
1005              5
1006              7
1007             10
1008          0   0          0.0        0.0        0.0
1009          3   1          0.0        0.0        0.0
1010              5
1011              3
1012
1013
1014
1015
1016        4   3
1017
1018
1019
1020
```

Add two cards for angular orientation of column and wheel masses (G3).

Table 1. Listing of Baseline Unrestrained Occupant Data Set (Page 9 of 9).

Table 2. Force-Deflection Functions Retained from Baseline Data Set.

- seat cushion (kg)
- seat back force (kg)
- toeboard force (kg), renamed, toepan force (kg)
- windshield R function
- windshield G function
- constant F=0.40
- constant F=0.1
- upp I.P. load (kg), renamed, head/I.P. load (kgf)
- constant F=0.9
- toeboard F
- constant F=0.67
- underloading G function
- underloading R function
- windshield force (kg)
- windshield spike (kg)
- lower IP load (kg)
- toeboard G
- toeboard R
- windshield renamed windshield fric
- seat F
- body forces (kg) renamed I.P. (kgf)

```
02 FEB 1985                                                                          A.1.A
 GMCOL1. STEERING WHEEL SIMULATOR TEST.                                              A.1.B
                                                                                     A.1.C
CM. KG. SEC.O.          O.          980.665                                          A.3
   6 375.0004   .0001   .0004   .0001                                                A.4
 0 0 5 1 0 0 0 0 0 0 0 0 0 0 0 0 0 0 1                                               A.5
    19    18                                                                         B.1
  LT 517.331 2.479 2.479 1.468 12.00 12.50 18.50  1.70 0.000 -.350                   B.2.A
  CT 4 5.760 .3650 .3650 .2790 11.00 11.00 14.00 6.660 0.000 0.000                   B.2.B
  UT 317.227 2.504 2.504 2.170 12.75 12.75 15.00 3.610 0.000 0.000                   B.2.C
   N 2 1.545 0.060 0.060 0.006  4.30  4.30  7.00 1.670 .0000 0.000                   B.2.D
   H 1 4.545 .2190 .2060 .2060  7.75  7.75 11.00 1.500 .0000 0.000                   B.2.E
 LUL A 6.091 .6860 .6860 .1310  7.50  7.50 23.10 -0.94 .0000 .0000                   B.2.F
 LLL B 3.300 .7650 .7650 .0970  5.75  5.75 23.70 -4.22 .0000 .0000                   B.2.G
  LF C 1.227 .0550 .0550 .0150  3.    3.    9.00 .0000 .0000 .0000                   B.2.H
 RUL D 6.091 .6860 .6860 .1310  7.50  7.50 23.10 -0.94 .0000 .0000                   B.2.I
 RLL E 3.300 .7650 .7650 .097   5.75  5.75 23.70 -4.22 .0000 .0000                   B.2.J
  RF F 1.227 .0550 .0550 .0150  3.    3.    9.00 .0000 .0000 .0000                   B.2.K
 LUA 6 2.000 .1160 .1160 .0250  4.50  4.50 13.00 .0000 .0000 .0000                   B.2.L
 LLA 7 2.273 .3600 .3600 .0320  4.25  4.25 20.80  1.15 .0000 .0000                   B.2.M
 RUA 8 2.000 .1160 .1160 .0250  4.50  4.50 13.00 .0000 .0000 .0000                   B.2.N
 RLA 9 2.273 .3600 .3600 .0320  4.25  4.25 20.80  1.15 .0000 .0000                   B.2.O
  LH N 0.800 .0115 .0115 .0012  5.50  3.05  9.00  .000 .000  .0000                   B.2.P
  RH M 0.80  .0115 .0115 .0012  5.5   3.05  9.00  .000 .0000 .0000                   B.2.Q
MCOL C 7.442 .0237 2.286 2.286  1.49  1.49  1.49 15.00 0.000 0.000                   B.2.R
MWHL W 1.49  .4547 .2281 .2281  1.25 18.50 18.50  0.00 0.000 0.000                   B.2.S
   P O    1  -2-4.25 0.    -4.32 0.    0.    6.53                                          B.3.A1
               0.    0.     0.   0.    0.    0.                                            B.3.A2
   W P    2  -2-1.6  0.    -6.48 0.    0.    13.93                                         B.3.B1
               0.    0.     0.   0.    0.    0.                                            B.3.B2
  NP Q    3  -2-2.54 0.    -15.590.    0.    0.                                            B.3.C1
               0.    0.     0.   0.    0.    0.                                            B.3.C2
  HP R    4  -20.    0.    -9.59 0.    0.    4.78                                          B.3.D1
               0.    0.     0.   0.    0.    0.                                            B.3.D2
  LH W    1  -4-2.45 -8.85 2.57  0.    0.    -23.99                                        B.3.E1
             -90.    90.    0.   0.    4.76  0.    27.    -70.  0.                         B.3.E2
  LK X    6   10.    0.    16.18 0.    0.    -16.36                                        B.3.F1
               0.    0.     0.   0.    43.0  0.                                            B.3.F2
  LA G    7  -4-.25  0.    22.04 5.36  0.    -4.09                                         B.3.G1
              90.    0.    0.    90.   0.    0.    0.     79.   0.                         B.3.G2
  RH Y    1  -4-2.45 8.85  2.57  0.    0.    -23.99                                        B.3.H1
              90.    90.    0.   0.    4.76  0.    -27.   70.   0.                         B.3.H2
  RK Z    9   10.    0.    16.18 0.    0.    -16.36                                        B.3.I1
               0.    0.     0.   0.    43.   0.                                            B.3.I2
  RA H   10  -4-.25  0.    22.04 5.36  0.    -4.09                                         B.3.J1
              90.    0.     0.   90.   0.    0.    0.     79.   0.                         B.3.J2
  LS S    3  -40.45  -18.  -14.590.    0.    -13.06                                        B.3.K1
               0.    0.    90.   0.    0.    0.    -55.   -65.  0.                         B.3.K2
  LE T   12  -40.    0.    13.07 0.    0.    -15.11                                        B.3.L1
              90.    0.     0.   90.   0.    0.    8.     70.   0.                         B.3.L2
  RS U    3  -40.45  18.   -14.590.    0.    -13.06                                        B.3.M1
               0.    0.    -90.  0.    0.    0.    55.    65.   0.                         B.3.M2
  RE V   14  -40.    0.    13.07 0.    0.    -15.11                                        B.3.N1
              90.    0.     0.   90.   0.    0.    -8.    70.   0.                         B.3.N2
  LW J   13   10.    0.    10.2  0.    0.    -5.11                                         B.3.O1
               0.    0.     0.   0.    -10.  0.                                            B.3.O2
  RW K-  15   10.    0.    10.2  0.    0.    -5.11                                         B.3.P1
               0.    0.     0.   0.    -10.  0.                                            B.3.P2
```

Table 3. Listing of Final Data Set Including Energy-Absorbing Column (Page 1 of 11).

59				0.	0.	0.	0.	0.	0.				B.3.Q1
60													B.3.Q2
61				0.	0.	0.	0.	0.	0.				B.3.R1
62													B.3.R2
63	115.8	0.	0.2	0.5	90.		115.8	0.	0.2	0.5	70.0		B.4.A
64	115.8	0.	0.2	0.5	90.		115.8	0.	0.2	0.5	70.		B.4.B
65	30.	.108	0.	0.5	60.		150.	.108	0.	0.5	60.		B.4.C
66	30.	.108	0.	0.5	60.		150.	.108	0.	0.5	60.		B.4.D
67	6.	.25	0.	0.5	10.		2.972	.1088	0.	0.5	100.		B.4.E1
68	16.	160.	160.	0.5	60.		0.	0.	0.	0.	0.		B.4.E2
69	0.	10.	10.	0.95	45.		0.	0.	0.	0.95	0.		B.4.F
70	1.	10.	10.	0.95	50.		1.	10.	10.	0.95	42.		B.4.G1
71	0.	0.	0.	0.	0.		0.	0.	0.	0.	0.		B.4.G2
72	6.	.25	0.	0.5	10.		2.972	.1088	0.	0.5	100.		B.4.H1
73	16.	160.	160.	0.5	60.		0.	0.	0.	0.	0.		B.4.H2
74	0.	10.	10.	0.95	45.		0.	0.	0.	0.95	0.		B.4.I
75	1.	10.	10.	0.95	50.		1.	10.	10.	0.95	42.		B.4.J1
76	0.	0.	0.	0.	0.		0.	0.	0.	0.	0.		B.4.J2
77	14.	0.	0.	.5	125.		14.	0.	0.	.5	60.		LS1
78	0.	0.	0.	0.	0.		0.	0.	0.	0.	0.		B.4.K2
79	14.	20.	0.	.5	45.		14.	0.	0.	.5	70.		LE1
80	0.	0.	0.	0.	0.		0.	0.	0.	0.	0.		B.4.L2
81	14.	0.	0.	.5	125.		14.	0.	0.	.5	60.		RS1
82	0.	0.	0.	0.	0.		0.	0.	0.	0.	0.		B.4.M2
83	14.	20.	0.	.5	45.		14.	0.	0.	.5	70.		RE1
84	0.	0.	0.	0.	0.		0.	0.	0.	0.	0.		B.4.N2
85	14.	20.	0.	.5	60.		14.	20.	0.	.5	60.		LW
86	14.	20.	0.	.5	60.		14.	20.	0.	.5	60.		RW
87													B.4.Q
88													B.4.R
89	1.4	1000.	200.	174.5	0.				0.	0.			B.5.A
90	1.4	1000.	200.	105.0	0.				0.	0.			B.5.B
91	.2	20.	200.	174.5	0.				0.	0.			B.5.C
92	.2	20.	200.	180.9	0.				0.	0.			B.5.D
93	1.2	500.	200.	180.9	0.				0.	0.			B.5.E
94	1.2	500.	200.	180.9	0.				0.	0.			B.5.F
95	1.2	500.	200.	180.9	0.				0.	0.			B.5.G
96	1.2	125.	10.	15.4	0.				0.	0.			B.5.H
97	.6	20.	10.	30.	0.				0.	0.			B.5.I
98	.6	20.	10.	30.	0.				0.	0.			B.5.J
99	0.	0.	10.	0.	0.				0.	0.			B.5.K
100	1.2	500.	200.	180.9	0.				0.	0.			B.5.L
101	1.2	500.	200.	180.9	0.				0.	0.			B.5.M
102	1.2	500.	200.	180.9	0.				0.	0.			B.5.N
103	1.2	125.	10.	15.4	0.				0.	0.			B.5.O
104	.6	20.	10.	30.	0.				0.	0.			B.5.P
105	.6	20.	10.	30.	0.				0.	0.			B.5.Q
106	0.	0.	10.	0.	0.				0.	0.			B.5.R
107	.1	125.	400.	65.	0.				0.	0.			B.5.S
108	.1	50.	400.	65.	0.				0.	0.			B.5.T
109	0.	0.	400.	0.	0.				0.	0.			B.5.U
110	.1	175.	100.	60.	0.				0.	0.			B.5.V
111	.1	175.	100.	60.	0.				0.	0.			B.5.W
112	0.	0.	100.	0.	0.				0.	0.			B.5.X
113	.1	125.	400.	65.	0.				0.	0.			B.5.Y
114	.1	50.	400.	65.	0.				0.	0.			B.5.Z
115	0.	0.	400.	0.	0.				0.	0.			B.5.AA
116	.1	175.	100.	60.	0.				0.	0.			B.5.AB

Table 3. Listing of Final Data Set Including Energy-Absorbing Column (Page 2 of 11).

```
117     .1    175.   100.   60.    0.                          0.     0.                  B.5.AC
118     0.    0.     100.   0.     0.                          0.     0.                  B.5.AD
119     .1    50.    100.   25.    0.                          0.      0.                 B.5.AE
120     .1    50.    100.   25.    0.                          0.      0.                 B.5.AF
121                                                                                       B.5.AG
122                                                                                       B.5.AH
123                                                 00.1 00.10 00.10 00.01  00.01  00.01B.6
124                                                 00.1 00.10  00.1                       B.6
125                                                 00.1 00.10 00.10                      B.6
126                                                 00.1 00.10 00.10                      B.6
127                                                 00.1 00.10 00.10                      B.6
128                                                 00.1 00.10 00.10                      B.6
129                                                 00.1 00.10 00.10                      B.6
130                                                 00.1 00.10 00.10                      B.6
131                                                 00.1 00.10 00.10                      B.6
132                                                 00.1 00.10 00.10                      B.6
133                                                 00.1 00.10 00.10                      B.6
134                                                 00.1 00.10 00.10                      B.6
135                                                 00.1 00.1  00.1                       B.6
136                                                 00.1 00.1  00.1                       B.6
137                                                 00.1 00.1  00.1                       B.6
138                                                 00.1 00.1  00.1                       B.6
139                                                 00.1 00.1  00.1                       B.6
140                                                 00.1 00.10 00.10 00.01  00.01  00.01B.6
141                                                 00.1 00.10 00.10 00.01  00.01  00.01B.6
142   FRONT BARRIER PULSE   PRIMARY VEHICLE MOTION                                        C.1.A
143   0.    0.    0.    1361. 0.    0.    0.    0.       210.    .01   0                 C.2.A
144   0.    8.7   19.9  26.   28.   25.1  21.5  17.1  12.7  3.5   -1.7  0.            C.3
145   0.    0.    0.    0.    0.    0.    0.    0.    0.                                C.3
146       25    0     0     4     0     4                                               D.1
147     1    FLOORPAN                                                                  D.2.1A
148   96.8        50.          19.                                                     D.2.1B
149   96.8        -50.         19.                                                     D.2.1C
150   -13.2       50.          19.                                                     D.2.1D
151     2    TOEPAN                                                                    D.2.2A
152   123.1       -50.         -26.3                                                   D.2.2B
153   86.8        -50.         23.7                                                    D.2.2C
154   123.1       50.          -26.3                                                   D.2.2D
155     3    KNEE RESTRAINT                                                            D.2.3A
156   51.4        -50.         -31.3                                                   D.2.3B
157   70.         -50.          3.7                                                    D.2.3C
158   51.4        50.          -31.3                                                   D.2.3D
159     4    WINDSHIELD                                                                 D.2.4A
160   36.8        -50.         -114.6                                                  D.2.4B
161   66.8        -50.         -47.2                                                   D.2.4C
162   36.8        50.          -114.6                                                  D.2.4D
163     5    HEAD RESTRAINT                                                            D.2.5A
164   51.8        50.          -50.1                                                   D.2.5B
165   106.8       50.          -42.9                                                   D.2.5C
166   51.8        -50.         -50.1                                                   D.2.5D
167     6    INSTRUMENT PANEL                                                          D.2.6A
168   56.5        -50.         -56.3                                                   D.2.6B
169   56.5        -50.         -26.3                                                   D.2.6C
170   56.5        50.          -56.3                                                   D.2.6D
171     7    SB1                                                                       D.2.7A
172   -13.71      50.          -13.97                                                  D.2.7B
173   -5.21       50.          3.43                                                    D.2.7C
174   -13.71      -50.         -13.97                                                  D.2.7D
```

Table 3. Listing of Final Data Set Including Energy-Absorbing Column (Page 3 of 11).

```
175        8     SB2
176    -20.81          50.          -41.87
177    -13.71          50.          -13.97
178    -20.81         -50.          -41.87
179        9     SC1
180    -5.91           50.           7.13
181    9.09            50.           7.13
182    -5.91          -50.           7.13
183       10     SC2
184    9.09            50.           7.13
185    19.09           50.           2.73
186    9.09           -50.           7.13
187       11     SC3
188    19.09           50.          2.73
189    34.09           50.          2.73
190    19.09          -50.          2.73
191       12     SC4
192    34.09           50.          2.73
193    41.19           50.          7.13
194    34.09          -50.          2.73
195       13     COLEAT
196    102.889594      3.          -19.776993
197    34.823699       3.0         -36.108169
198    102.889594     -3.          -19.776993
199       14     COLEAB
200    102.889594      3.          -16.681747
201    102.889594     -3.          -16.681747
202    34.823699       3.          -33.022923
203       15     COLEAR
204    102.09          1.5         -14.79
205    34.03           1.5         -31.16
206    103.73          1.5         -21.67
207       16     COLEAL
208    102.09         -1.5         -14.79
209    103.73         -1.5         -21.67
210    34.03          -1.5         -31.16
211       17     BOTOUT
212    89.567743      -5.          -16.280587
213    89.567743       5.          -16.280587
214    91.902197      -5.          -26.004287
215       18     COLT
216    -28.75         -22.         -18.5
217    -28.75          22.         -18.5
218    -41.75         -22.         -18.5
219       19     COLB
220    -28.75          22.          18.5
221    -28.75         -22.          18.5
222    -41.75          22.          18.5
223       20     COLR
224    -28.75          18.5         22.
225    -41.75          18.5         22.
226    -28.75          18.5        -22.
227       21     COLL
228    -41.75         -18.5         22.
229    -28.75         -18.5         22.
230    -41.75         -18.5        -22.
231       22     COLA
232    -40.            22.          22.
```

```
D.2.8A
D.2.8B
D.2.8C
D.2.8D
D.2.9A
D.2.9B
D.2.9C
D.2.9D
D.2.10A
D.2.10B
D.2.10C
D.2.10D
D.2.11A
D.2.11B
D.2.11C
D.2.11D
D.2.12A
D.2.12B
D.2.12C
D.2.12D
D.2.13A
  D2
D.2.13C
  D2
D.2.14A
  D2
  D2
  D2
D.2.15A
  D2
  D2
  D2
D.2
  D2
  D2
  D2
D.2
D.2
D.2
D.2
D.2
D.2
D.2
D.2
D.2
D.2
D.2
D.2
D.2
D.2
D.2
D.2
D.2
D.2
D.2
D.2
D.2
D.2
D.2
D.2
D.2
```

Table 3. Listing of Final Data Set Including Energy-Absorbing Column (Page 4 of 11).

```
233     -40.          -22.          22.                                                                  D.2
234     -40.          22.           -22.                                                                 D.2
235       23    COLP                                                                                     D.2
236     -37.5         -22.          22.                                                                  D.2
237     -37.5         22.           22.                                                                  D.2
238     -37.5         -22.          -22.                                                                 D.2
239       24    HUB                                                                                      D.2
240     -36.          -18.5         18.5                                                                 D.2
241     -36.          18.5          18.5                                                                 D.2
242     -36.          -18.5         -18.5                                                                D.2
242.2     25    KNEE RESTRAINT                                                                           D.2.3A
242.4   51.4          -50.          -31.3                                                                D.2.3B
242.6   70.           -50.          3.7                                                                  D.2.3C
242.8   51.4          50.           -31.3                                                                D.2.3D
243         211.49  1.49  1.49  -10.  0.    0.    0.    0.    0.                                       D.5
244         221.24  1.24  1.24  0.    0.    -17.250.    0.    0.                                       D.5
245         231.24  1.24  1.24  0.    -17.2517.25 0.    0.    0.                                       D.5
246         241.24  1.24  1.24  0.    17.25 17.25 0.    0.    0.                                       D.5
247                                                                                                    D.7
248                                                                                                    D.7
248.1   18 200.     0.    0.    54.2710.    -29.91-10.      33    00.   0.      D8
248.2   19 180.     0.    -17.25-40.  0.    -17.25-1.25     34    00.   0.      D8
248.3   19 180.     -17.2517.25 -40.  -17.2517.25 -1.25     35    00.   0.      D8
248.4   19 180.     17.25 17.25 -40.  17.25 17.25 -1.25     35    00.   0.      D8
249       1     SEAT CUSION FORCE(KG)                                                                  E.1
250   0.              -14.          0.          1.                                                     E.2
251         6                                                                                          E.4
252   0.              0.            2.          20.         4.          45.                            E.4
253   6.              80.           8.          130.        10.         200.                           E.4
254   12.             300.          14.         450.                                                   E.4
255       2     SEATBACK FORCE(KG)                                                                     E.1
256   0.              -16.          0.          1.                                                     E.2
257         8                                                                                          E.4
258   0.              0.            1.          7.5         2.          20.                            E.4
259   3.              50.           4.          90.         6.          200.                           E.4
260   10.             500.          16.         1000.                                                  E.4
261       3     TOEPAN FORCE (KG)                                                                      E.1
262   0.              -10.          0.          1.                                                     E.2
263         18                                                                                         E.4
264   0.              0.            0.1         14.         0.2         22.                            E.4
265   0.3             40.           0.4         56.         0.5         74.                            E.4
266   0.6             95.           0.7         115.        0.8         145.                           E.4
267   1.              150.          2.0         240.        3.          300.                           E.4
268   4.              350.          5.          500.        6.          900.                           E.4
269   7.              1300.         9.          1650.       10.         1800.                          E.4
270       4     WNDSHLD R FUNCTION                                                                     E.1
271   0.              -20.          0.                                                                 E.2
272         4                                                                                          E.4
273   0.              1.            2.          0.5         9.          0.25                           E.4
274   20.             0.                                                                               E.4
275       5     WNDSHLD G FUNCTION                                                                     E.1
276   0.              -20.          0.                                                                 E.2
277         4                                                                                          E.4
278   0.              0.            2.          .75         9.          0.95                           E.4
279   20.             0.95                                                                             E.4
280       6     CONSTANT F=0.4                                                                         E.1
281   0.              0.            0.4                                                                E.2
282       7     CONSTANT F=0.05                                                                        E.1
```

Table 3. Listing of Final Data Set Including Energy-Absorbing Column (Page 5 of 11).

```
283     0.          0.          0.05                                        E.2
284        8    HEAD/IP LOAD (KGF)                                         E.1
285     0.          -24.        0.                    1.                    E.2
286           7                                                            E.4
287     0.          0.          3.          80.       6.          120.      E.4
288     9.          240.        12.         560.      18.         1150.     E.4
289     24.         1800.                                                  E.4
290        9    CONSTANT F=0.9                                             E.1
291     0.          0.          0.9                                        E.2
292       10    TOEBRD F                                                   E.1
293     0.          0.          0.95                                       E.2
294       11    CONSTANT F=0.67                                            E.1
295     0.          0.          0.67                                       E.2
296       12    UNLOADING G FUNCTION                                       E.1
297     0.          -1000.      0.                                         E.2
298           4                                                            E.4
299     0.          0.          0.5         0.        0.6         0.95      E.4
300     1000.       0.05                                                   E.4
301       13    UNLOADING R FUNCTION                                       E.1
302     0.          -1000.      0.                                         E.2
303           4                                                            E.4
304     0.          1.          0.5         1.        0.6         0.05      E.4
305     1000.       0.05                                                   E.4
306       14    WNDSHLD FORCE (KG)                                         E.1
307     0.          -20.        0.                    1.                    E.2
308             16                                                         E.4
309     0.          0.          1.          70.       2.          110.      E.4
310     3.          145.        4.          170.      5.          182.      E.4
311     6.          188.        7.          190.      8.          189.      E.4
312     9.          176.        10.         166.      11.         153.      E.4
313     12.         130.        13.         90.       15.         0.        E.4
314     20.         0.                                                     E.4
315       15    WSHLD SPIKE (KG)                                           E.1
316     0.          -2.5        0.          1.5       1.                    E.2
317           13                                                           E.4
318     0.          0.          0.4         60.       0.5         120.      E.4
319     0.7         160.        0.9         190.      1.          200.      E.4
320     1.2         190.        1.4         160.      1.5         130.      E.4
321     1.7         80.         2.0         40.       2.2         20.       E.4
322     2.5         0.                                                     E.4
323       16    LWR IP LOAD (KG)                                           E.1
324     0.          -40.        0.                    0.                    E.2
325             17                                                         E.4
326     0.          0.          1.          200.      2.          320.      E.4
327     3.          390.        4.          420.      5.          450.      E.4
328     6.          465.        7.          485.      8.          495.      E.4
329     11.         525.        13.         550.      15.         600.      E.4
330     17.         700.        19.         900.      20.         1070.     E.4
331     21.         1300.       40.5        160000.                         E.4
332       17    TOEBRD G                                                   E.1
333     0.          -10.        0.                    0.                    E.2
334           8                                                            E.4
335     0.          0.          0.2         0.05      0.4         0.13      E.4
336     0.65        0.22        1.5         0.55      2.2         0.8       E.4
337     2.8         0.92        10.         0.99                            E.4
338       18    TOEBRD R                                                   E.1
339     0.          -10.        0.                    0.                    E.2
340           8                                                            E.4
```

Table 3. Listing of Final Data Set Including Energy-Absorbing Column (Page 6 of 11).

```
341     0.          0.          0.2         0.47        0.4         0.37        E.4
342     0.65        0.31        1.5         0.26        2.2         0.24        E.4
343     2.8         0.22        10.         0.01                                E.4
344       19    WNDSHLD FRIC                                                    E.1
345     0.          10.                                                         E.2
346     0.76        0.156       0.                                              E.3
347       20    SEAT F                                                          E.1
348     0.          10.                                                         E.2
349     0.3         0.1         0.                                              E.3
350       21    MID I.P. (KGF)                                                  E.1
351     0.          -2.5        0.                      1.                      E.2
352           6                                                                 E.4
353     0.          0.          0.4         4.          1.          8.          E.4
354     1.5         16.         2.0         18.         2.5         30.         E.4
355       22    CHESTST                                                         E.1
356     0.          -7.         0.                                              E.2
357           5                                                                 E.4
358     0.          0.          1.          541.        2.2         892.        E.4
359     4.          1243.       7.          1541.                               E.4
360       23    CHEST G                                                         E.1
361     0.          -7.         0.                                              E.2
362           5                                                                 E.4
363     0.          0.          1.          0.2         2.2         0.275       E.4
364     4.          0.270       7.          0.357                               E.4
365       24    CHEST R                                                         E.1
366     0.          -7.         0.                                              E.2
367           5                                                                 E.4
368     0.          0.          1.          0.48        2.2         0.356       E.4
369     4.          0.352       7.          0.218                               E.4
370       25    COLUMN EA                                                       E.1
371     0.          -20.        0.                                              E.2
372           4                                                                 E.4
373     0.          0.          1.          1000.       2.          2500.         E4
374     3.          8900.                                                       E4
375       26    COLUMN G                                                      E.1
376     0.          0.          0.01                                          E.2
377       27    COLUMN R                                                      E.1
378     0.          0.          0.99                                          E.2
379       28    HUB  FD                                                       E.1
380     0.          -20.        0.                                            E.2
381           5                                                               E.4
382     0.          0.          1.          500.        2.          1000.         E4
383     4.          4000.       5.          10000.                            E4
384       29    HUB G                                                       E.1
385     0.          0.          0.95                                        E.2
386       30    HUB R                                                       E.1
387     0.          0.          0.01                                        E.2
388       31    BOTOUT FD                                                   E.1
389     0.          100.                    0.                              E.2
390     0.          800.        0.                                          E.3
390.1     32    CONST. F=0.                                                   E1
390.11  0.          0.          0.                                            E2
390.2     33    COL.SP.DAMP.                                                  E1
390.21  0.          -20.        0.                                            E2
390.22        4                                                               E4
390.23  0.          0.          .5          815.7       12.5        815.7       E4
390.24  20.         4000.                                                     E4
390.3     34    WHL.SP.DAMP.TOP                                               E1
```

Table 3. Listing of Final Data Set Including Energy-Absorbing Column (Page 7 of 11).

```
390.31  0.          -15.          0.                                                    E2
390.32       6                                                                        E4
390.33  0.          0.            .8          398.          1.5          398.        E4
390.34  5.5         143.          9.1         143.          15.          1020.       E4
390.4     35    WHL.SP.DAMP.BOT.                                                      E1
390.41  0.          -15.          0.                                                    E2
390.42       6                                                                        E4
390.43  0.          0.            .8          199.          1.5          199.        E4
390.44  5.5         71.5          9.1         71.5          15.          510.        E4
390.5     36    ABDOMEN FD                                                            E1
390.51  0.          -14.          0.                                                    E2
390.511      5                                                                        E4
390.52  0.          0.            2.          541.          4.4          892.          E4
390.53  8.          1243.         14.         1541.                                   E4
390.57    37    LWR IP LOAD (KG)                                                    E.1
390.61  0.          -40.          0.                        0.                        E.2
390.65       17                                                                     E.4
390.69  0.          0.            1.          20.           2.           50.         E4
390.73  3.          100.          4.          200.          5.           300.        E4
390.77  6.          400.           7.         485.          8.           495.      E.4
390.81  11.         525.          13.         550.          15.          600.      E.4
390.85  17.         700.          19.         900.          20.          1070.     E.4
390.89  21.         1300.         40.5        160000.                               E.4
391      999                                                                       E.4
392        2   2   4   1,  1   4   2   2   2   3   3   1   2   2   2   2   1   3F.1
393        3   3   3   3   0   2   4                                             F.1
394        1  20   8   8   3       18  17  10                                    F.1
395        1  20  11  11   3       18  17  10                                    F.1
396        2  20   8   8   3       18  17  10                                    F.1
397        2  20  11  11   3       18  17  10                                    F.1
398        3  20   6   6  16       13  12   6                                    F.1
399        3  20   7   7  16       13  12   6                                    F.1
400        3  20   9   9  16       13  12   6                                    F.1
401        3  20  10  10  16       13  12   6                                    F.1
402        4  20   5   5  14  15    4   6  19                                    F.1
403        5  20   5   5   8       13  12   7                                    F.1
404        6  20  13  13  37       13  12   9                                    F.1
405        6  20  15  15  37       13  12   9                                    F.1
406        6  20  16  16  37   0   13  12   7                                    F.1
407        6  20  17  17  37       13  12   7                                    F.1
408        7  20   1   1   2       13  12   7                                    F.1
409        7  20   2   2   2       13  12   7                                    F.1
410        8  20   2   2   2       13  12   7                                    F.1
411        8  20   3   3   2       13  12   7                                    F.1
412        9  20   1   1   1       13  12   7                                    F.1
413        9  20   2   2   1       13  12   7                                    F.1
414       10  20   1   1   1       13  12  20                                    F.1
415       10  20   6   6   1       13  12  20                                    F.1
416       10  20   9   9   1       13  12  20                                    F.1
417       11  20   1   1   1       13  12   7                                    F.1
418       11  20   6   6   1       13  12   7                                    F.1
419       11  20   9   9   1       13  12   7                                    F.1
420       12  20   1   1   1       13  12   7                                    F.1
421       13  20  18  18  25       30  29  32                                    F.1
422       13  20  18  21  25       30  29  32                                    F.1
423       14  20  18  18  25       30  29  32                                     F.1
424       14  20  18  21  25       30  29  32                                    F.1
425       15  20  18  18  25       30  29  32                                    F.1
```

Table 3. Listing of Final Data Set Including Energy-Absorbing Column (Page 8 of 11).

```
426      15  20  18  21  25      30  29  32                    F.1
427      16  20  18  18  25      30  29  32                    F.1
428      16  20  18  21  25      30  29  32                    F.1
429      17  20  18  18  31      13  12  32                    F.1
430      18  18  19  22  28      30  29  32                    F.1
431      18  18  19  23  28      30  29  32                    F.1
432      18  18  19  24  28      30  29  32                    F.1
433      19  18  19  22  28      30  29  32                    F.1
434      19  18  19  23  28      30  29  32                    F.1
435      19  18  19  24  28      30  29  32                    F.1
436      20  18  19  22  28      30  29  32                    F.1
437      20  18  19  23  28      30  29  32                    F.1
438      20  18  19  24  28      30  29  32                    F.1
439      21  18  19  22  28      30  29  32                    F.1
440      21  18  19  23  28      30  29  32                    F.1
441      21  18  19  24  28      30  29  32                    F.1
442      22  18  19  22  28      30  29  32                    F.1
443      22  18  19  23  28      30  29  32                    F.1
444      22  18  19  24  28      30  29  32                    F.1
448      24  18   2   2  28      30  29   7                    F.1
449      24  18   3   3  28      30  29   7                    F.1
449.01   25  20  13  13  37      13  12   7                      F1
449.02   25  20  15  15  37      13  12   7                      F1
449.1    25  20  16  16  37      13  12   7                      F1
449.2    25  20  17  17  37      13  12   7                      F1
450       2   3   5   1   1   0   0   0   0                    F.3
451                                                            F.3
452       1   1  13  13   3      13  12   7                    F.3
453       1   1  15  15   3      13  12   7                    F.3
454       2   2  16  16  21      13  12   7                    F.3
455       2   2  17  17  21      13  12   7                    F.3
456       2   2  19  19  36      24  23   9                    F.3
457       3   3  13  13   3      13  12   7                    F.3
458       3   3  15  15   3      13  12   7                    F.3
459       3   3  16  16  21      13  12   7                    F.1
460       3   3  17  17  21      13  12   7                    F.1
461       3   3  19  19  22      24  23   9                    F.1
462       4   4  19  19  22      24  23   9                    F.1
463       5   5  19  19  22      24  23   9                    F.1
464                                                            F.4
465   10.         30.         1.                               G.1
466   1.38        0.          -3.34                            G.2
467   63.994797   0.          -27.562185                       G.2
468   26.315462   0.          -36.608193                       G.2
469   0.          22.5        0.                               G.3
470   0.          15.         0.                               G.3
471   0.          -2.         0.                               G.3
472   0.          -15.        0.                               G.3
473   0.          -15.        0.                               G.3
474   0.          103.822     0.                               G.3
475   0.          57.         0.                               G.3
476   0.          144.        0.                               G.3
477   0.          103.822     0.                               G.3
478   0.          57.         0.                               G.3
479   0.          144.        0.                               G.3
480   0.          5.          0.                               G.3
481   17.5        81.         0.                3  2  1       G.3
482   0.          5.          0.                               G.3
```

Table 3. Listing of Final Data Set Including Energy-Absorbing Column (Page 9 of 11).

```
 483    -17.5      81.       0.                                  3  2  1   G.3
 484     17.5      81.       0.                                  3  2  1   G.3
 485    -17.5      81.       0.                                  3  2  1   G.3
 486     0.       -13.5      0.                                              G.3
 487     0.       -13.5      0.                                              G.3
1000
1001     0.        150.      0.          0                                     HO2
1002        1  2   3   4   5   6   7   8   9  12                             HO2
1003                                                                         H.0.3
1004           19  0  10.          0.          0.                           H.1.A
1005               0  20.          0.          0.                           H.1.B
1006               0  30.          0.          0.                           H.1
1007               0  40.          0.          0.                           H.1
1008               0  50.          0.          0.                           H.1
1009               0  60.          0.          0.                           H.1
1010               0  70.          0.          0.                           H.1
1011               0  80.          0.          0.                           H.1
1012               0  90.          0.          0.                           H.1
1013               0 100.          0.          0.                           H.1
1014               0 110.          0.          0.                           H.1
1015               0 120.          0.          0.                           H.1
1016               0 130.          0.          0.                           H.1
1017               0 140.          0.          0.                           H.1
1018               0 150.          0.          0.                           H.1
1019               0 160.          0.          0.                           H.1
1020               0 170.          0.          0.                           H.1
1021               0 180.          0.          0.                           H.1
1022               0 190.          0.          0.                           H.1
1023           19  0  10.          0.          0.                           H.2.A
1024               0  20.          0.          0.                           H.2.B
1025               0  30.          0.          0.                           H.2
1026               0  40.          0.          0.                           H.2
1027               0  50.          0.          0.                           H.2
1028               0  60.          0.          0.                           H.2
1029               0  70.          0.          0.                           H.2
1030               0  80.          0.          0.                           H.2
1031               0  90.          0.          0.                           H.2
1032               0 100.          0.          0.                           H.2
1033               0 110.          0.          0.                           H.2
1034               0 120.          0.          0.                           H.2
1035               0 130.          0.          0.                           H.2
1036               0 140.          0.          0.                           H.2
1037               0 150.          0.          0.                           H.2
1038               0 160.          0.          0.                           H.2
1039               0 170.          0.          0.                           H.2
1040               0 180.          0.          0.                           H.2
1041               0 190.          0.          0.                           H.2
1042           19  0  10.          0.          0.                           H.3.A
1043               0  20.          0.          0.                           H.3.B
1044               0  30.          0.          0.                           H.3
1045               0  40.          0.          0.                           H.3
1046               0  50.          0.          0.                           H.3
1047               0  60.          0.          0.                           H.3
1048               0  70.          0.          0.                           H.3
1049               0  80.          0.          0.                           H.3
1050               0  90.          0.          0.                           H.3
1051               0 100.          0.          0.                           H.3
1052               0 110.          0.          0.                           H.3
```

Table 3. Listing of Final Data Set Including Energy-Absorbing Column (Page 10 of 11).

```
1053              0 120.          0.          0.                              H.3
1054              0 130.          0.          0.                              H.3
1055              0 140.          0.          0.                              H.3
1056              0 150.          0.          0.                              H.3
1057              0 160.          0.          0.                              H.3
1058              0 170.          0.          0.                              H.3
1059              0 180.          0.          0.                              H.3
1060              0 190.          0.          0.                              H.3
1061         19    1    2    3    4    5    6    7    8    9   10          11H.4
1062              12   13   14   15   16   17   18   19                       H.4
1063         19    1    2    3    4    5    6    7    8    9   10          11H.5
1064              12   13   14   15   16   17   18   19                       H.5
1065         19    1    2    3    4    5    6    7    8    9   10          11H.6
1066              12   13   14   15   16   17   18   19                       H.6
1067         16    1    2    3    4    5    6    7    8    9   10          11H.7
1068              12   13   14   15   16                                      H.7
1069       5   3                                                            H.8
2001    0 1 1 1 0 1 1 0
2002  0.       .15      .01
2003  0.       0.       0.
2004  1.       0.       0.
2005  0.       1.       0.
2006  0.       0.       1.
2007  1.       0.       0.
2008  0.       1.       0.
2009  0.       0.       -1.
2010  .5       .5       11.      8.5
2011  .5       .5       10.      7.
2012  -30.     -32.     160.     112.     .3
2013  GMCOL1.  XZ
2014  0.       -1.      0.
2015  1.       0.       0.
2016  0.       0.       1.
2017  .5       9.       11.      8.5
2018  .5       .5       10.      7.
2019  -80.     -80.     160.     112.     .3
2020  GMCOL1.  YZ
2021  1.       0.       0.
2022  0.       0.       1.
2023  0.       -1.      0.
2024  .5       17.5     11.      8.5
2025  .5       .5       10.      7.
2026  -30.     -56.     160.     112.     .3
2027  GMCOL1.  XY
```

Table 3. Listing of Final Data Set Including Energy-Absorbing Column (Page 11 of 11).

Table 4. Allowed Contacts

Surface or Ellipsoid Number	Surface or Ellipse Name	Ellipse (number)
1	Floorpan	Left foot, right foot (8,11)
2	Toepan	Left foot, right foot (8,11)
3	Knee restraint	Left and right upper and lower legs (6,7,9,10)
4	Windshield	Head (5)
5	Head restraint (Instrument panel top)	Head (5)
6	Instrument panel	Left and right lower arms and hands (13,15,16,17)
7	SB1 (Bottom seat back)	Lower and center torso (1,2)
8	SB2 (Top of seat back)	Center and upper torso (2,3)
9	SC1 (rearmost seat cushion segment)	Lower and center torso (1,2)
10	SC2 (Seat cushion segment)	Left and right upper legs, lower torso (1,6,9)
11	SC3 (Seat cushion segment)	Left and right upper legs, lower torso (1,6,9)
12	SC4 (Forwardmost seat cushion segment	Lower torso (1)
13	COLEAT (Top of column)	The two spheres on the column mass (18,21)
14	COLEAB (Bottom of column)	The two spheres on the column mass (18,21)
15	COLEAR (Right side of column	The two spheres on the column mass (18,21)

Table 4. Allowed Contacts (continued)

Surface or Ellipsoid Number	Surface or Ellipse Name	Ellipse (number)
16	COLEAL (Left side of column	The two spheres on the column mass (18,21)
17	BOTOUT (Stop at bottom of column	The bottom sphere on the column mass (18)
18	COLT (Top of wheel mass retainer)	The three spheres on the wheel mass (22,23,24)
19	COLB (Bottom wheel mass mass retainer	The three spheres on the wheel mass (22,23,24)
20	COLR (Right wheel mass retainer)	The three spheres on the wheel mass (22,23,24)
21	COLL (Left wheel mass retainer)	The three spheres on the wheel mass (22,23,24)
22	COLA (Wheel mass retainer toward vehicle front)	The three spheres on the wheel mass (22,23,24)
23	COLP (Wheel mass retainer nearest occupant)	The three spheres on the wheel mass (22,23,24)
24	HUB (Steering column hub on column mass)	Center and upper torso (2,3)
25	Knee Restraint	Left and right lower arms and hands (13,15,16,17)
1	Lower torso	Left and right lower arms (13,15)
2	Center torso	Left and right hands, steering wheel (16,17,19)
3	Upper torso	Left and right lower arms and hands, steering wheel (13,15,16,17,19)
4	Neck	Steering Wheel (19)
5	Head	Steering Wheel (19)

Table 5. New Force-Deflection Functions

Name	Number	Function
CHESTST	22	Static force-deflection curve for chest.
CHESTG	23	Permanent deflection ratio for chest.
CHESTR	24	Conserved energy ratio for chest.
COLUMNEA	25	Static force-deflection curve for column.
COLUMNG	26	Permanent deflection ratio for column.
COLUMNR	27	Conserved energy ratio for column.
HUBFD	28	Static force-deflection curve for hub.
HUBG	20	Permanent deflection ratio for hub.
HUBR	30	Conserved energy ratio for hub.
BOTOUTFD	31	Column bottom out force-deflection curve.
CONST. F=0	32	Zero friction
COL.SP.DAMP.	33	Force-deflection for column spring/dampers.
WHL.SP.DAMP.TOP	34	Force-deflection for spring/dampers.
WHL.SP.DAMP.BOT.	35	Force-deflection for spring/dampers at bottom of wheel.
ABDOMEN FD	36	Force-deflection curve for abdomen
LWR IP LOAD (KG)	37	Alternate force-deflection curve for lower instrument panel.

4.0 SIMULATION RESULTS

The simulation results are presented as seven groups of figures as follows:

- Occupant position (Figures 11-15)
- Comparison of simulation with test results (Figures 16-25)
- Predicted accelerations (Figures 26-28)
- Vehicle/occupant interactions (Figures 29-34)
- Column and wheel dynamics (Figures 35-39)
- Vehicle deceleration (Figure 40)
- Force-deflection curves for column and wheel spring-dampers (Figures 41-42).

The first group of figures presents computer-generated schematics of occupant position. The initial position is shown in Figure 11. By 50 milliseconds (Figure 12), the abdomen ellipsoid has contacted the lower rim of the steering wheel. This has produced deformation and rotation of the wheel in the direction of column collapse as was observed in the test. A variety of additional interactions have been initiated by 70 milliseconds (Figure 13). These include substantial penetration of the:

- seat cushion by the pelvis,
- toepan and floor by the feet,
- knee restraint by knees, hands, and lower arms, and,
- wheel rim and hub by the chest

The upper torso is rotating the column and pushing it upwards as can be observed by the restraining forces produced by the housing of the energy-absorbing column. By 100 milliseconds (Figure 14), the head has rotated into the rim and also contacted the windshield. It should also be noted that there is no force generated on the lower leg ellipsoid. This is due to the location of the center of the ellipsoid with respect to the end of the knee restraint. A small modification to the geometry of the lower leg ellipsoids would lead to the production of significant forces, likely leading to a reduction of the penetration of the foot into the toepan. Figure 15 shows the beginnings of rebound. During

this period, the upper torso rides up the wheel rim and causes the top of the rim to rotate toward the column as was observed in the test movie. After this point in time, contacts are gradually released.

Figures 16-25 present comparisons of simulation results with those from the test. Head, chest, and pelvis accelerations are shown in Figure 16. In general the agreement is good. It should be noted that the simulation output has not been filtered. The spike in the head acceleration at about 90 milliseconds reflects the interaction with the upper rim of the steering wheel. The spike near the beginning of the chest acceleration curve occurs at initial contact. The oscillations indicate a springiness in the wheel/column interaction with the upper torso. Perhaps a parameter study should be undertaken to see what parameters (damping, energy-absorption, friction, etc.) could be better defined to reduce what appears to be a somewhat underdamped interaction.

Figure 17 shows a comparison between measured and predicted forces in the upper legs. There is a basic difference between the two quantities. The test results present the load measured in the femur load cells which includes loads transmitted from the hip joint, the seat cushion, the knee joint, and contacts of the knee with the knee restraint. Because of this, even the contacts of the feet with the floor and toeboard will be reflected in the test values. The predicted quantities are based on the direct contact of the upper leg ellipsoids with the knee restraint and include no additional loadings. Under these circumstances, the agreement is quite good. However, further study is warranted to determine whether the predicted force lag is related to poorly placed contact ellipsoids, a small error in occupant positioning, or is actually an accurate prediction.

Figure 18 shows a comparison of predicted and measured head angular orientation. Agreement is much better than for head forward motion which is shown in Figure 19. Predicted head motion is approximately 2 centimeters less than that which was measured. The predicted forward motions of the hip and leg (See Figures 20 and 21) are larger than would be expected. This probably points out the need for improved force-deformation data for one or more of the seat cushion, knee restraint, floor, and toepan.

Figures 22 through 25 compare various aspects of the steering column performance. The predictions in Figure 22 show about 3 centimeters more collapse of the column than was observed in the test. In addition, the column rebounds much more quickly than occurred during the test. The addition of more energy absorption will be required in the force-deflection functions for the spring/damper elements to improve this aspect of model performance. Figure 23 compares predicted and measured axial column accelerations. Again it should be noted that the output from the simulation was not filtered. A visual observation shows that these two curves follow the same general path. Figure 24 compares the predicted upward-directed loads applied to the steering column with those which were measured. The forces predicted for the column were those occurring due to contacts of the ellipsoids on the column with the vehicle surfaces which formed the sleeve. It is not known where the force transducer was located in the test buck. The important item to note is that forces of approximately the same magnitude were produced in both cases and their phasing was good. In all probability the interaction of the abdomen with the lower rim of the steering wheel was responsible for the first of the predicted spikes. Figure 25 compares

lateral loads on the vehicle due to the column. Although these values can be predicted, their meaning is unclear due to lack of knowledge of transducer placement. It would be expected, however, that the predicted forces would be lower due to the approximate symmetry of the simulation.

Figure 26 through 28 present predictions which were not verifiable by comparable measurements. Figure 26 shows the similarity between accelerations in the abdomen (center torso) and the thorax. The initial higher spike in the center torso is due to the initial contact of the abdomen with the steering wheel rim. Figure 27 shows expanded versions of the head and pelvis accelerations. The predicted initial high acceleration in the upper legs (See Figure 28) follows the shape of the femur load cell results (See Figure 17) more closely than the predictions of force at the knees. This lends some credibility to the idea that femur load cell results reflect more dynamic interaction than merely knee impact.

Figure 29 through 34 describe interactions of various body segments with the vehicle. Figure 29 shows the timing of abdomen (CT), thorax (UT), and head contacts with the wheel ellipsoid (Whl) and the hub. As expected, the initial contact is between the abdomen and the wheel rim. This is followed by a high level interaction between the thorax and the hub. The column reacts dynamically and completely releases the force before contact is reestablished about 10 milliseconds later. It is likely that damping properties added to the spring/damper representing column collapse would improve the dynamic coupling. Parameter studies would be necessary to develop appropriate tuning. The contacts of the thorax with the wheel rim were better tuned. An interaction between the head and the wheel rim began at 84 milliseconds and continued until

approximately 120 milliseconds. Figure 30 shows windshield/head contact which follows the wheel/head contact by about 10 milliseconds.

Figure 31 shows details of the interaction of the left knee with the knee restraint. All interactions of the hands and lower arms with the lower instrument panel (knee restraint surface) are shown in Figure 32. It should be noted that the left and right hands do not interact at the same time. The reason for this is not known, but some asymmetry is to be expected due to round-off errors when the Euler angles that are supplied as impact data are transformed into direction cosines within the program. The reason could also be an undiscovered problem with the initial baseline data set. Further work is necessary to solve this problem.

The various interactions of the pelvis (lower torso) with the seat back and cushion are shown in Figure 33. The four segments of the seat cushion are labeled SC1, SC2, SC3, and SC4. The surface SC1 is closest to the seatback while SC4 is closest to the front of the vehicle. Initial forces are generated by the seatback (lo st bk) and surface SC1. As the simulation progresses, the occupant moves forward and interacts with one after the other of the surfaces. Although the total force curve is fairly smooth, it appears possible that the abrupt change in force at about 50 milliseconds may be unrealistic and could be reflected in the predicted dynamics from that point on. Also, it is not known whether this seat cushion model reflects the seat used in the test.

Figure 34 shows interactions of the feet with the toepan. Asymmetry of loading can be noted. The overall effect on occupant dynamics was not significant.

Figures 35-39 present predictions of column performance. Axial loadings on the column are shown in Figure 35. Until about 47 milliseconds the loadings are due to vehicle deceleration. At 47 milliseconds the initial contact of the abdomen with the lower wheel rim is reflected into the column. By 60 milliseconds the upper torso is loading the column directly through the hub. The large increase in force after 80 milliseconds is due to the bottoming of the column. A second surface (Col Btm Out) had little effect in restraining column motion due to the small diameter of the sphere attached to the column in comparison to the large motions which were necessary.

Figure 36 shows the forces restraining up-and-down motions of the column within the restraining sleeve. Forces generated by both contact sensing spheres attached to the column mass are presented. The curves labeled Col Top and Col Top2 refer respectively to interactions of the sphere nearest the occupant and the sphere nearest to the front of the vehicle with the surface restraining the column from upward movement. Similarly Col Bot and Col Bot2 show the resistance to downward movement. The maximum loading is at about 70 milliseconds when the occupant is tending to push the steering column upward. To resist this torque the sphere nearest the occupant is restrained from upward movement (Col Top2) while the sphere nearest the front of the vehicle is restrained from downward movement (Col Bot). Figure 37 shows details of the resistance to lateral motions. The quantities R Col and L Col show interactions of the sphere nearest the front of the vehicle with the right and left restraining surfaces. The fact that these small asymmetric loads exist at all is due to the slight asymmetry of the occupant which exists even before contact is initiated.

The curves in Figure 38 show the loadings applied to the rim as reflected in the forces generated in the three spring/dampers that attach the wheel mass to the column mass. The initial interaction is with the lower section of the rim. This is reflected in both spring dampers attached to the bottom of the wheel. Substantial loading of the upper portion of the wheel contact ellipsoid does not occur until after 60 milliseconds. It is not until after 80 milliseconds that the bulk of the load transfers to the upper half of the wheel causing rotation of the top of the rim toward the front of the vehicle. Figure 39 shows the accelerations predicted for the wheel and column masses.

Figures 40-42 reflect input data. Figure 40 shows the input deceleration function that was derived from data supplied with the impact sled test information. Figures 41-42 are force-deflection curves for the spring-dampers. These curves were prepared using simulation output. The curve for column axial resistance was developed from data supplied with sled test information. The rim resistance data input was developed from tests conducted at General Motors specifically for this project. In both cases, an estimate of force unloading should be developed to improve that aspect of the simulation.

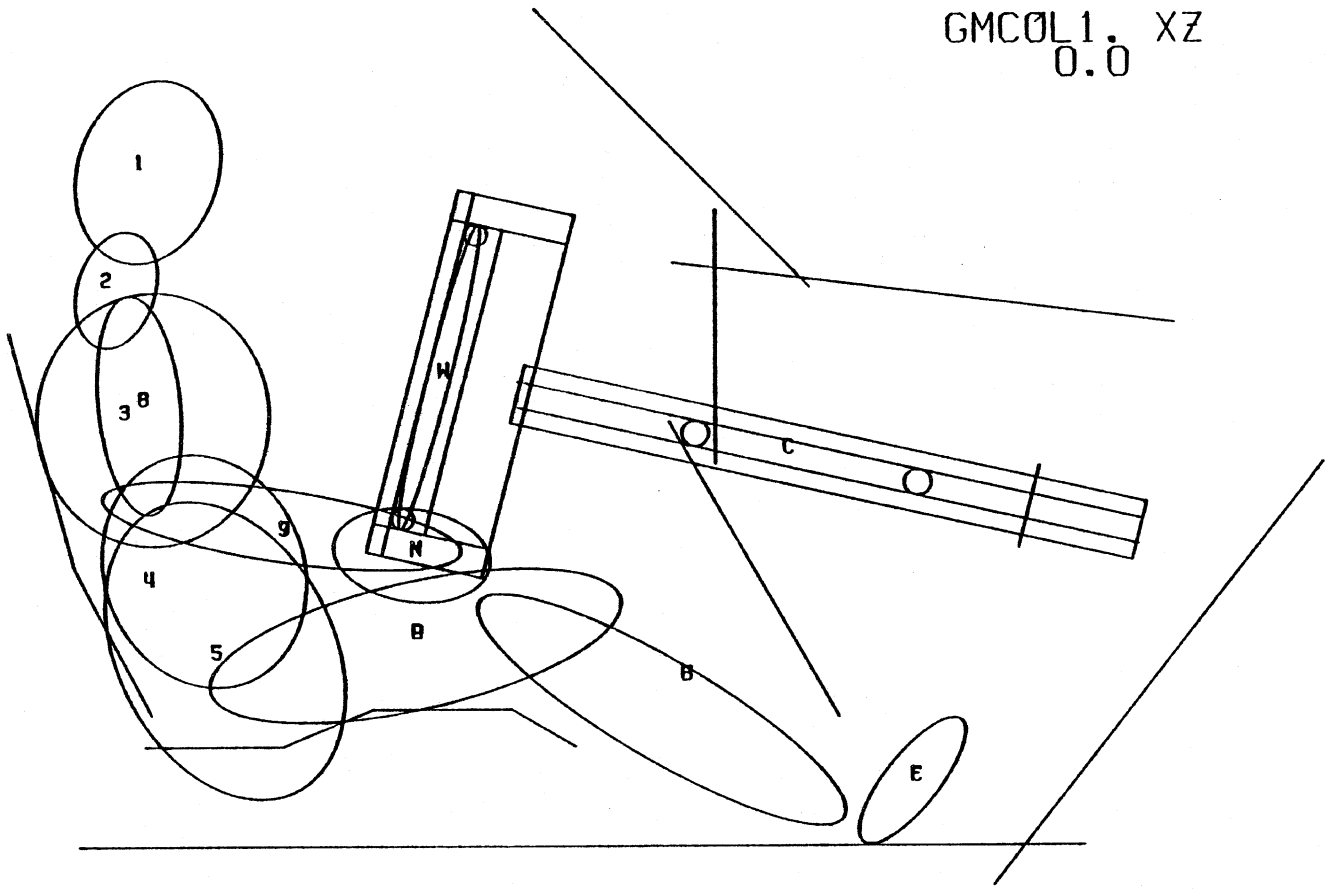

Figure 11. Side view of occupant position. t=0ms.

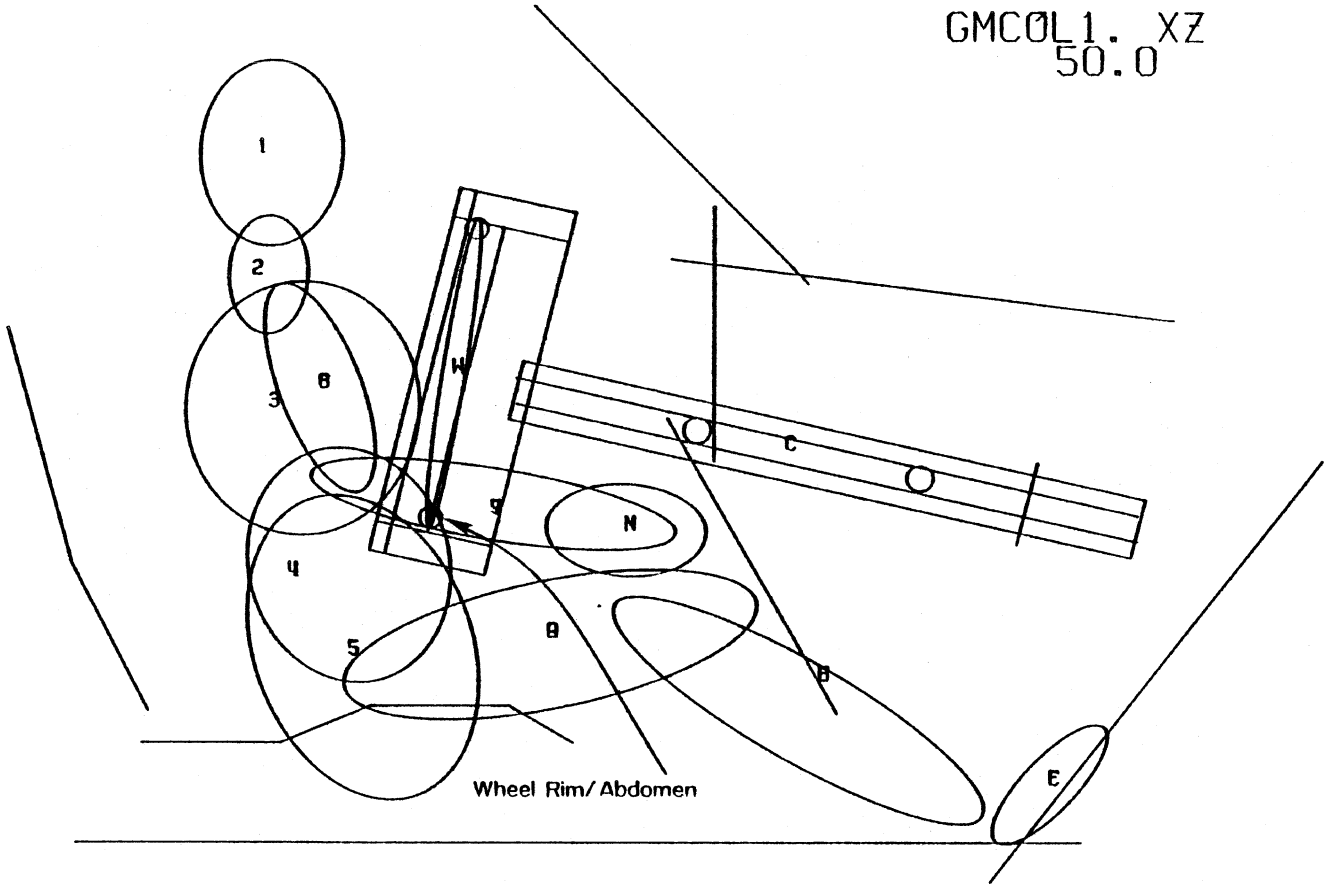

Figure 12. Side view of occupant position. t=50ms.

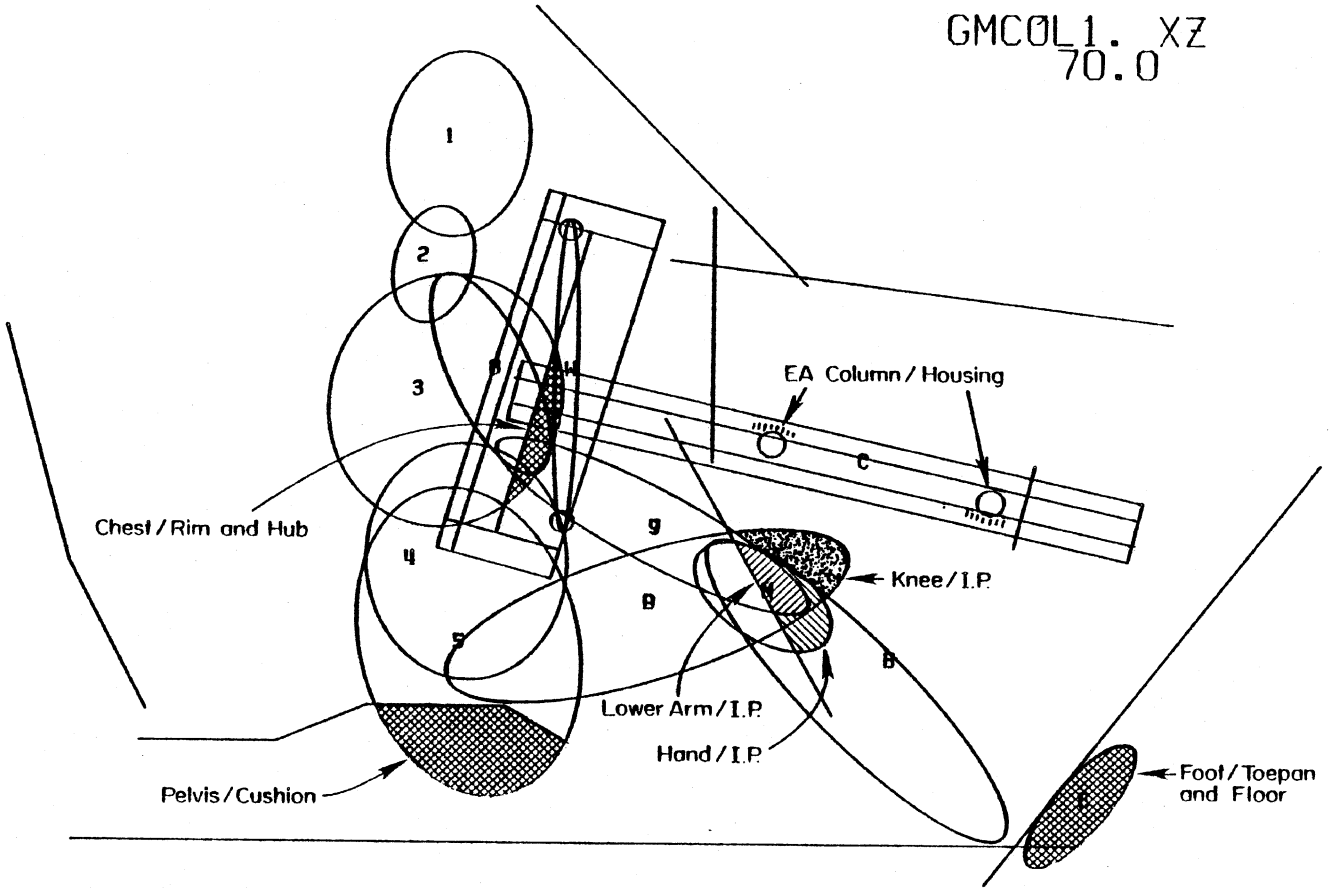

Figure 13. Side view of occupant position. t=70ms.

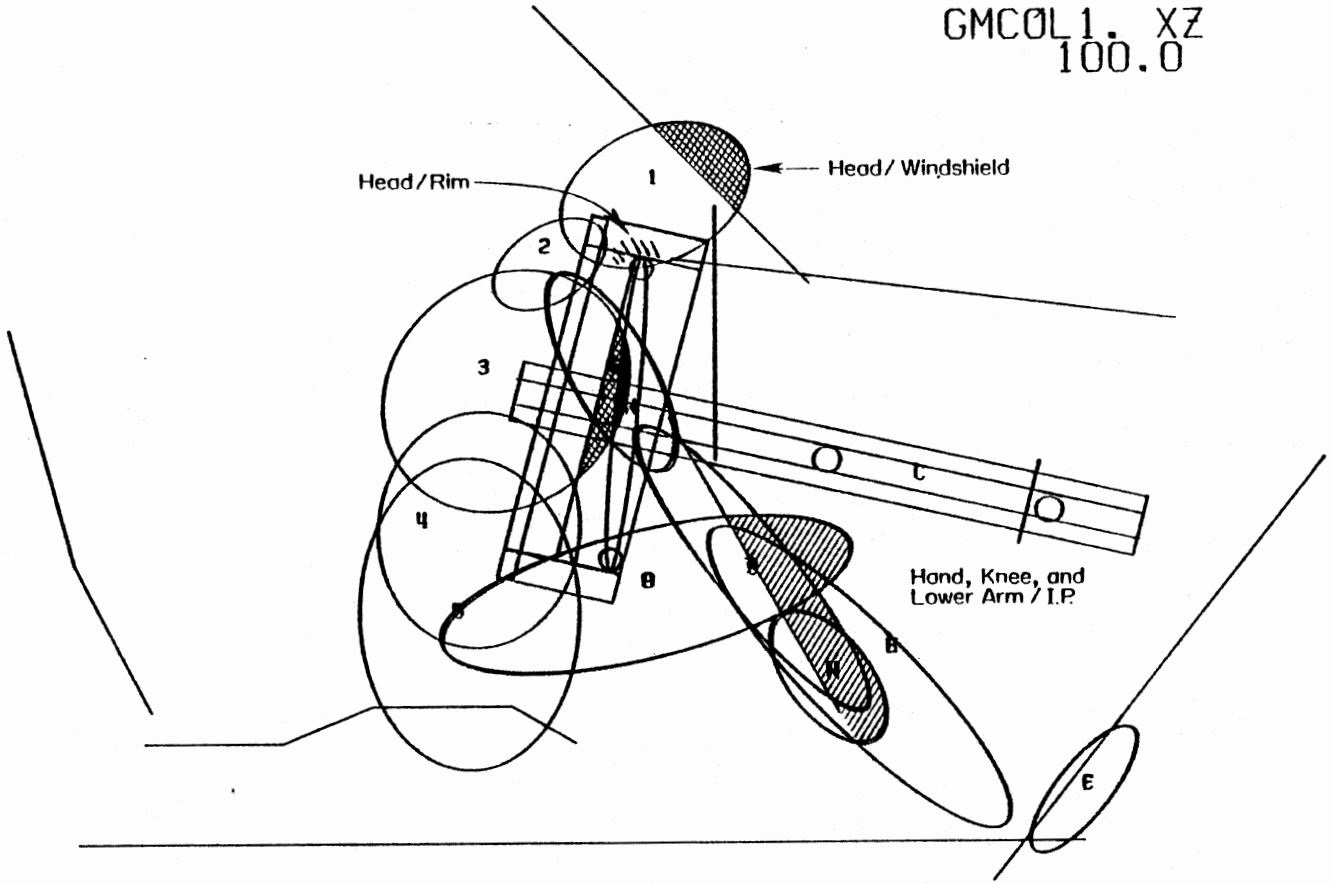

Figure 14. Side view of occupant position. t=100ms.

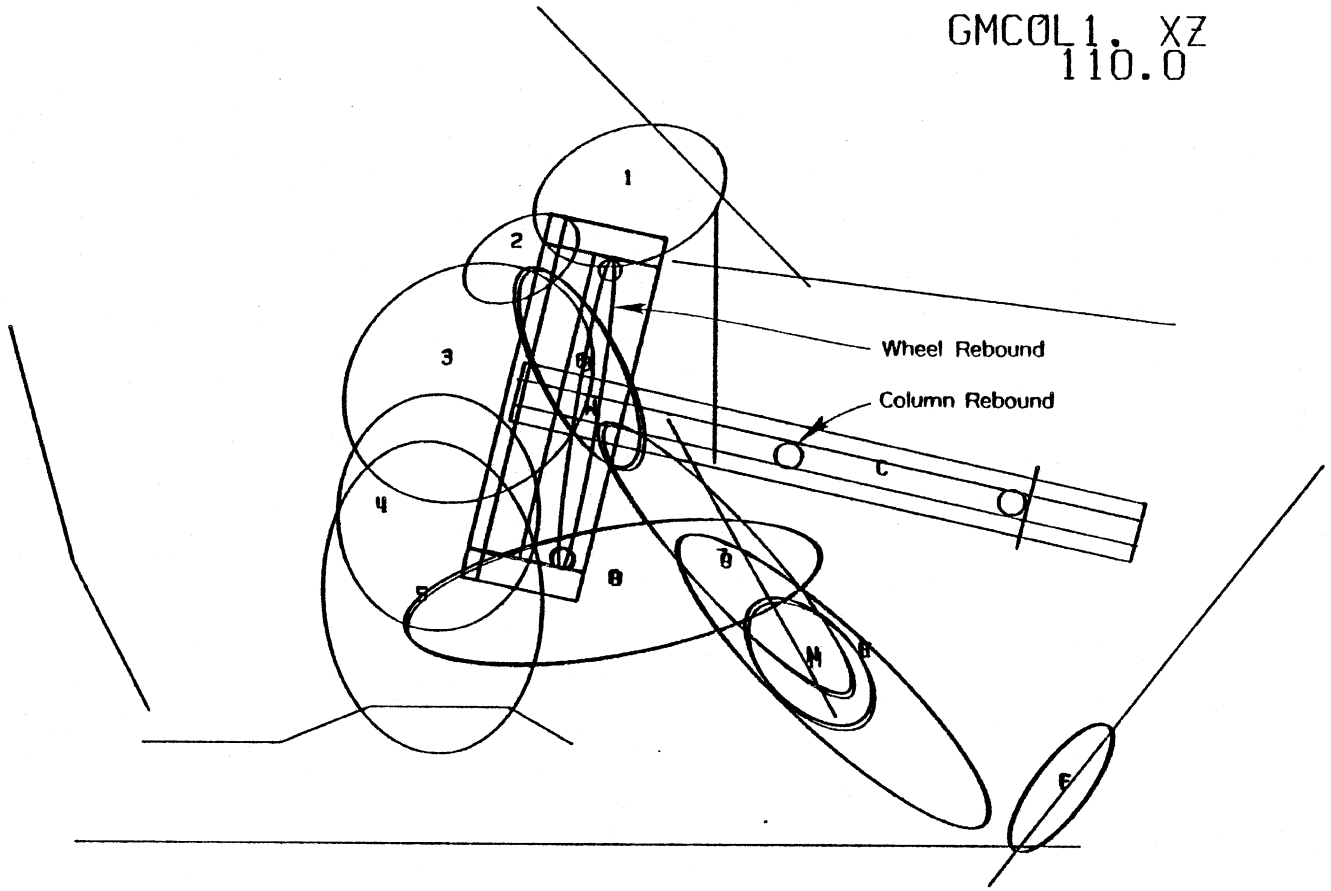

Figure 15. Side view of occupant position. t=110ms.

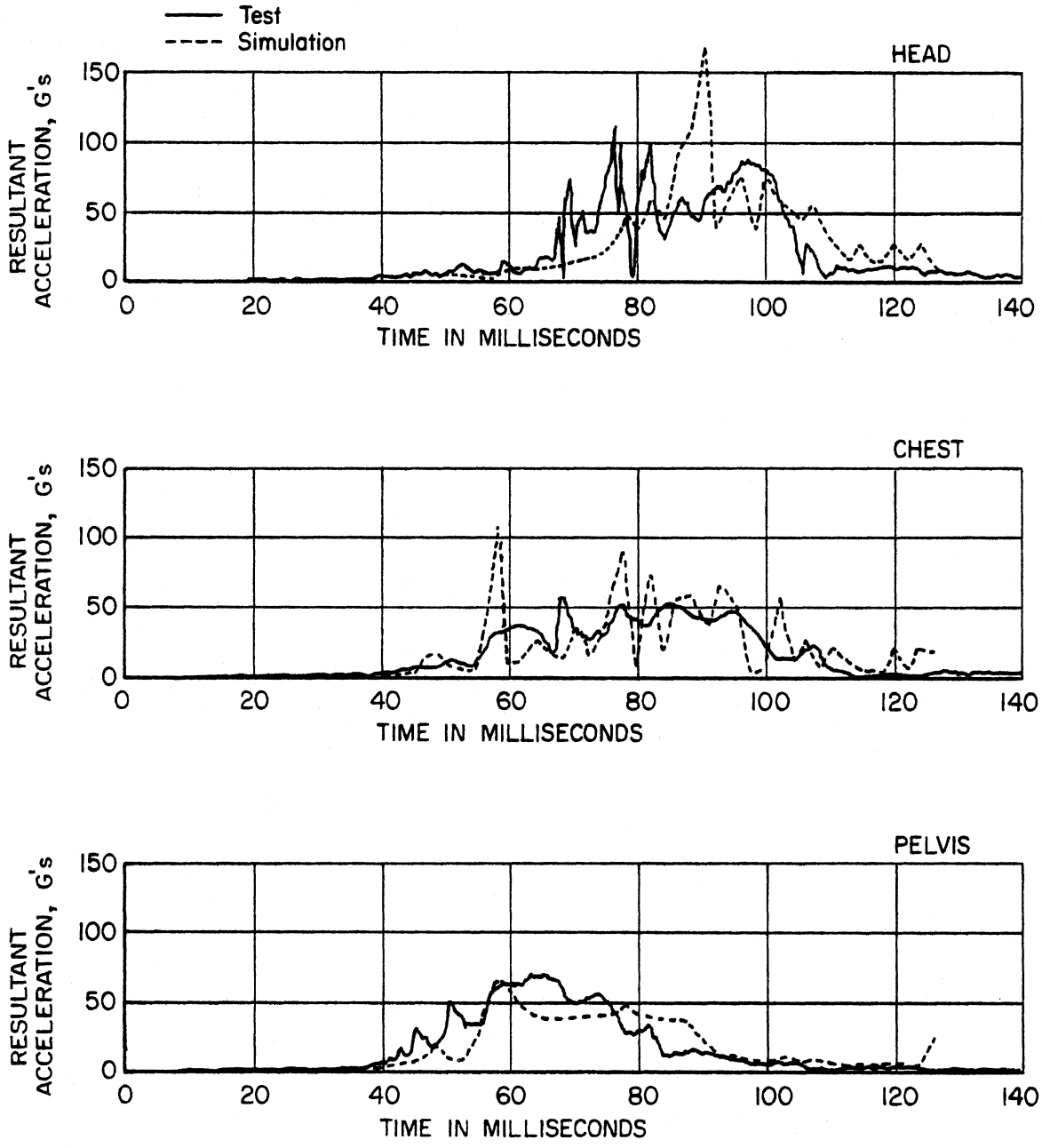

Figure 16. Comparison of predicted and measured head, chest, and pelvis accelerations.

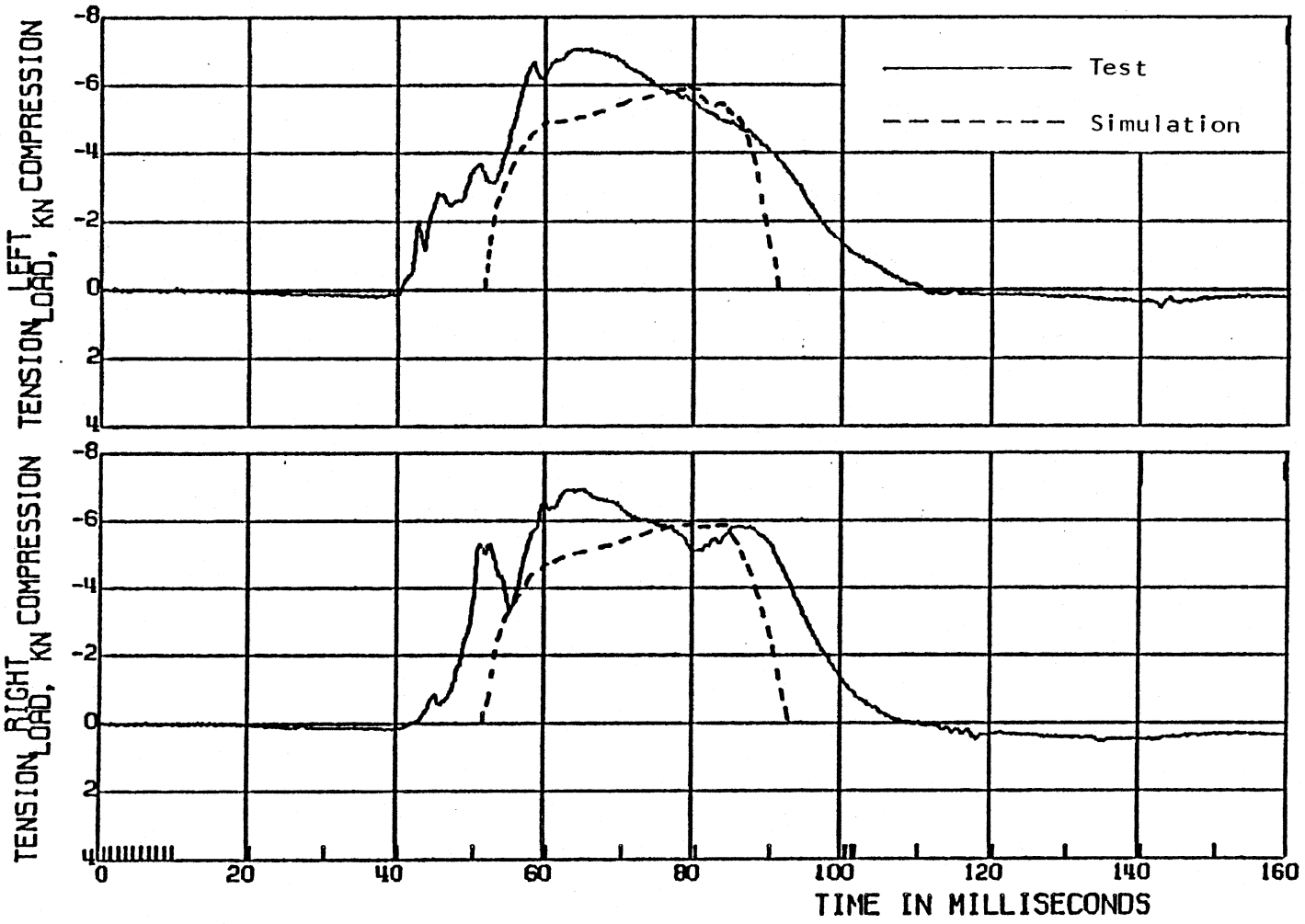

Figure 17. Comparison of measured femur loads with predicted applied force at the knees.

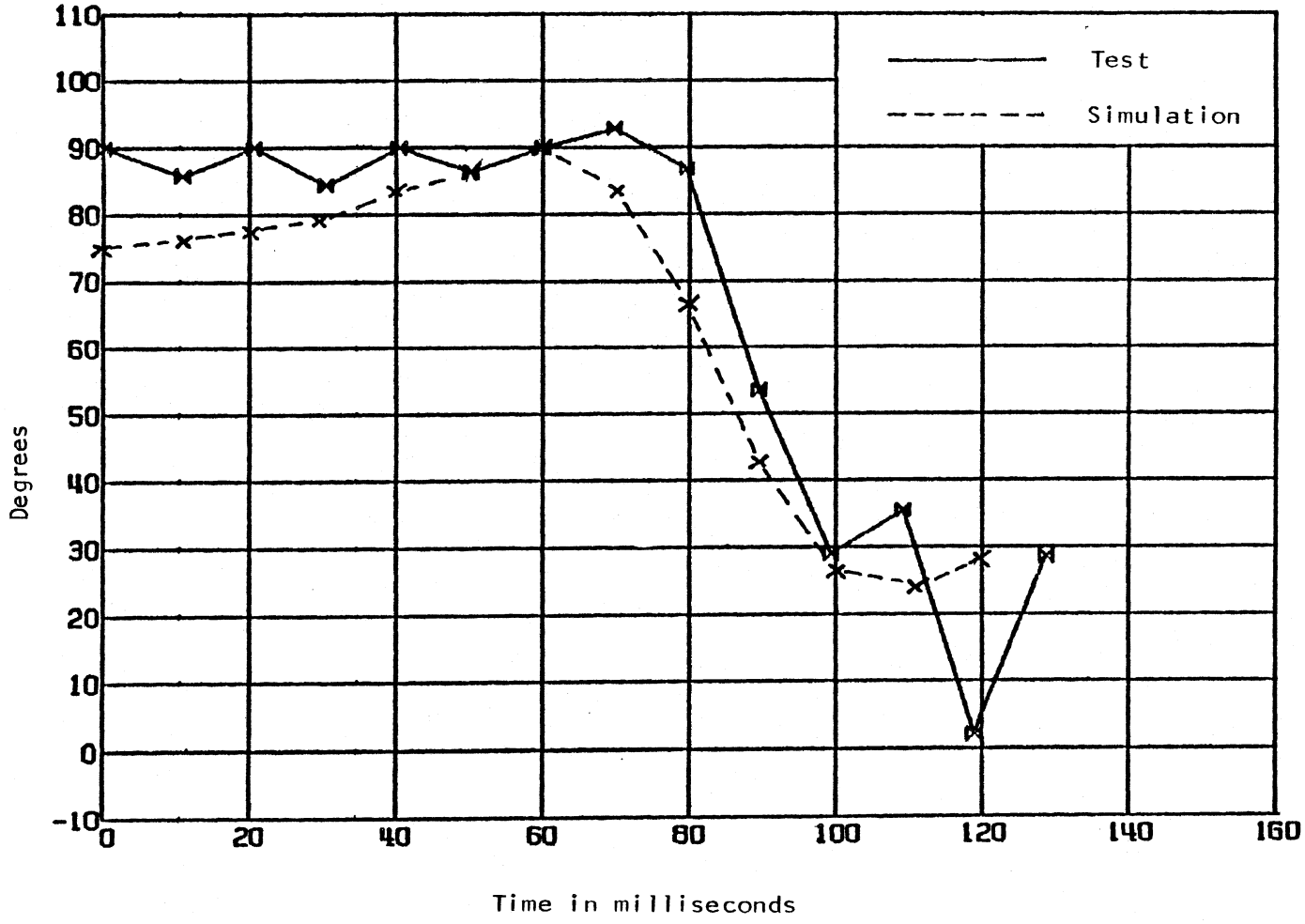

Figure 18. Comparison of predicted and measured head angular orientation.

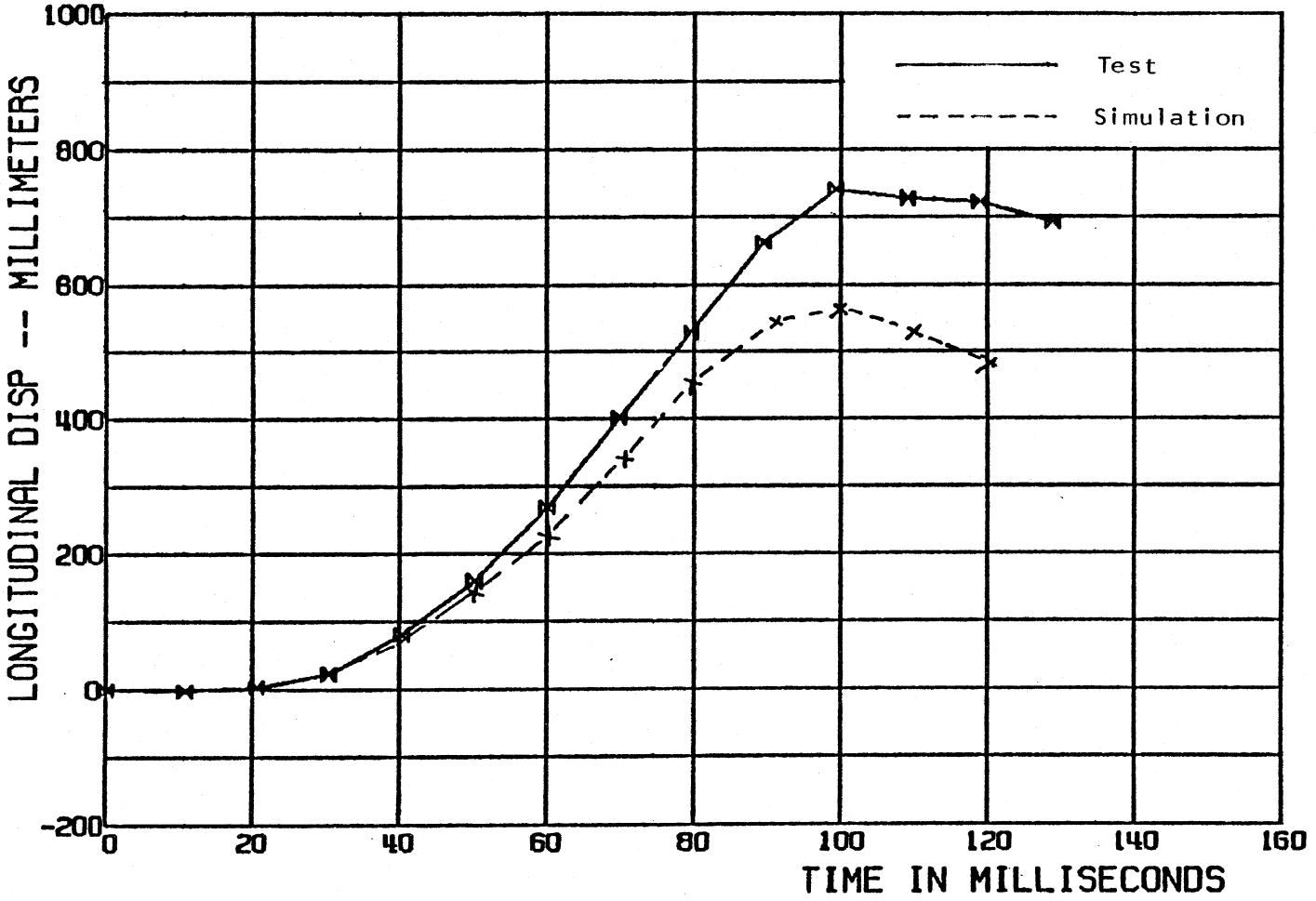

Figure 19. Comparison of predicted and measured head longitudinal displacement.

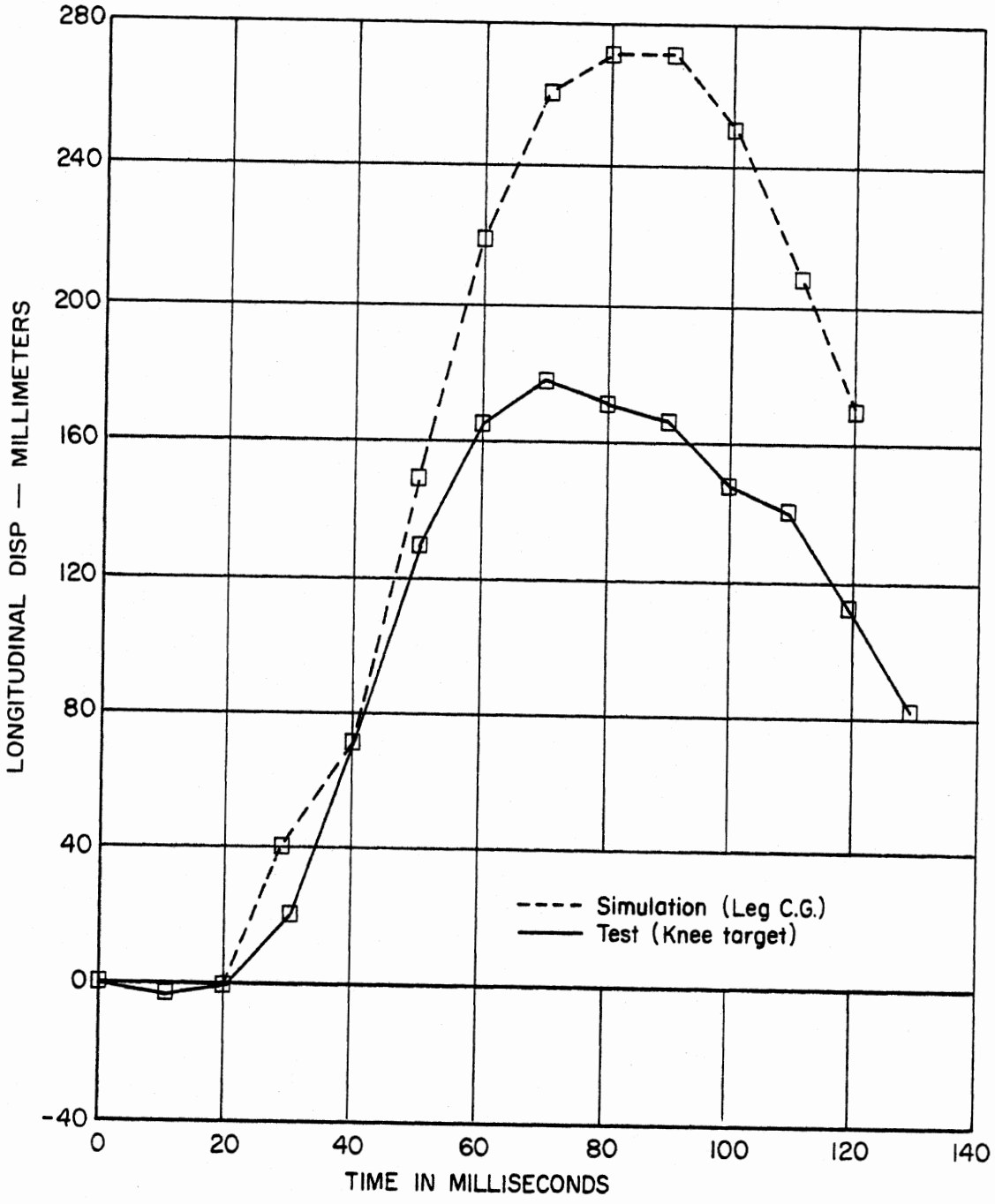

Figure 20. Comparison of predicted and measured leg longitudinal displacement.

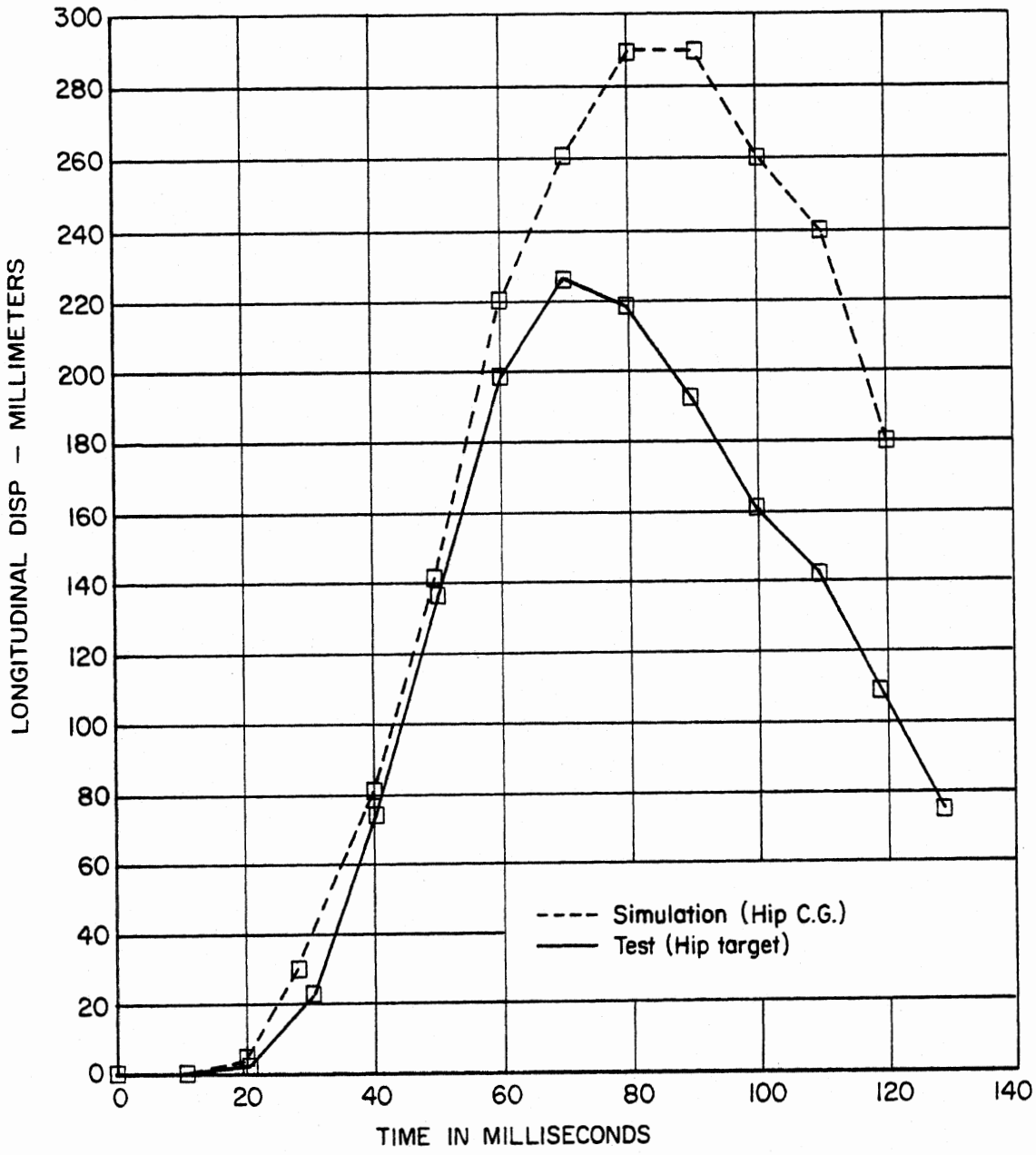

Figure 21. Comparison of predicted and measured hip longitudinal displacement.

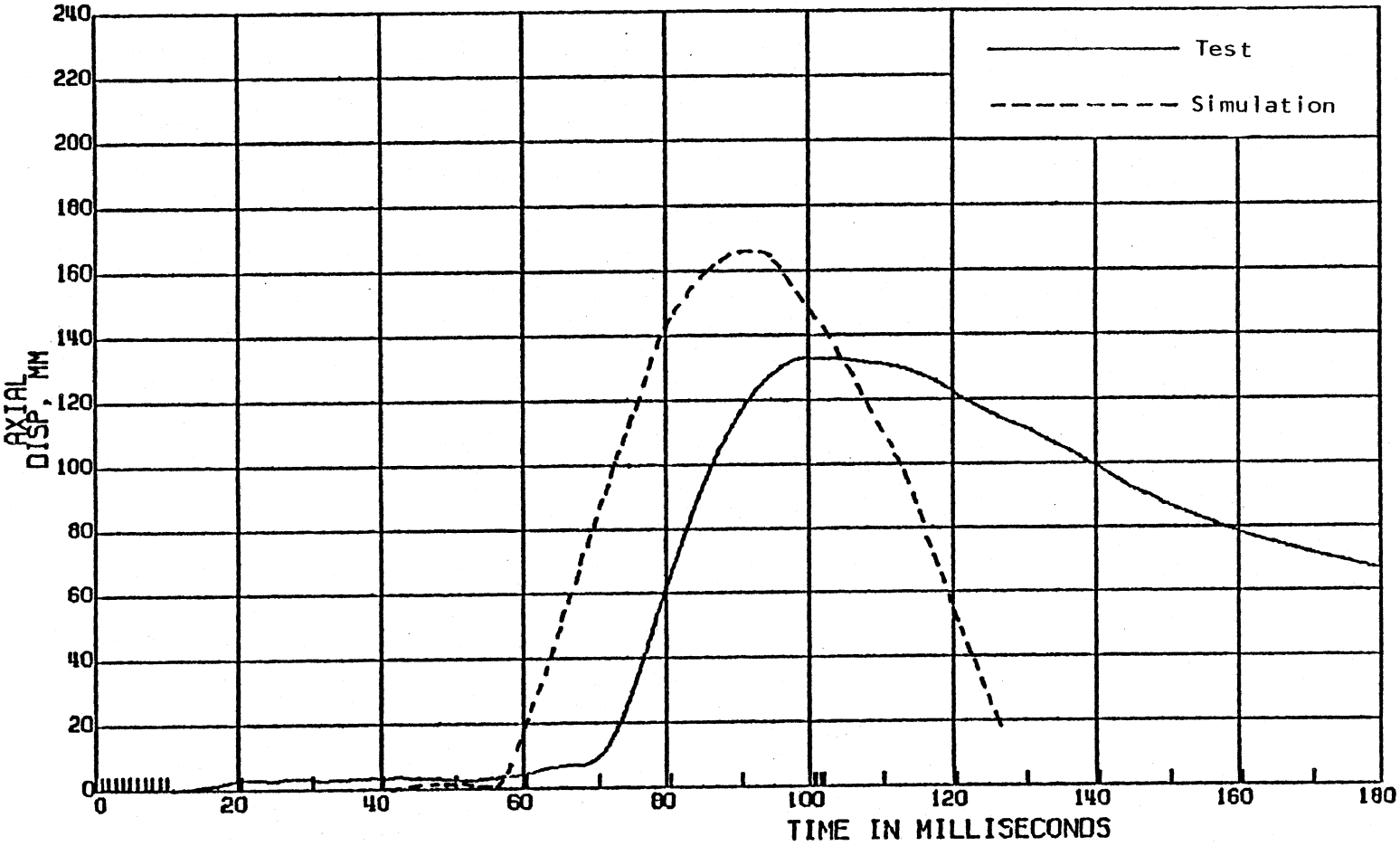

Figure 22. Comparison of predicted and measured steering column displacement.

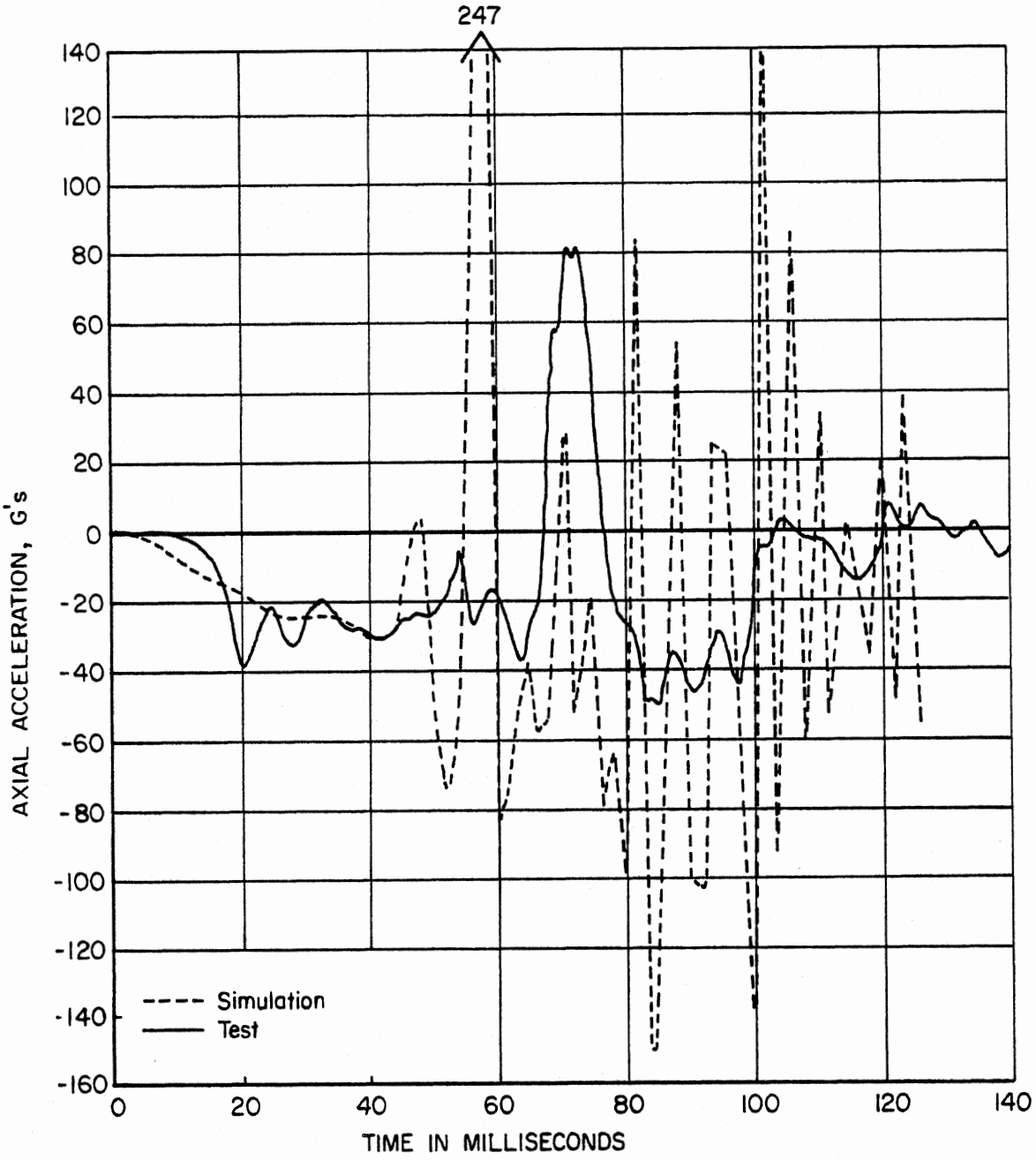

Figure 23. Comparison of predicted and measured steering column acceleration.

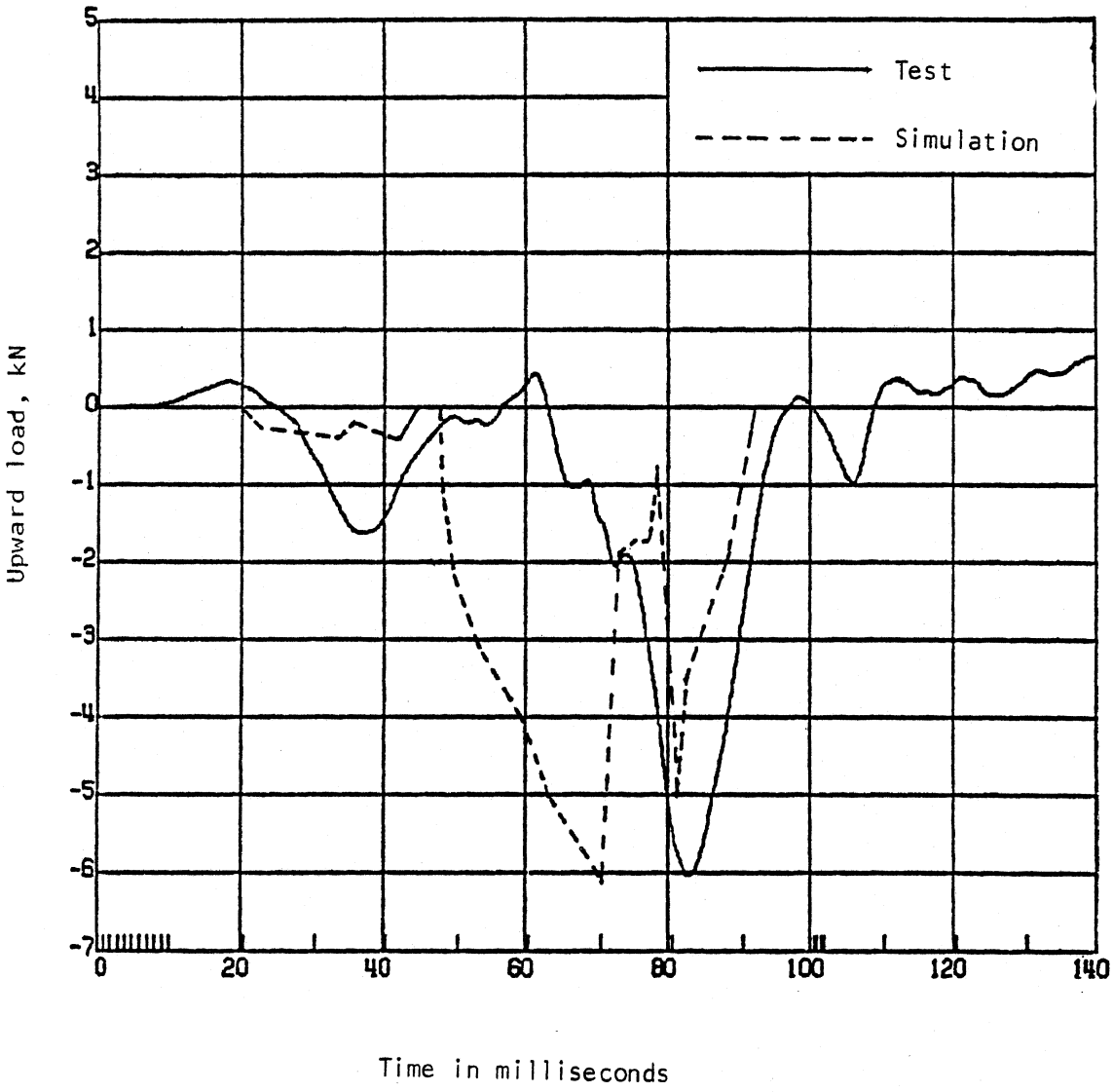

Figure 24. Comparison of predicted and measured upward steering column load.

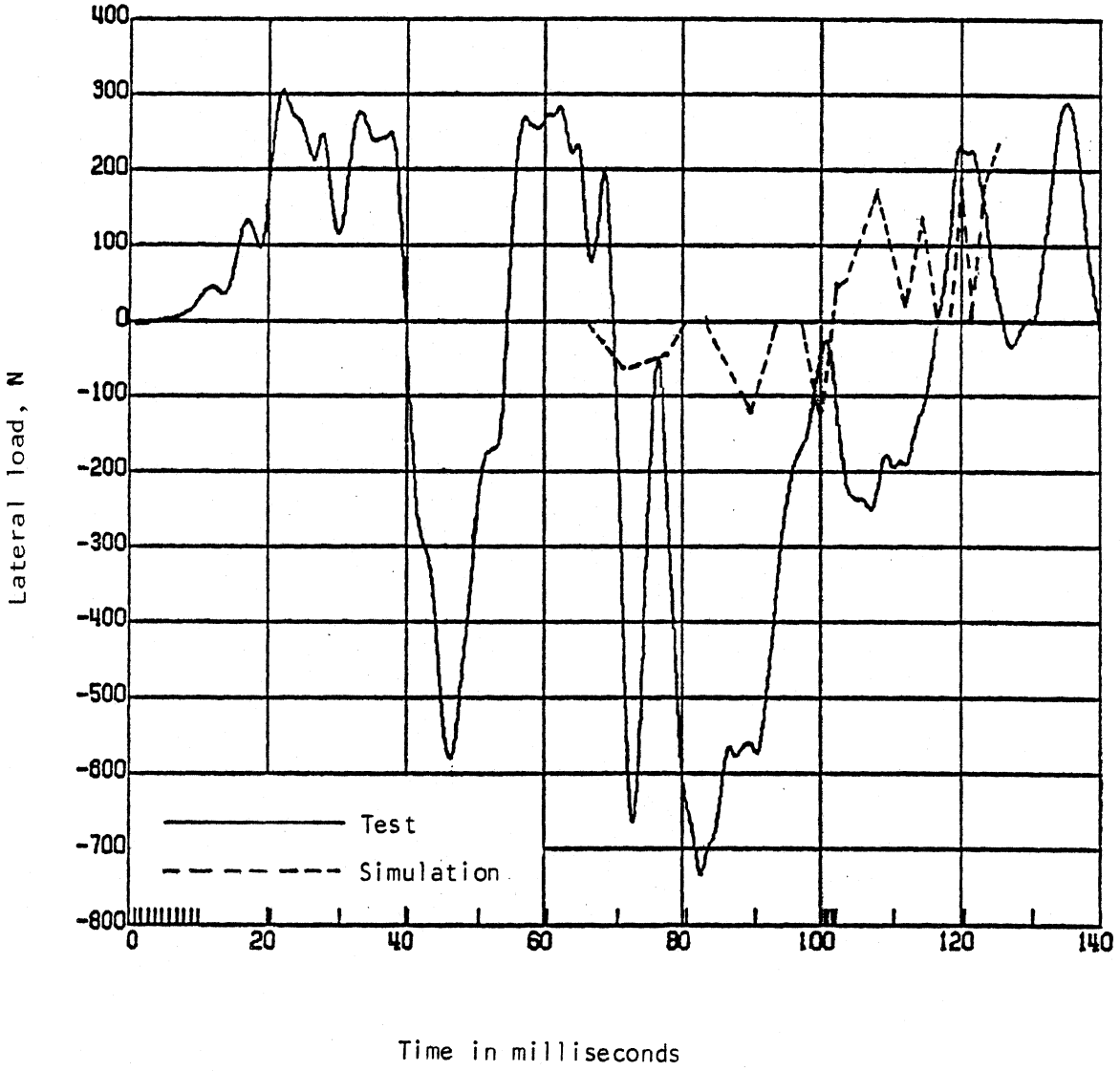

Figure 25. Comparison of predicted and measured lateral steering column load.

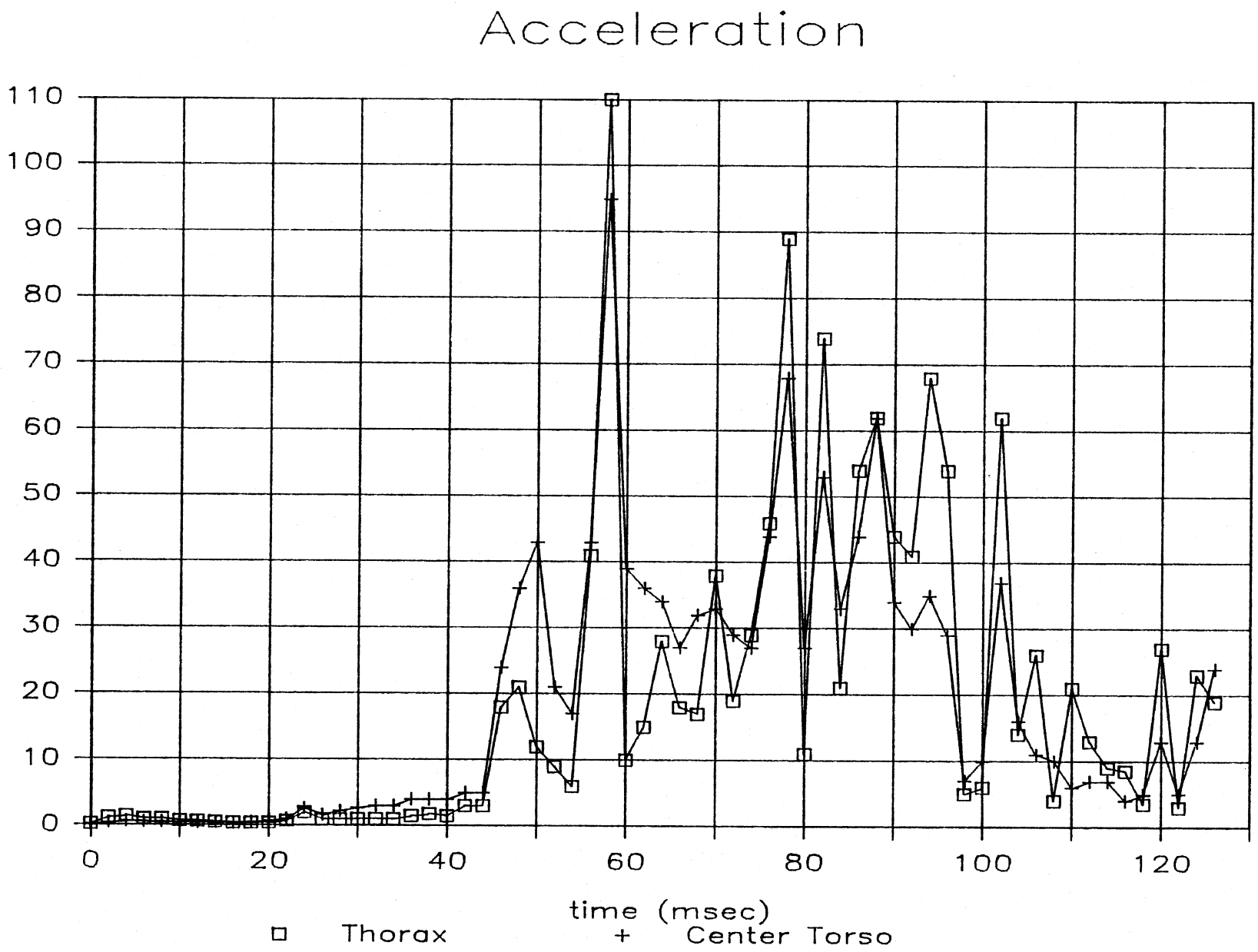

Figure 26. Predicted thorax and abdomen acceleration.

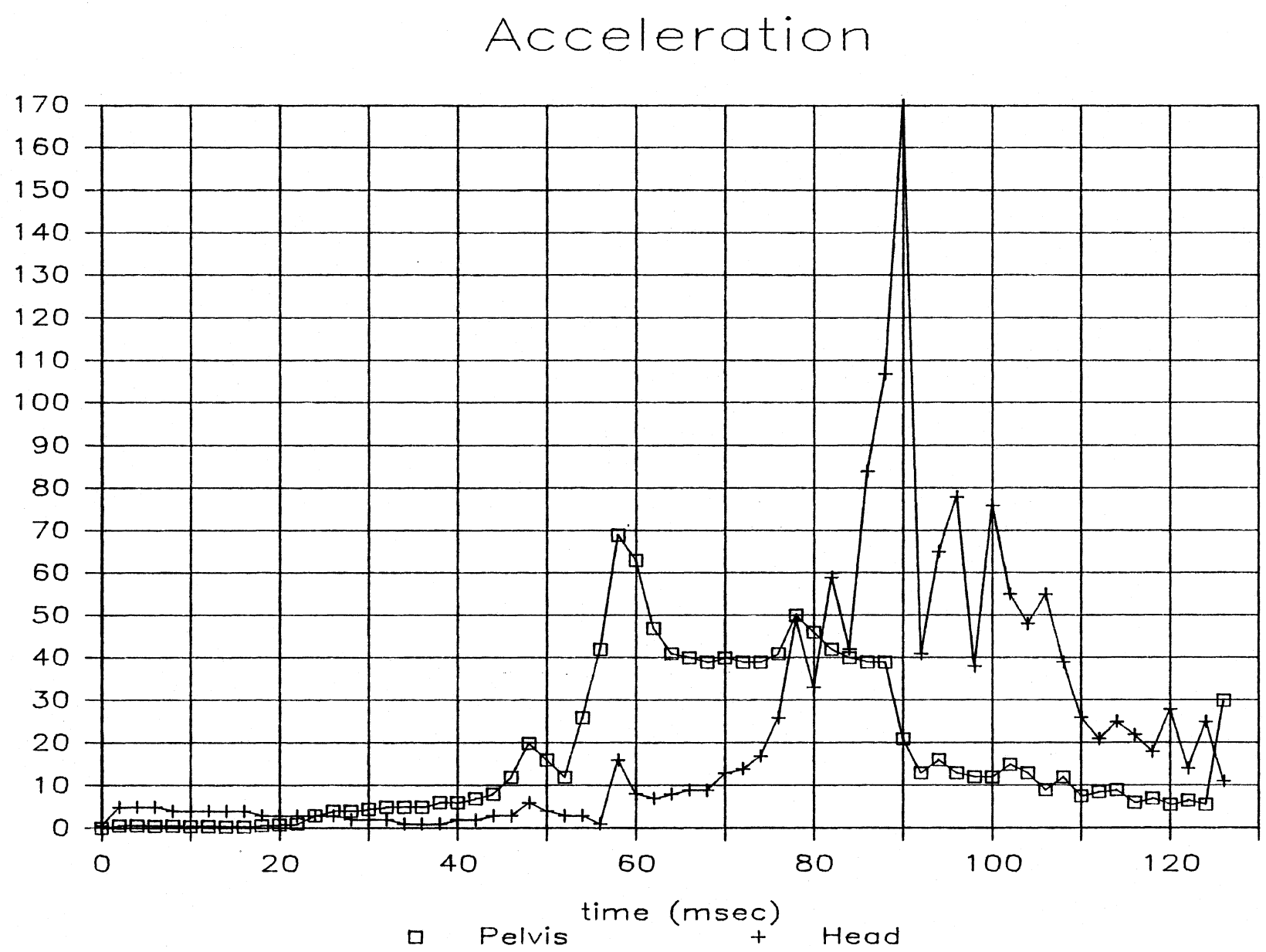

Figure 27. Predicted pelvis and head acceleration.

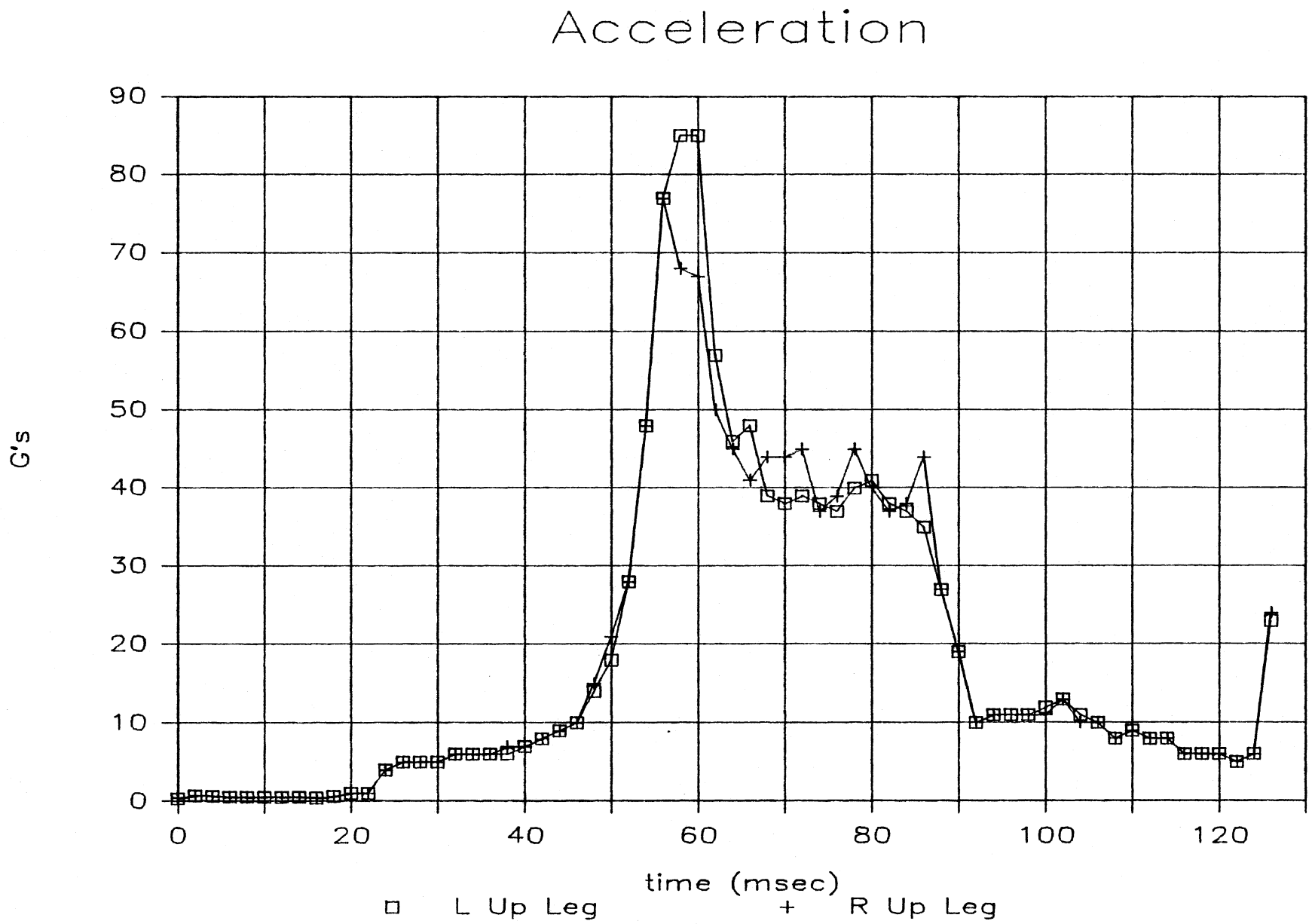

Figure 28. Predicted upper leg acceleration.

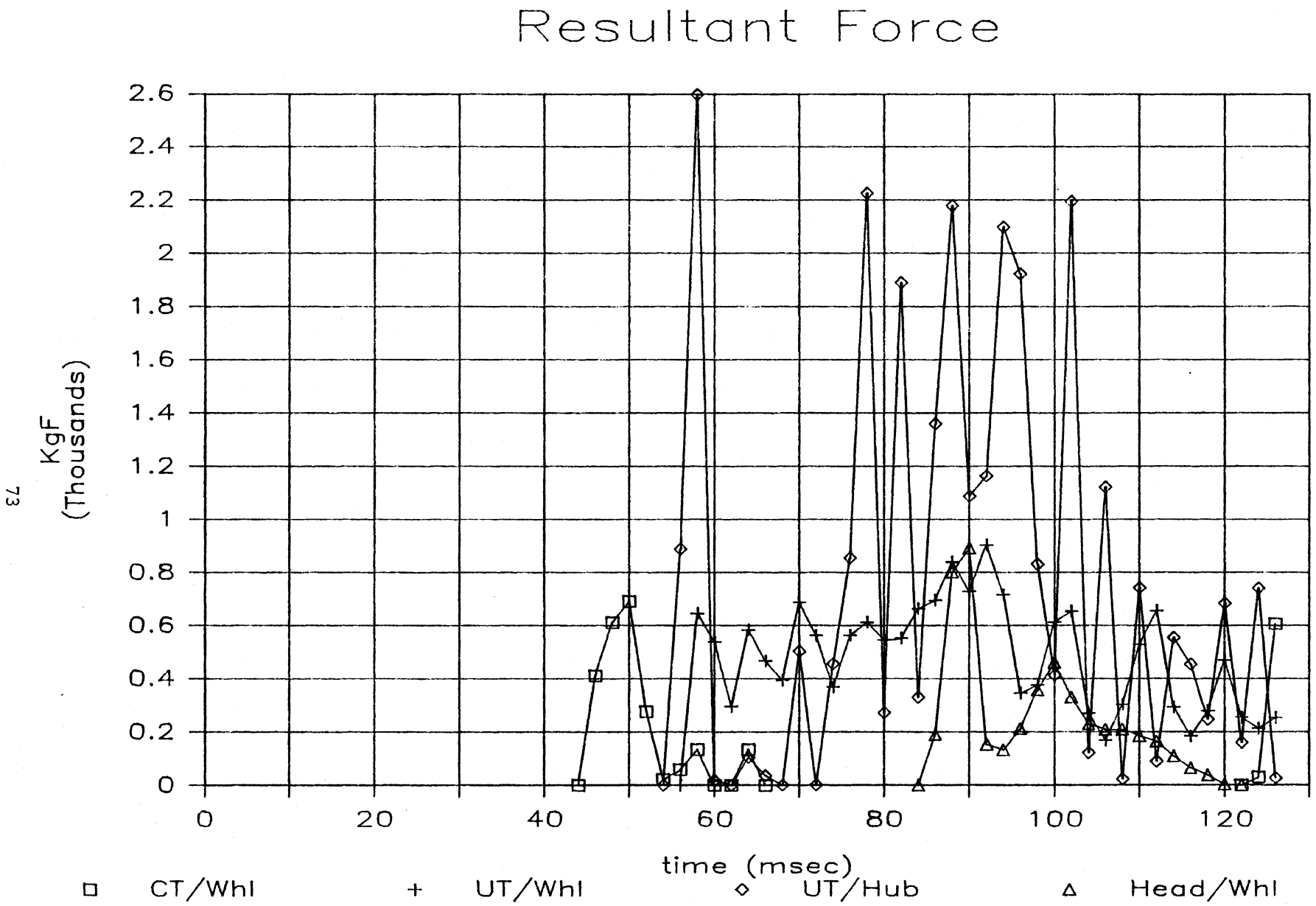

Figure 29. Predicted interactions of the chest and abdomen with the steering wheel and hub.

Figure 30. Predicted interaction of the head with the windshield.

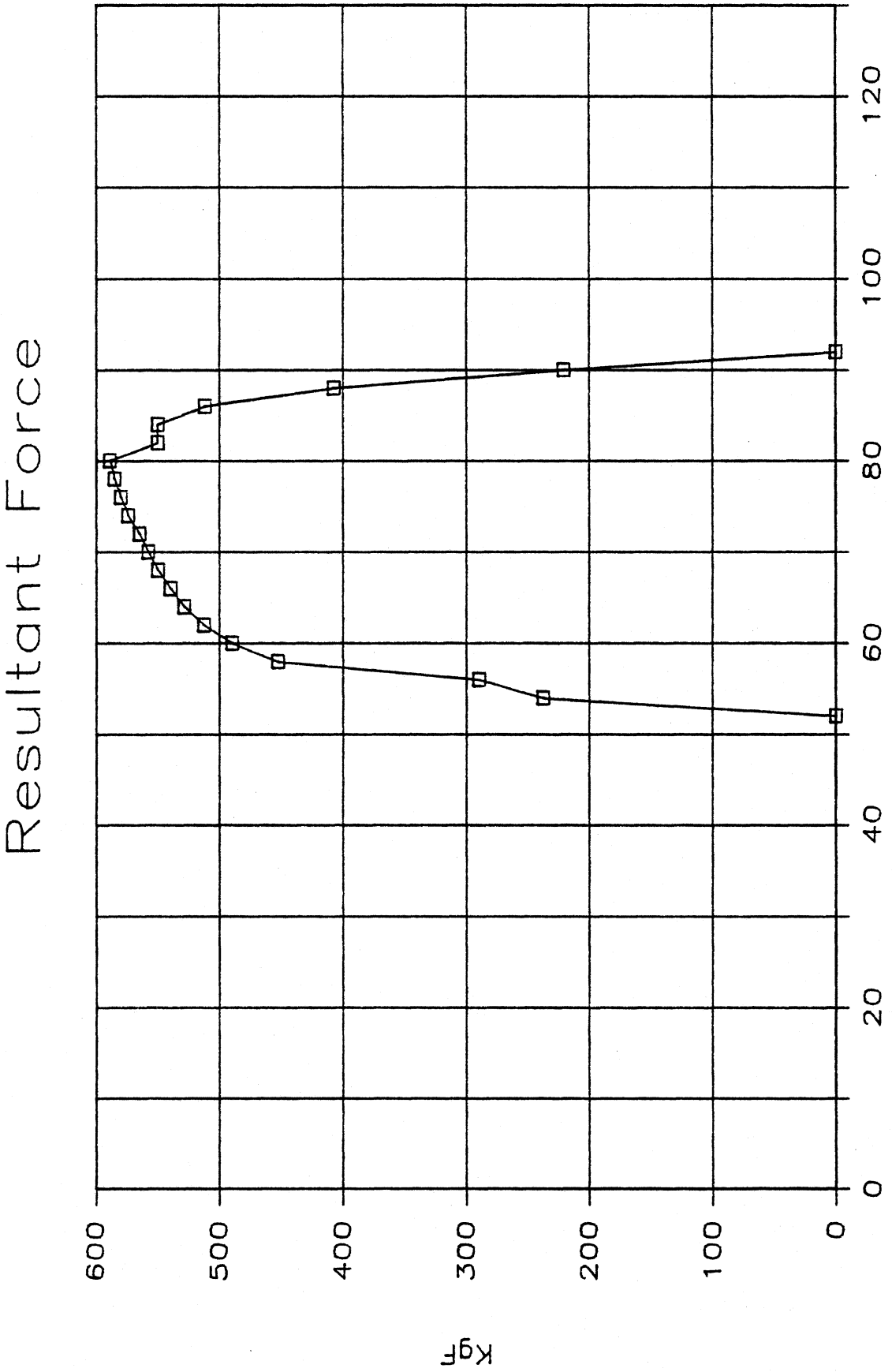

Figure 31. Predicted interaction of the left upper leg with the knee restraint.

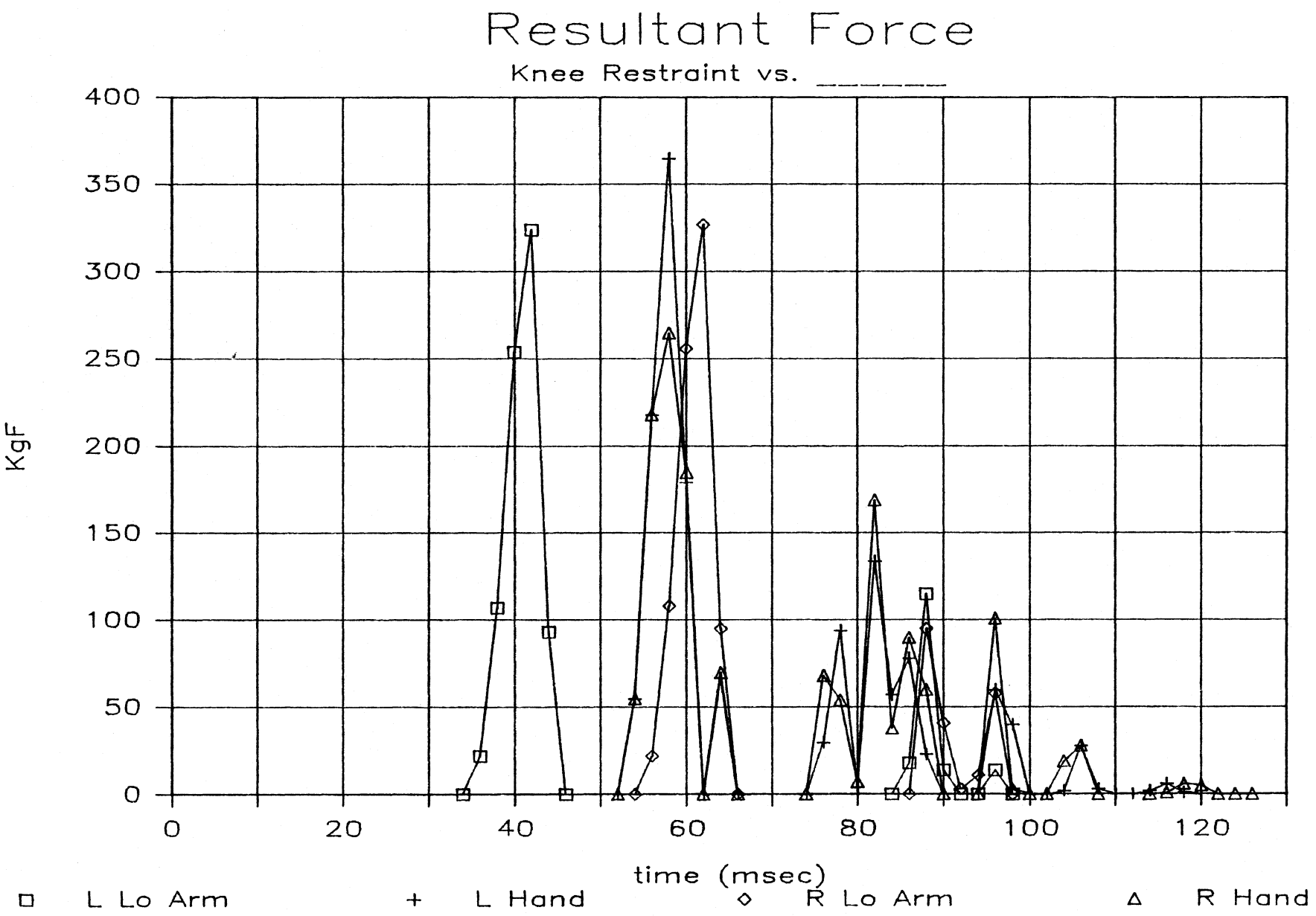

Figure 32. Predicted interactions of the hands and lower arms with the knee restraint.

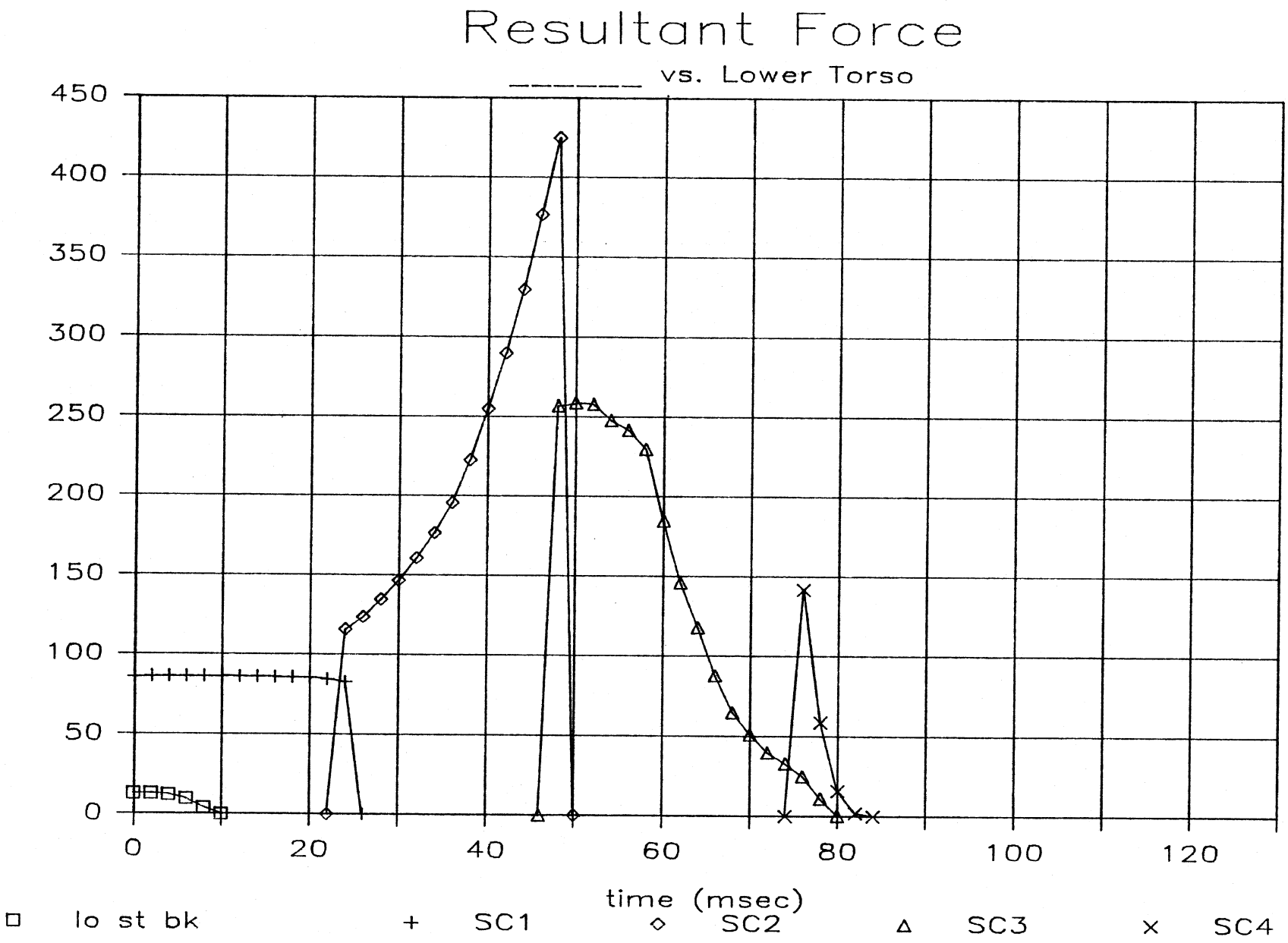

Figure 33. Predicted interaction of the pelvis with the seat cushion.

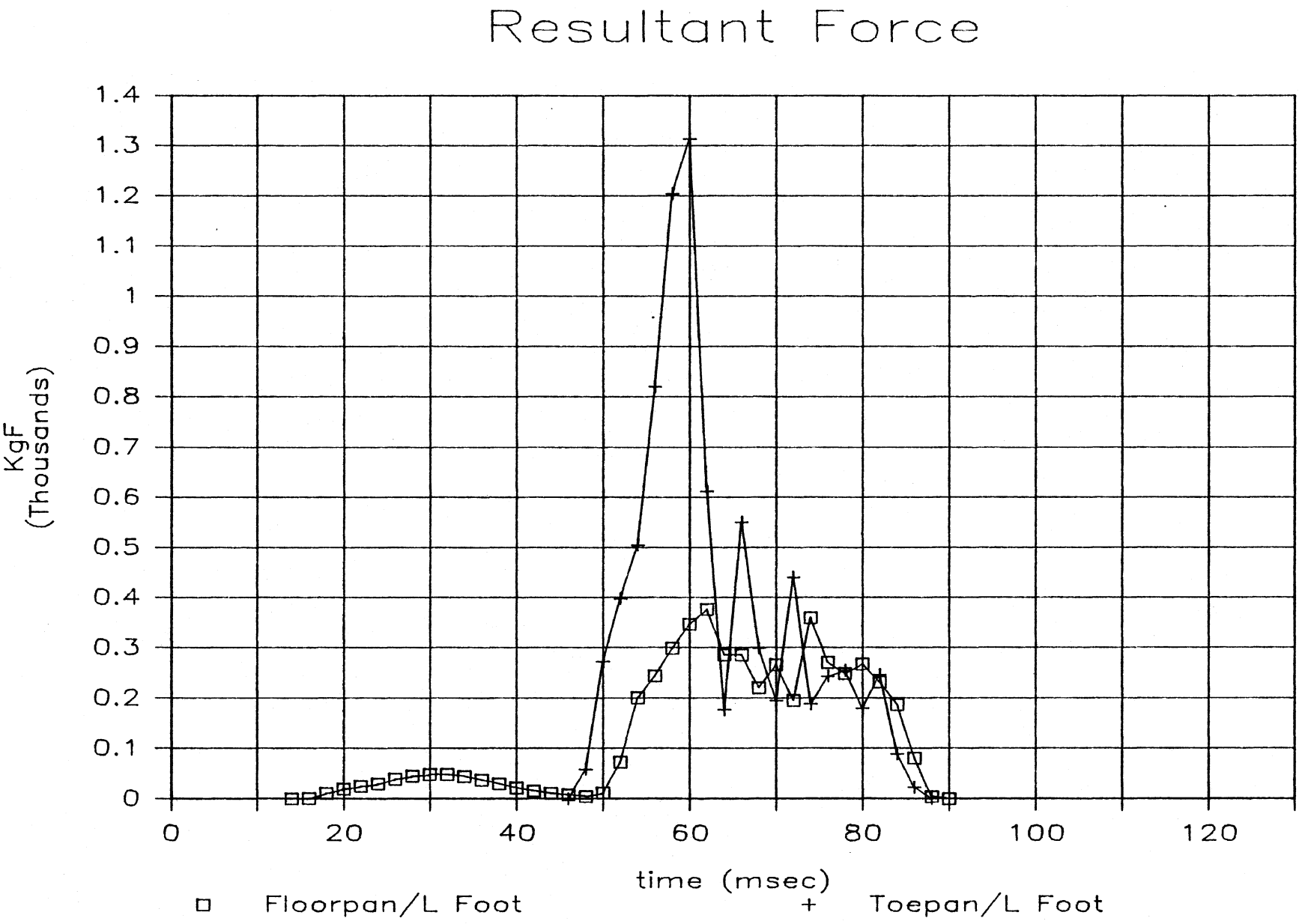

Figure 34. Predicted interaction of the left foot with the floorpan and toepan.

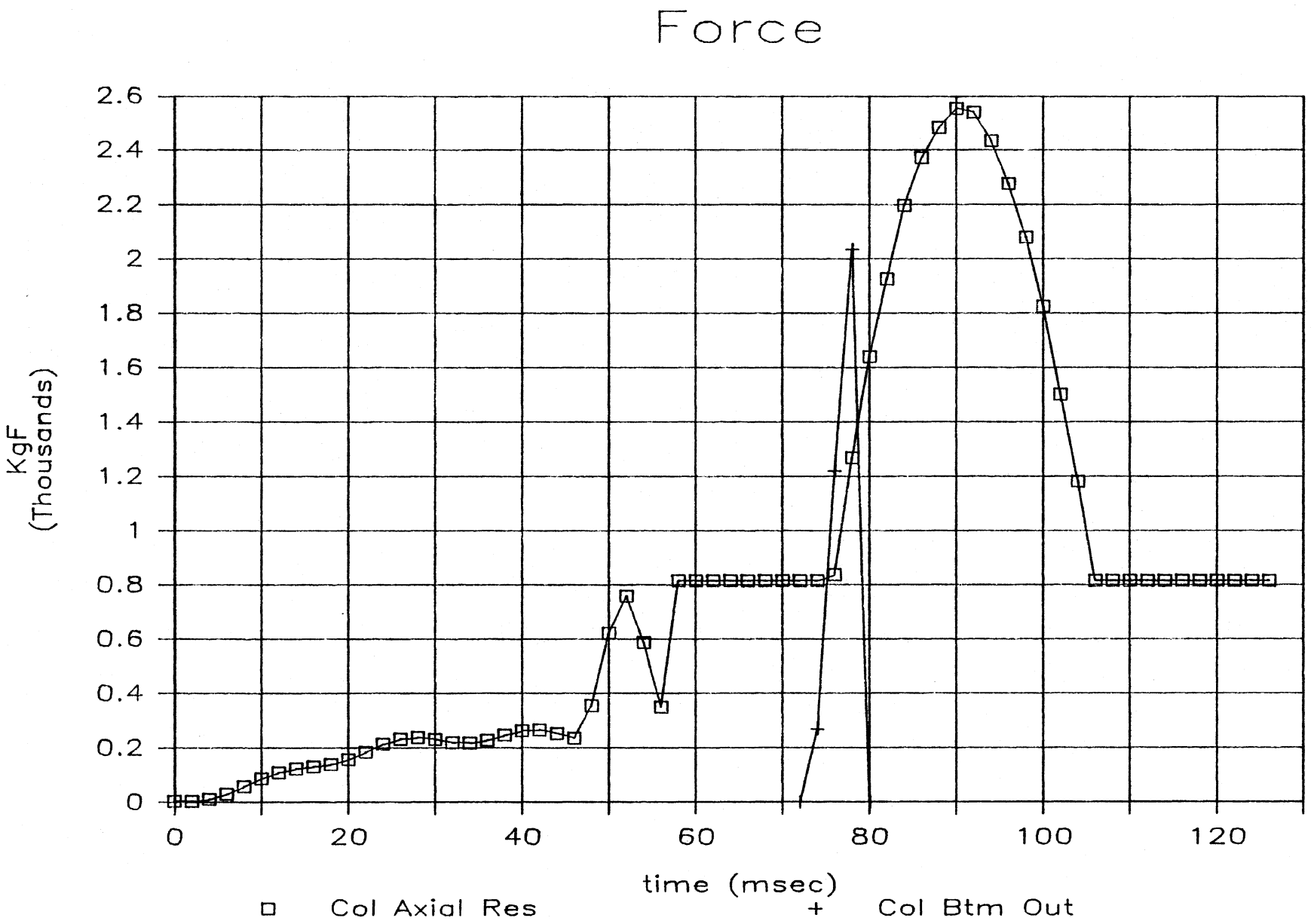

Figure 35. Predicted forces restraining the column from collapse.

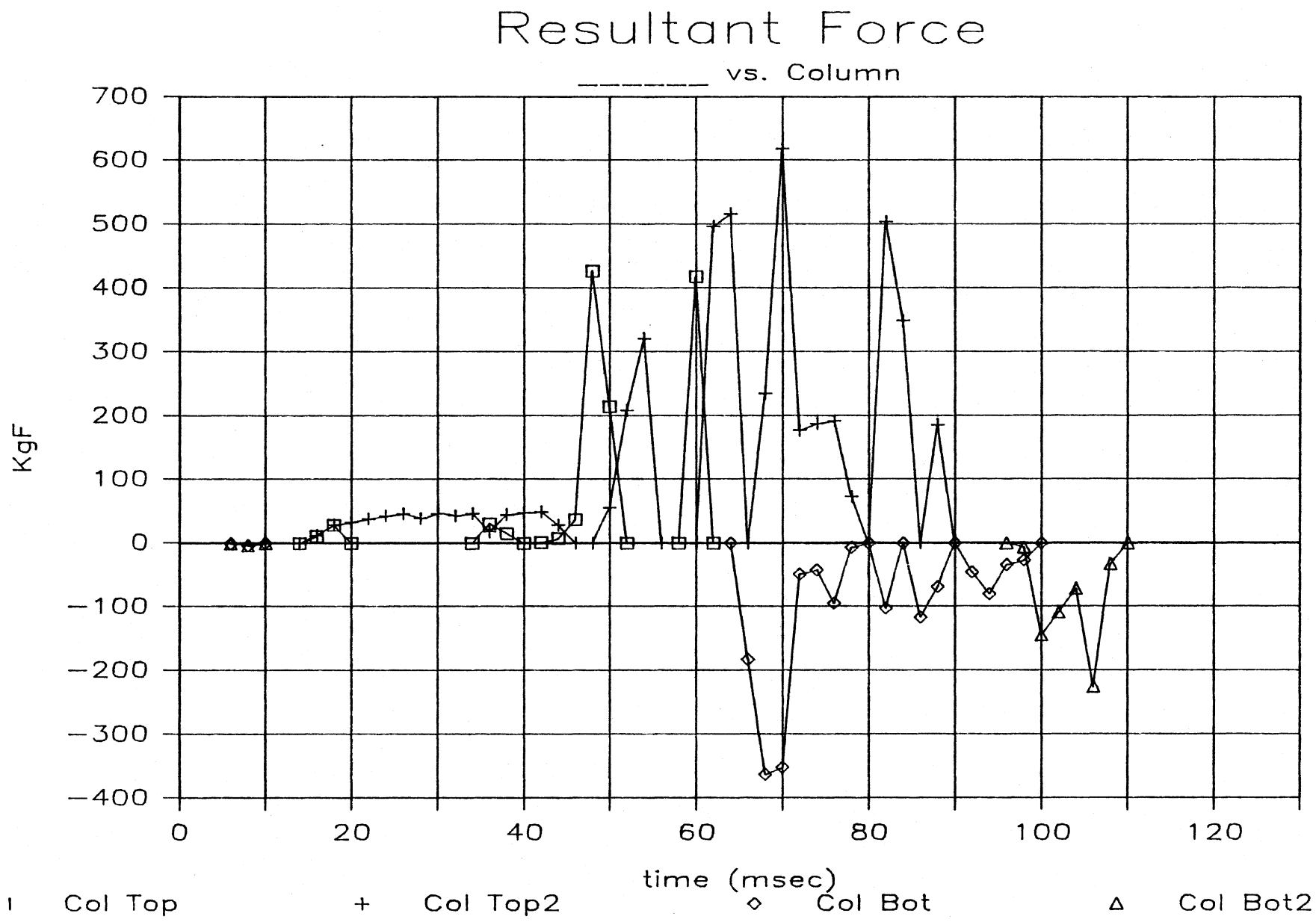

Figure 36. Predicted forces restraining the column from upward or downward motion.

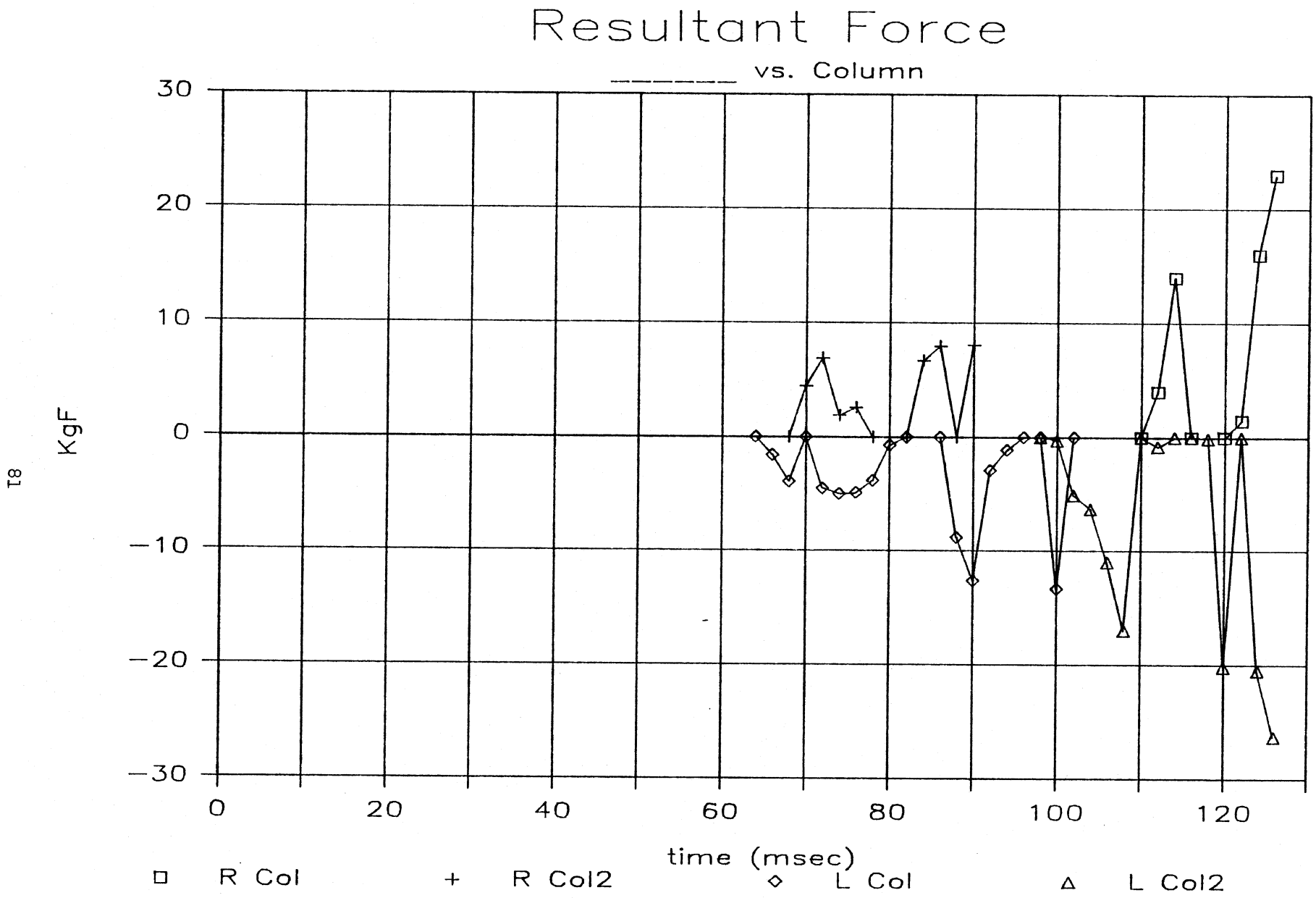

Figure 37. Predicted forces restraining the column from lateral motion.

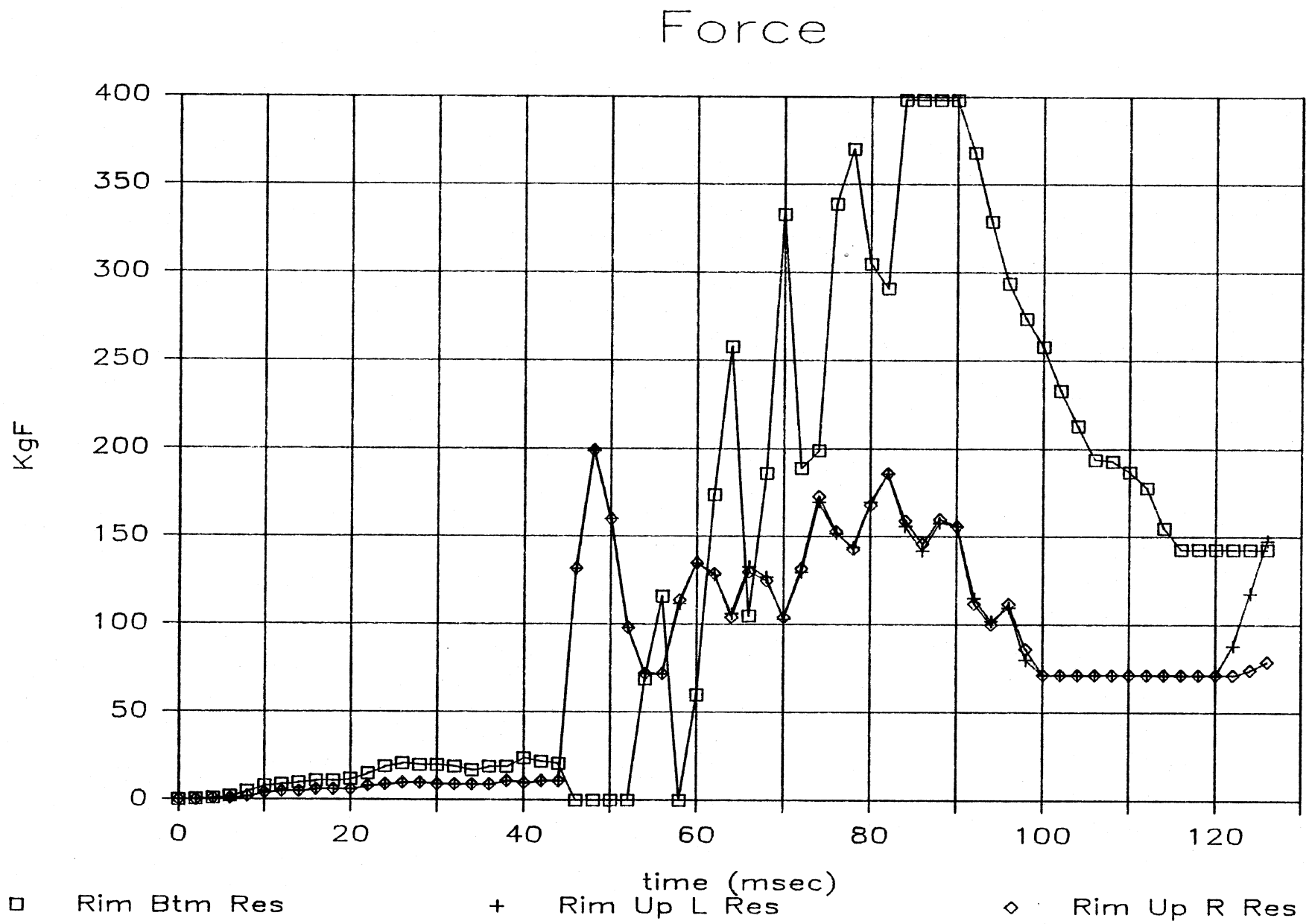

Figure 38. Predicted forces restraining the wheel rim from axial motion.

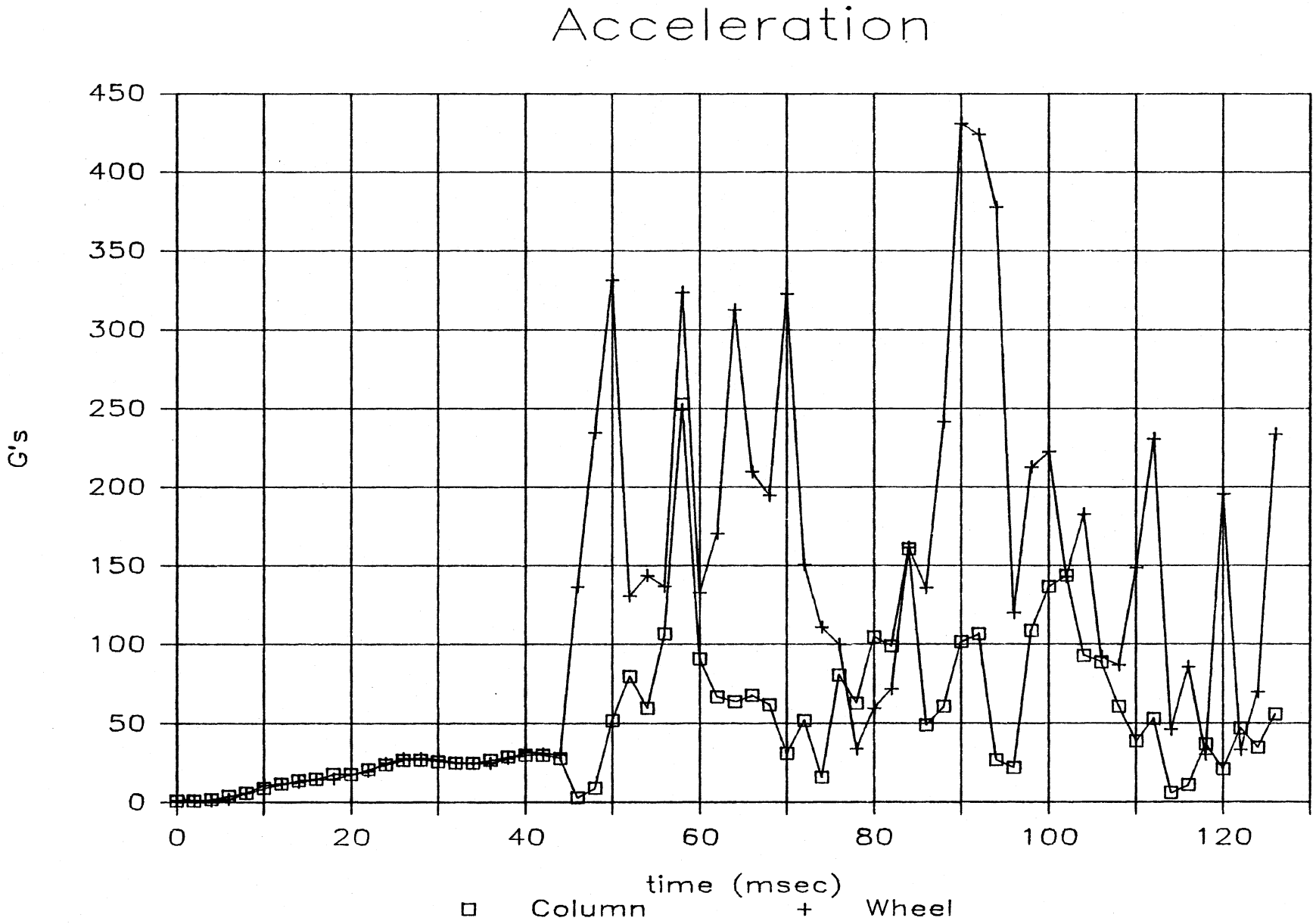

Figure 39. Predicted column and wheel accelerations.

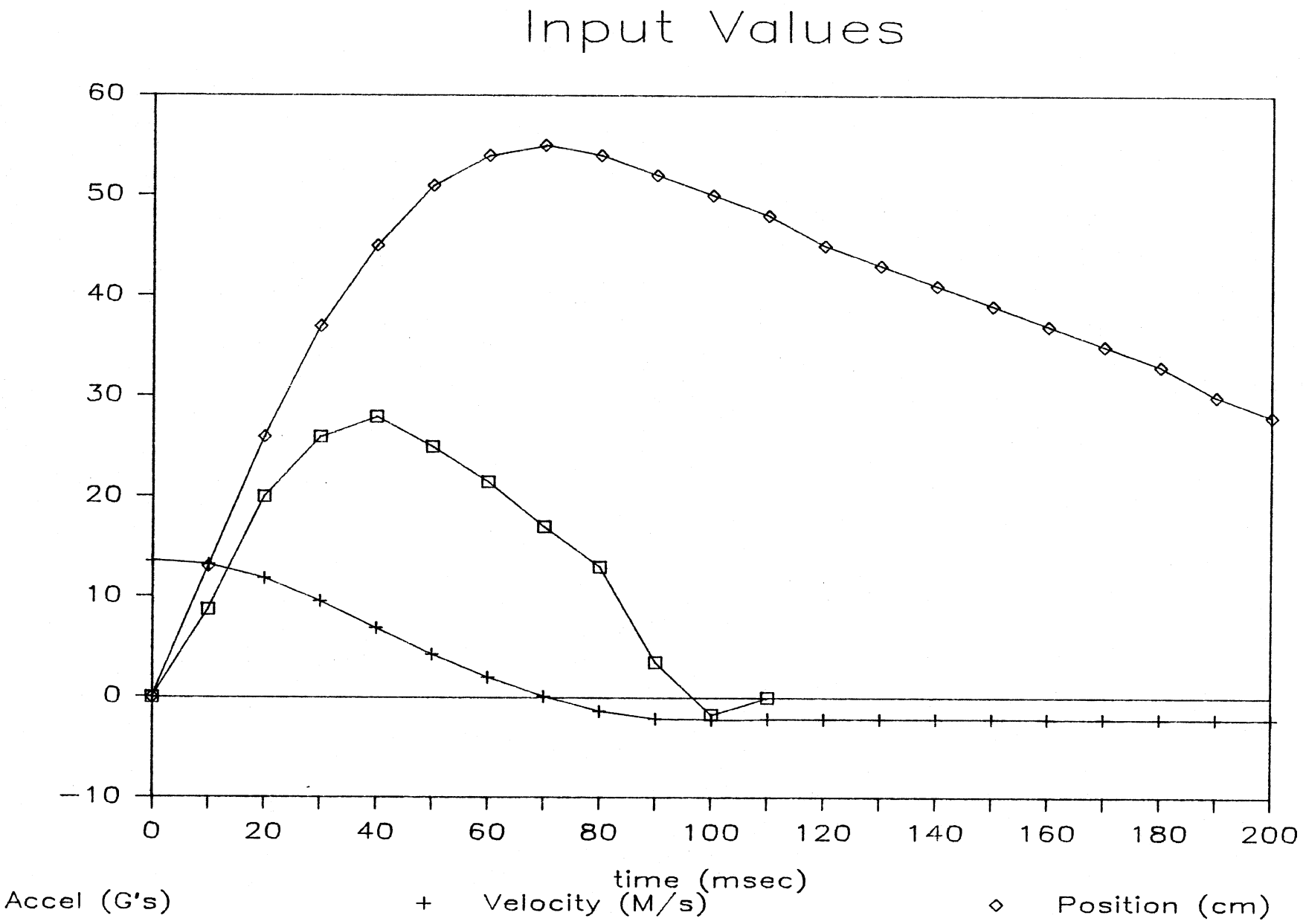

Figure 40. Vehicle input deceleration.

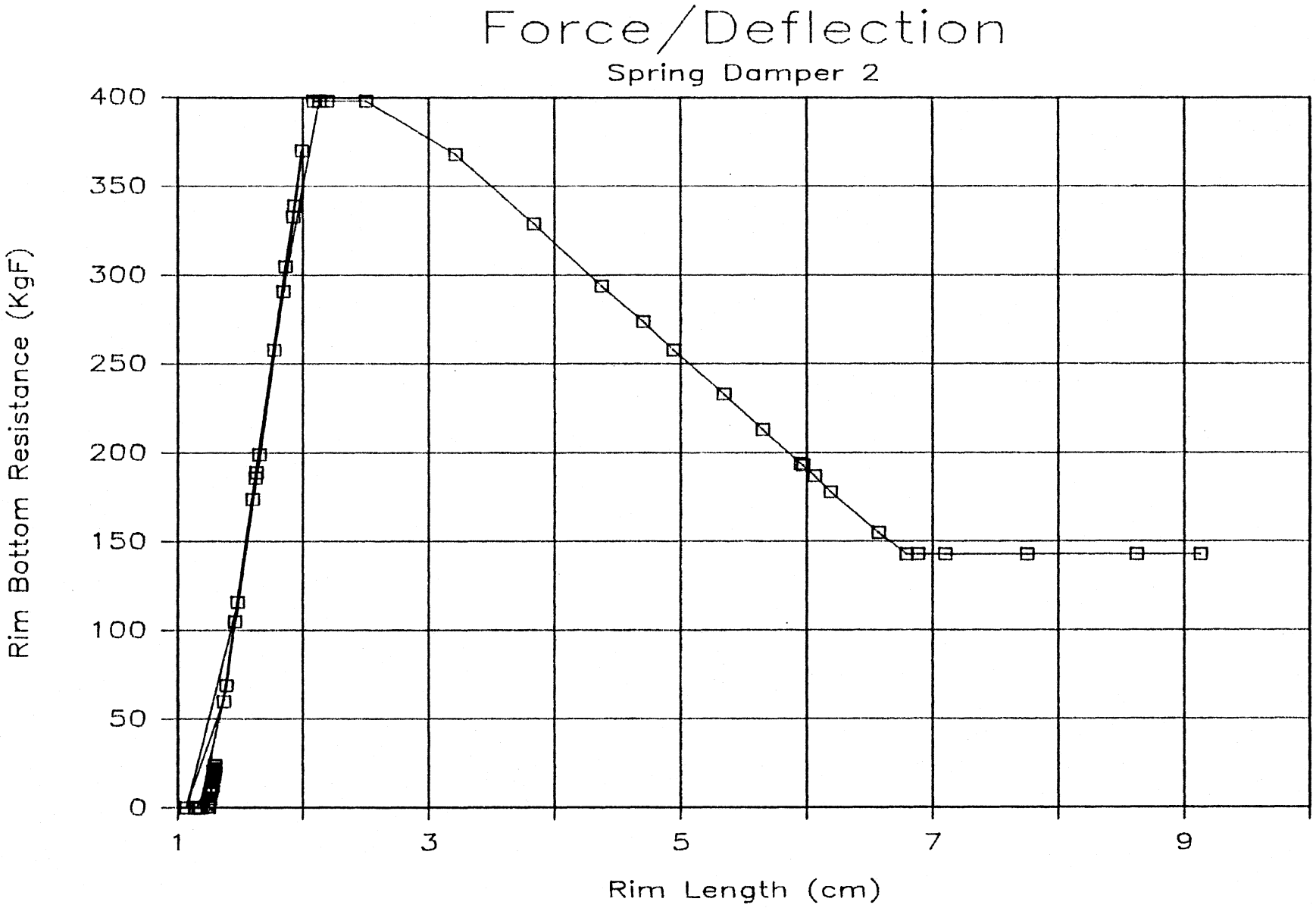

Figure 41. Force vs. deflection for rim bottom spring-damper.

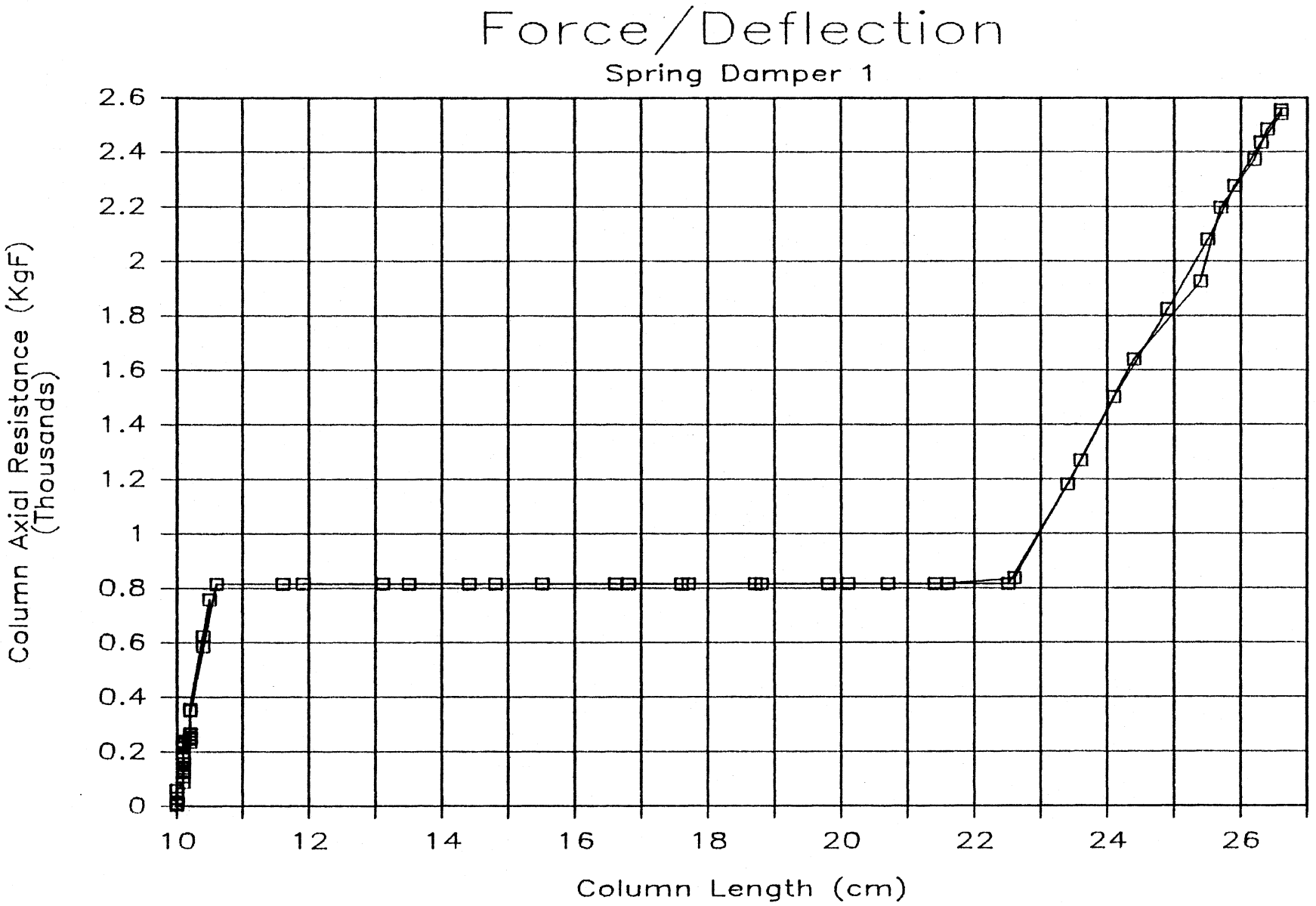

Figure 42. Force vs. deflection for column spring-damper.

5.0 CONCLUSIONS

Two basic conclusions have been reached with regard to the results generated during this project. The first is that a steering assembly model is feasible and has been demonstrated. A comparison between predictions and test data indicates similar results. This conclusion is tempered somewhat by the observation that 3D-CVS software is hard to use.

The second conclusion is that simulation accuracy improves with the quality of the available input data. This conclusion can be reached for all projects involving simulation of occupant dynamics. Any application of software of this type places the burden on the user of obtaining physical data to describe:

- the occupant (test dummy)
- the three-dimensional geometry of the vehicle
- the dynamic deflection and force response of vehicle components to interaction with an occupant, or with each other in the case of the column model
- the initial conditions describing the location of the occupant in the vehicle along with the forcing function (vehicle deceleration).

The better the quality of the data--the better the quality of results. It is essential that baseline experimental data related to the design task at hand be available before simulation is attempted. This emphasizes the importance of coordinating the efforts of analytical, design, and test staff in order to gain optimum results from a simulation activity such as the wheel/column model. Access to and communication with all of these groups aided this investigator greatly in reaching a reasonably successful solution to the problem.

In order to improve the quality of this simulation result and others which will be accomplished in the future, several recommendations can be made about:

- Improved graphic output.
- Development of new column test procedures.
- Use of accident reconstruction techniques to develop initial occupant position.
- Modification of the 3D-CVS friction model to include static friction.
- Improvement of the integration algorithm to decrease stepsize more accurately.
- Improvement of ellipsoid/surface contact algorithm.

Data set preparation is awkward for the user. The first and most basic aid should be the development of documented baseline data sets describing the physical properties of the dummies which are in use. The documentation should include test reports and a rationale for each entry to the data file. Volume 2 of Fleck's report (1) is a good point at which to start. In addition, automated procedures should be developed for preparing vehicle geometric models using quantities obtained directly from vehicle drawings as input. Likewise, automated procedures should be developed for occupant positioning. A particular problem is defining the angular degrees of freedom for the various segments and the initial joint orientations. A most effective means for accomplishing this would use an interactive display of the occupant in a vehicle. Targets developed from test or design data would be entered on the screen for positioning known points on the occupant (H-point, knee-point, heel-point, eye point, and any others). The location of these same points on the dummy could then be adjusted by moving them on command to coincide with the targets. When an appropriate position is reached, a command to the software would automatically compute all angular parameters needed for input. The procedure could also be coupled with the existing 3D-CVS equilibrium sub-program or with a procedure modeled after the HELPER program (5) developed for the MVMA-2D occupant motion simulation package. In many ways the package which has

been proposed is not unlike some of the design tools used in Human Factors studies (SAMMIE, CYBERMAN) of occupant position, clearance, and reach.

Improved interactive graphics output would be an important aid both in data set preparation and analysis of results. The wireframe models which exist can be modified to improve hidden line removal, if desired, and to provide a graphic display of contacts which occur and the vector direction and location of the resulting forces applied to the occupant.

With respect to wheel/column modeling, new test procedures should be developed to determine the conditions under which binding will occur to form the basis for realistic modeling of this phenomenon. The capability to generate forces in particular directions exists within the software and awaits a physical description for implementation.

An improvement to modeling technique is recommended based on the accident reconstruction work reported by Robbins, et al. (6). The procedure is to overlay the simulated occupant linkage on a photograph (slide) of the test setup in order to select the proper location and orientation of contact ellipsoids to be attached to the occupant.

The remaining three recommendations have to do with changes in the existing 3D-CVS code. The first is to modify the current friction model to include static friction. As described in Section 2.2, this lack of an effective static friction model almost caused abandonment of the project. The necessary changes appear to be feasible and, when implemented for linear motions, produce somewhat the same effect as locking and unlocking of joints, only at prescribed values of force. It should be noted that the same problem also exists with the MVMA-2D Code.

The second coding change which is recommended has to do with the integration procedure. There is a tendency for the simulation to stop when step sizes have to be suddenly decreased, usually due to the beginning of a contact interaction or the sudden application of internal joint torques. This appears to be related to lack of storage of previously computed numerical information which can serve to aid the process of step size reduction. Again, this is a feasible improvement which could aid immensely in the solutions for stiff interactions. Related to this should be an effort to reintroduce the RESTART option in the General Motors version of the 3D-CVS code. When stiff interactions are anticipated, the execution can be stopped and restarted using more satisfactory integration parameters for the region of the solution in question.

The final recommendation has also been discussed in Section 2.2 and is relatively easy to solve. This is the reduction of force to zero when an ellipsoid has passed completely through a contact surface. This is a particularly severe problem when the dimensions of the ellipsoid are small with respect to the deformation of the surface.

6.0 REFERENCES

1. Fleck, J.T., Butler, F.E., and DeLeys, N.J., Validation of the Crash Victim Simulator, Report ZS-5881, Calspan Corporation, Buffalo, NY, December 1982, 3 Vols.

2. CAL-3D User Conference Proceedings, Sponsored by MVMA and NHTSA, Dearborn, MI., May 1981.

3. Bowman, B.M., Bennett, R.O., and Robbins, D.H., MVMA Two-Dimensional Crash Victim Simulation, Version 3, Report No. UMTRI-85-24-1,2,3. 3 Vols. University of Michigan Transportation Research Institute, Ann Arbor, June 1985.

4. Robbins, D.H. and Bennett, R.O., Three-Dimensional Occupant Dynamics Software: Belt Model Use, Report No. UMTRI-85-45. University of Michigan Transportation Research Institute, Ann Arbor, October 1985.

5. Bowman, B.M. and Pope, M.E., MVMA-2D Occupant Positioning for Approximate Initial Equilibrium, Report GMR-4198, General Motors Research Laboratories, Warren, MI, September 1982.

6. Robbins, D.H., Huelke, D.F., and Sherman, H.W., Biomechanical Accident Investigation Methodology: Second Phase Case Reports and Guidelines for Application, Report No. UMTRI-85-36, University of Michigan Transportation Research Institute, Ann Arbor, August, 1985.